AD_____

Award Number: W81XWH-09-1-0185

TITLE: Defining the Role of BTLA in Breast Cancer Immunosurveillance and Selective Targeting of the BTLA-HVEM-LIGHT Constimulatory System

PRINCIPAL INVESTIGATOR: Kenneth M. Murphy, M.D.
William E. Gillanders, M.D.

CONTRACTING ORGANIZATION:
Washington University
St. Louis, MO 63130-4862

REPORT DATE: May 2011

TYPE OF REPORT: Annual

PREPARED FOR: U.S. Army Medical Research and Materiel Command
Fort Detrick, Maryland 21702-5012

DISTRIBUTION STATEMENT:

X Approved for public release; distribution unlimited

REPORT DOCUMENTATION PAGE

Form Approved
OMB No. 0704-0188

1. REPORT DATE *(DD-MM-YYYY)*	**2. REPORT TYPE**	**3. DATES COVERED** *(From - To)*
31-MAY-2011	Annual	01 MAY 2010 - 30 APR 2011

4. TITLE AND SUBTITLE
Defining the Role of BTLA in Breast Cancer Immunosurveillance

and Selective Targeting of the BTLA-HVEM-LIGHT Constimulatory

System

5a. CONTRACT NUMBER

5b. GRANT NUMBER
W81XWH-09-1-0185

5c. PROGRAM ELEMENT NUMBER

6. AUTHOR(S)
Kenneth Murphy, William Gillanders

kmurphy@wustl.edu

5d. PROJECT NUMBER

5e. TASK NUMBER

5f. WORK UNIT NUMBER

7. PERFORMING ORGANIZATION NAME(S) AND ADDRESS(ES)
Washington University

Saint Louis, MO 63130-4862

8. PERFORMING ORGANIZATION REPORT NUMBER

9. SPONSORING / MONITORING AGENCY NAME(S) AND ADDRESS(ES)
US Army Medical Research and
Materiel Command
Fort Detrick, Maryland
21702-5012

10. SPONSOR/MONITOR'S ACRONYM(S)

11. SPONSOR/MONITOR'S REPORT NUMBER(S)

12. DISTRIBUTION / AVAILABILITY STATEMENT

Approved for public release, distribution unlimited.

13. SUPPLEMENTARY NOTES

14. ABSTRACT

None provided.

15. SUBJECT TERMS
Anti tumor therapy, graft vs host disease, regulatory T cell (Treg), B&T lymphocyte attenuator.

16. SECURITY CLASSIFICATION OF:			**17. LIMITATION OF ABSTRACT**	**18. NUMBER OF PAGES**	**19a. NAME OF RESPONSIBLE PERSON**
a. REPORT	**b. ABSTRACT**	**c. THIS PAGE**			USAMRMC
U	U	U	UU	76	**19b. TELEPHONE NUMBER** *(include area code)*

Table of Contents

INTRODUCTION: The current reporting period represents the second year of the award. In the first year the primary goals of generating crosses between various genetic strains of mice were initiated. In the repost for the first year, described the discovery of a use for BTLA that could be applied to treatment of breast cancer in an unanticipated manner. One therapy used to treat metastatic breast cancer is autologous stem cell transplantation, or bone marrow transplantation (BMT), which however can cause serious or even lethal graft versus host disease (GvHD). GvHD therefore presents a real limitation to the use of BMT in treating metastatic breast cancer. In our previous report, we described our discovery that administration of anti-BTLA antibodies at the time of bone marrow transplantation permanently prevent GvHD in murine models. In the second year, we pursued to determine the mechanistic basis for this effect. This work was very successful, and we have now published our study in the Journal of Experimental Medicine.

Targeting of B and T lymphocyte associated (BTLA) prevents graft-versus-host disease without global immunosuppression. Albring JC, Sandau MM, Rapaport AS, Edelson BT, Satpathy A, Mashayekhi M, Lathrop SK, Hsieh CS, Stelljes M, Colonna M, Murphy TL, Murphy KM. J Exp Med. 2010 207:2551-9.

The mechanism of anti-BTLA treatment at the time of BMT is a selective blockade of the dangerous alloreactive donor T cells, without a blockade in the expansion and effector activities of normally protective and pathogen-specific donor T cells. More importantly, we showed that blockade of GvHD by anti-BTLA antibody did not prevent the elimination of tumor cells by the newly established donor-derived immune system.

WE now intend to seek additional funding to develop anti-human BTLA antibodies and to move this discovery into the clinic. Our initial target disease will be in the setting of acute myeloid leukemia where patient's may not always have well-matched bone marrow donors, and where autologous transplantation does not deliver anti-tumor activity. Our finding that anti-tumor responses from the donor T cells are intact makes it possible anti-BTLA modified BMT may prevent GvHD while retaining the desirable anti-tumor effects of BMT.

Our funds from the DOD grant are now exhausted, but they provided critical means by which an important discovery were made.

The award was in the format of a synergistic idea award to Dr. Gillanders, a cancer surgeon, and Dr. Murphy, a basic immunologist. The overall aim was to evaluate the potential of manipulating the BTLA inhibitory receptor on lymphocytes for the purpose of augmenting immunotherapy's directed at cancers, particularly in this instance breast cancer models in mice. The proposed plan was to use a spontaneous breast cancer mouse model in which the role of BTLA would be tested by introducing targeted genetically manipulations to BTLA. The scope of the evaluation is directed at the characterization of the T cell responses to tumors. The benefits of a spontaneous tumor model was intended to be used to evaluate the in-vivo role of manipulating BTLA for anti tumor therapies, but required a long lead time to generate the required genetic crosses, and also have the built in difficulty of the duration required for the generation of coherts in mice that develop the spontaneous cancers. During the study, the related utility of manipulating BTLA in the disease Graft versus Host Disease (GvHD) was evaluated. Graft versus Host Disease is a major limitation the use of bone marrow transplantation (BMT), which is a current therapy in the treatment of metastatic breast carcinoma. We discovered that administration of an anti-BTLA antibody at the time of BMT eliminated GvHD in chronic and lethal models through a mechanism that did not generate general immune suppression and left anti-tumor immune responses intact.

BODY: The tasks associated with specific aims 1, 2, and 3 that were specified for the first year of research are underway. The breeding between PD-1 and BTLA deficient mice has been completed, with no observation of spontaneous disease. Currently we know that T cells develop normally in the double-deficient mice with no obvious alteration in the development of major immune subsets. At present, no spontaneous tumors from Balb/c-new t mice have been evaluated due to the absence of mice of sufficient age and genetic background at this point.

Mechanistic work related to the BTLA/HVEM access has been carried out in a readily available model of murine Graft-versus-Host Disease (see accompanying manuscript). Based upon the likely similarity of the actions of BTLA on anti tumor T cells and in T cells expanding in the GVHD model, we have carried out a series of studies into the mechanism and effects of BTLA directed immunotherapy. In GVHD, T cells expanding following bone marrow transplantation not only manifest Graft-versus-Host Disease, but also mediate important anti-tumor effects in this setting that are used advantageously in the setting of certain cancers of lymphoid tissues. Therefore, we have carried out an analysis to evaluate the role of BTLA directed therapy in this setting during this period in which experimental mice colonies are being generated through breeding programs.

The model used during this period is the fully irradiated GVHD model. Two forms of this were tested, being a fully MHC-mismatched model of B6 transfer into Balb/c recipients, or a parental into f1 model. In both cases, either lethal or chronic GVHD is established, concurrent with significant weight loss, and a permanent mucosal inflammatory disease in the gut and elsewhere. Our essential finding is that the treatment of recipient mice with a single injection of anti-BTLA antibody (6a6) results in a permanent prevention of GVHD. We find that treatment at the time of bone marrow transplantation (BMT) leads to a permanent cure, but that treatment with antibody delayed by 7 or 14 days fails to have any impact on the prevention of GVHD. In analyzing this observation, we have found that the effect is mediated by the alteration of populations of T cells expanding during the period of lymphopenia immediately following BMT. The accompanying manuscript has been submitted to Nature Medicine, and has received favorable reviews with suggestions for additional experiments, which we are currently undertaking to perform. In these additional experiments, we have used Foxp3-reportor mice in a series of cellular adoptive transfer experiments and have evaluated the effects of BTLA-directed therapy. The results indicate that BTLA acts on the expanding effector cells, exerting a preferential inhibition of their expansion compared to the expansion of regulatory T cells. This may relate to our earlier observations that effector cells express high levels of BTLA, whereas regulatory T cells express lower levels of BTLA and therefore may be inhibited to a lesser extent than expanding effector T cells. This prevention of robust effector cell expansion during lymphopenia following BMT may have the effect of limiting the expansion of auto-reactive T cells that are driven to expand through antigen interactions during the period of lymphopenia. By allowing the establishment of an appropriate balance between regulatory T cell populations and the effector cells that they control, a permanent cure and prevention of GVHD appears to take place once lymphopenic homeostatic expansion ceases in the recipient about 7-14 days following BMT.

Of relevance to the current proposal, we have found that HVEM is not involved in the mechanisms of the beneficial effects of BTLA-directed therapy. During homeostatic expansion, HVEM is not engaged to limit the expansion of effector T cells after BMT. This observation may alter our future focus to concentrate on BTLA rather than HVEM manipulations in considering ways to augment anti-tumor vaccinations.

KEY RESEARCH ACCOMPLISHMENTS:

Generation of proposed genetic strains is completed or underway.

Identification of an effect of BTLA-directed therapy in the treatment of Graft-versus-Host Disease, which may impact anti-tumor T cell effects.

REPORTABLE OUTCOMES: The accompanying manuscript has been submitted to Nature Immunology and is currently under revision. This unanticipated result was obtained during the period of time in which the major activities involved generation of various mouse strains.

CONCLUSION: The current proposal as initially funded is not yet completed, intermediate conclusions relate to the beneficial effect of anti-BTLA therapy in Graft-versus-Host Disease. Analysis of mice generated in the next funding year will be required for additional conclusions.

REFERENCES:

1. M. A. Hurchla et al., *J Immunol* 174, 3377-3385 (2005).
2. M. A. Hurchla, J. R. Sedy, K. M. Murphy, *J Immunol* 178, 6073-6082 (2007).
3. J. R. Sedy et al., *Nat Immunol* 6, 90-98 (2005).
4. N. Watanabe et al., *Nat Immunol* 4, 670-679 (2003).
5. J.C. Albring et al., J Exp Med 12 2551-9 (2010).

APPENDICES: See attached PDF's

Figure 1

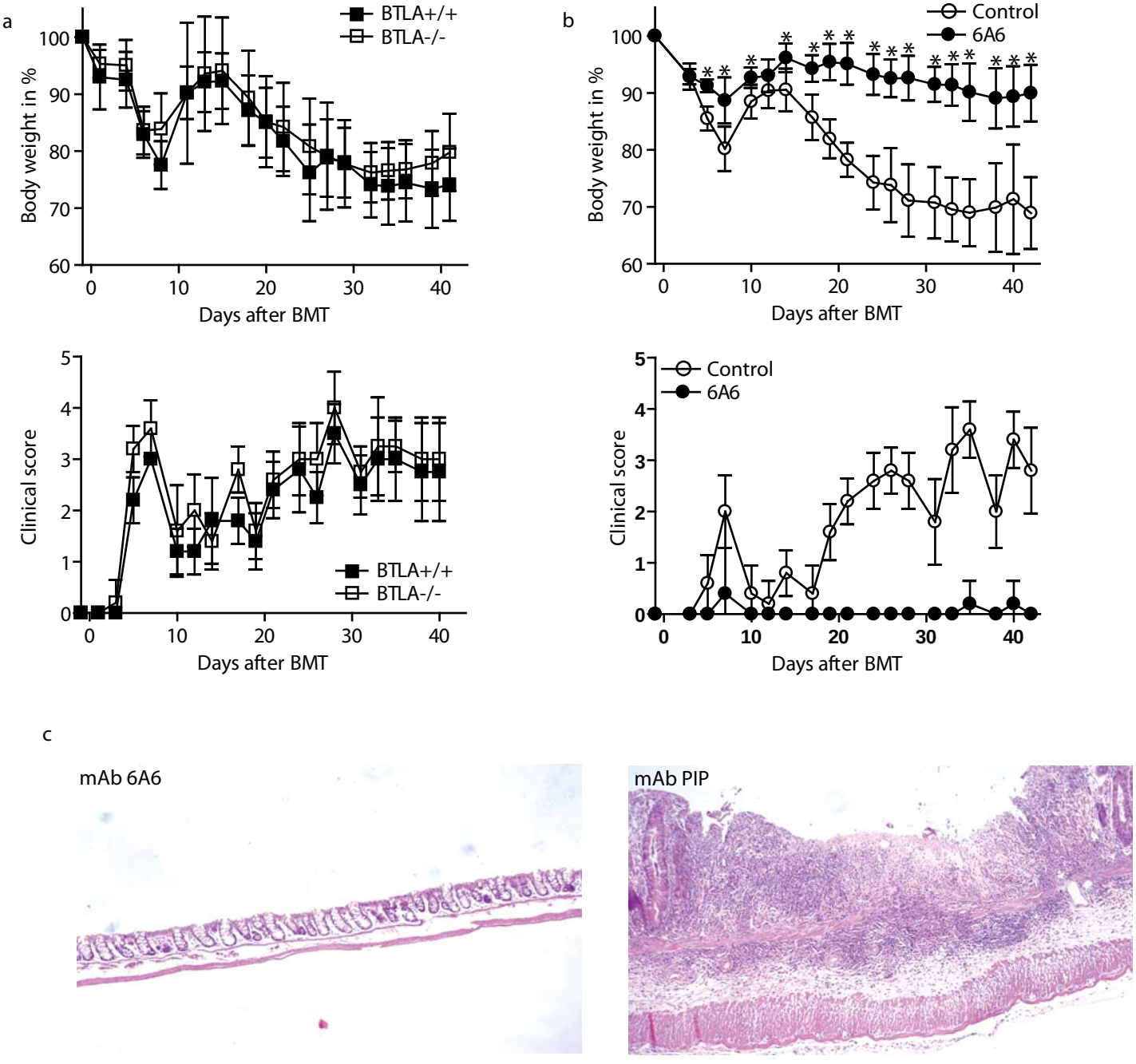
a
BTLA+/+
BTLA-/-
Body weight in %
Days after BMT
b
Control
6A6
Body weight in %
Days after BMT
Clinical score
BTLA+/+
BTLA-/-
Days after BMT
Control
6A6
Clinical score
Days after BMT

c

mAb 6A6
mAb PIP

Figure 2

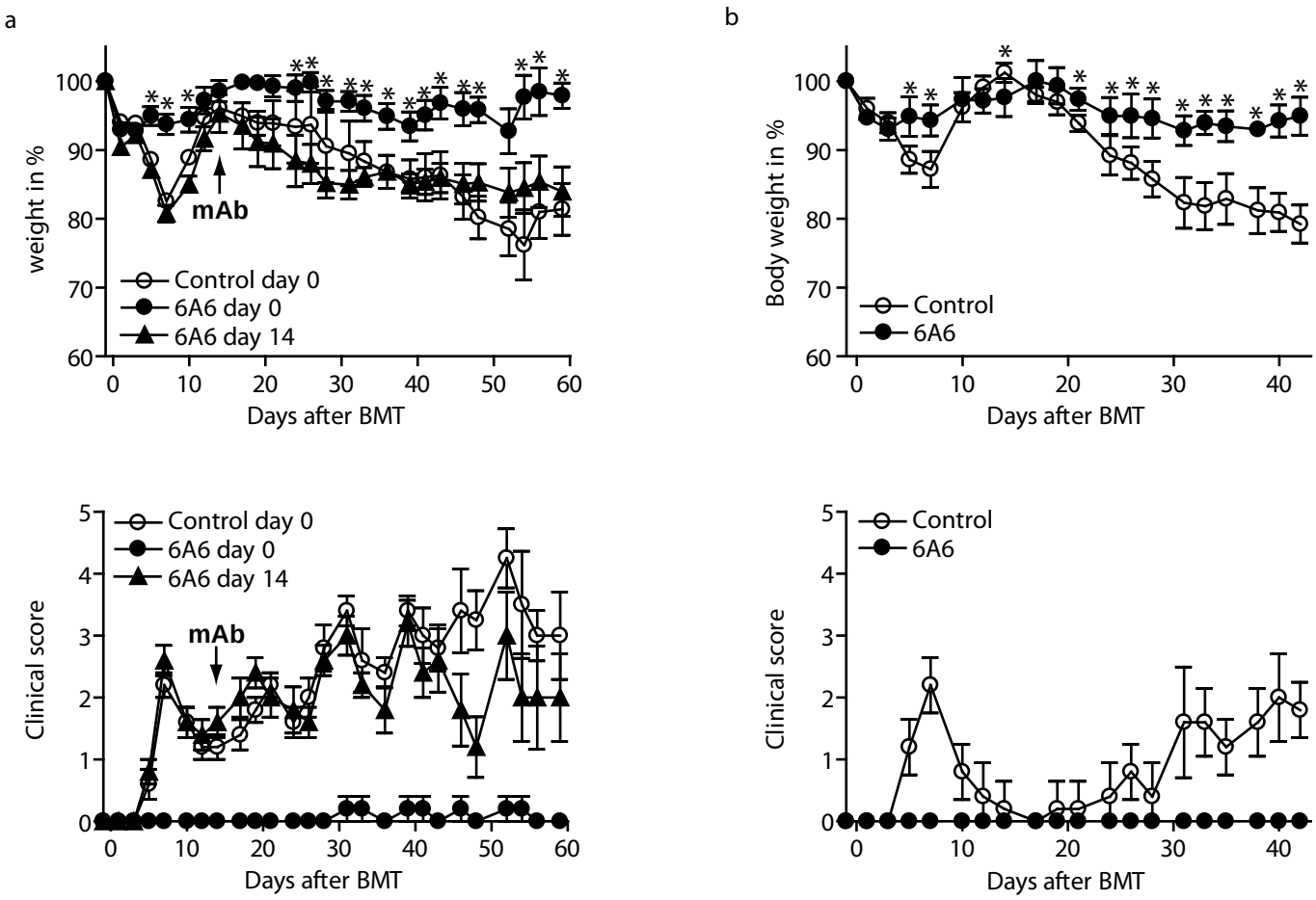
a
b
weight in %
Body weight in %
Days after BMT
mAb
Control day 0
6A6 day 0
6A6 day 14
Control
6A6
Clinical score

Figure 3

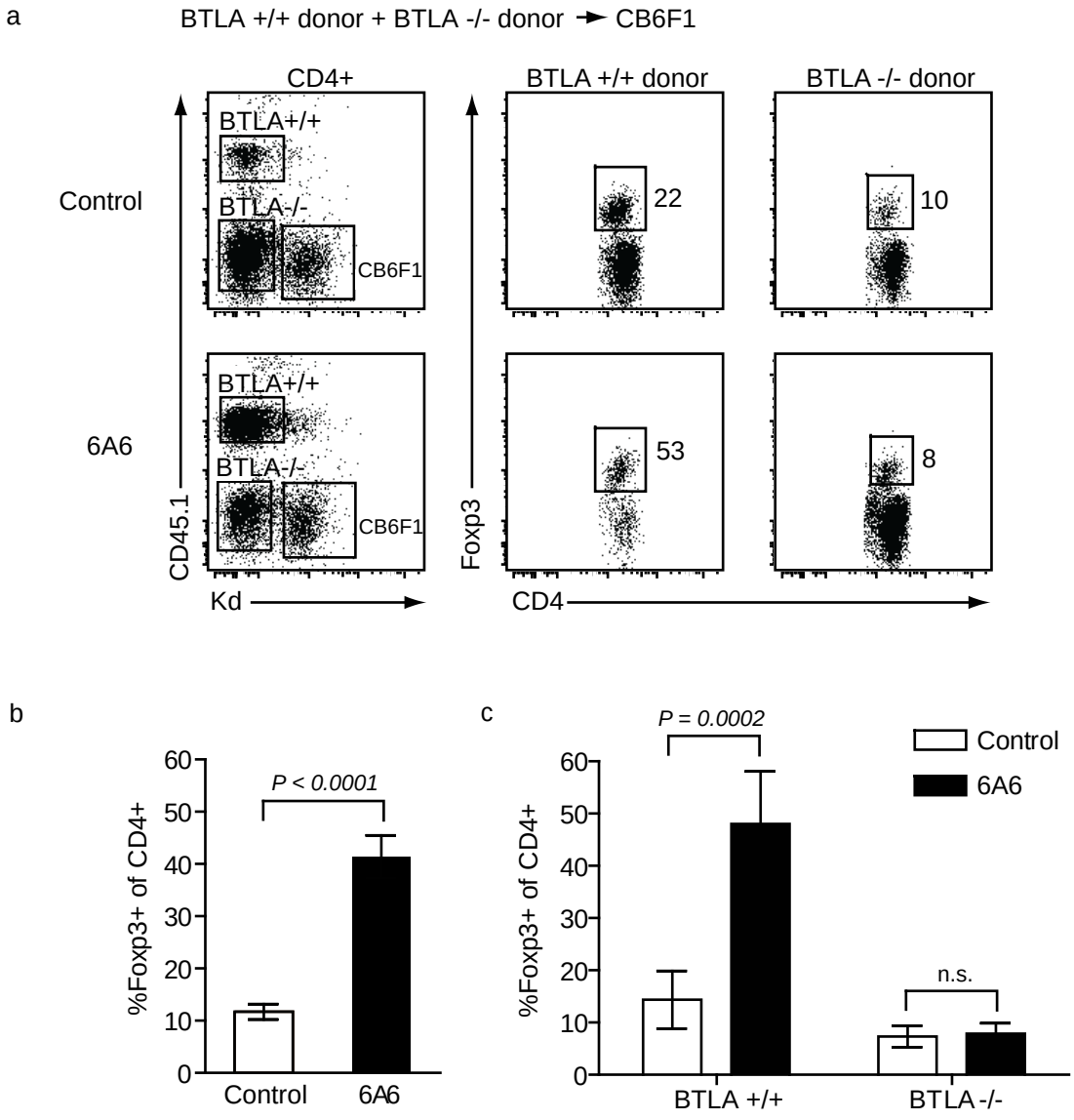
a
BTLA +/+ donor + BTLA -/- donor → CB6F1
CD4+
BTLA +/+ donor
BTLA -/- donor
Control
6A6
BTLA+/+
BTLA-/-
CB6F1
22
10
53
8
CD45.1
Kd
Foxp3
CD4
b
%Foxp3+ of CD4+
P < 0.0001
Control
6A6
c
P = 0.0002
Control
6A6
n.s.
BTLA +/+
BTLA -/-

Figure 4

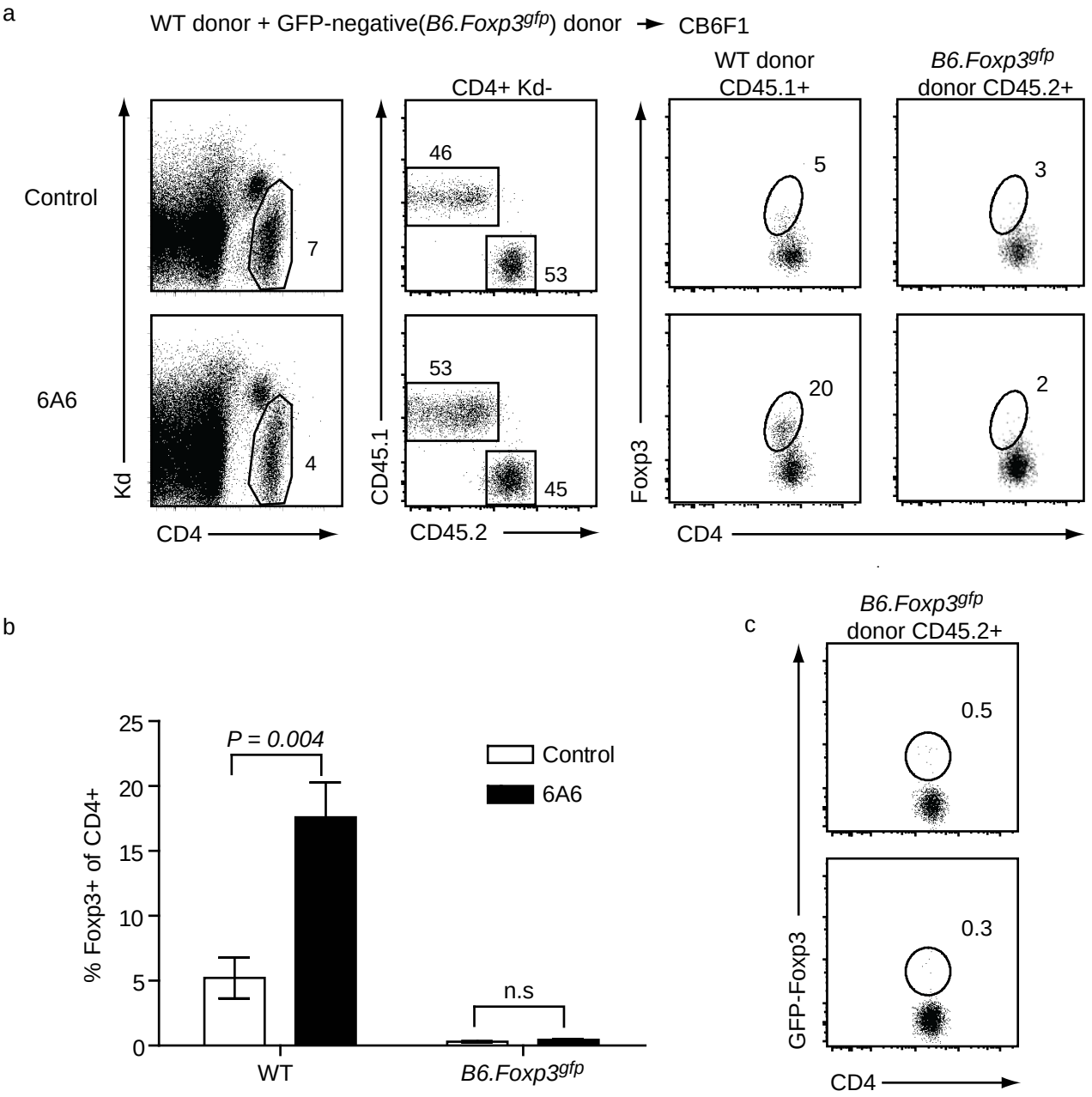
a
WT donor + GFP-negative(B6.Foxp3gfp) donor → CB6F1
CD4+ Kd-
WT donor CD45.1+
B6.Foxp3gfp donor CD45.2+
Control
6A6
Kd
CD4
7
4
46
53
53
45
CD45.1
CD45.2
5
20
3
2
Foxp3
CD4
b
P = 0.004
Control
6A6
% Foxp3+ of CD4+
25
20
15
10
5
0
n.s
WT
B6.Foxp3gfp
c
B6.Foxp3gfp donor CD45.2+
0.5
0.3
GFP-Foxp3
CD4

Supplemental Figure 1

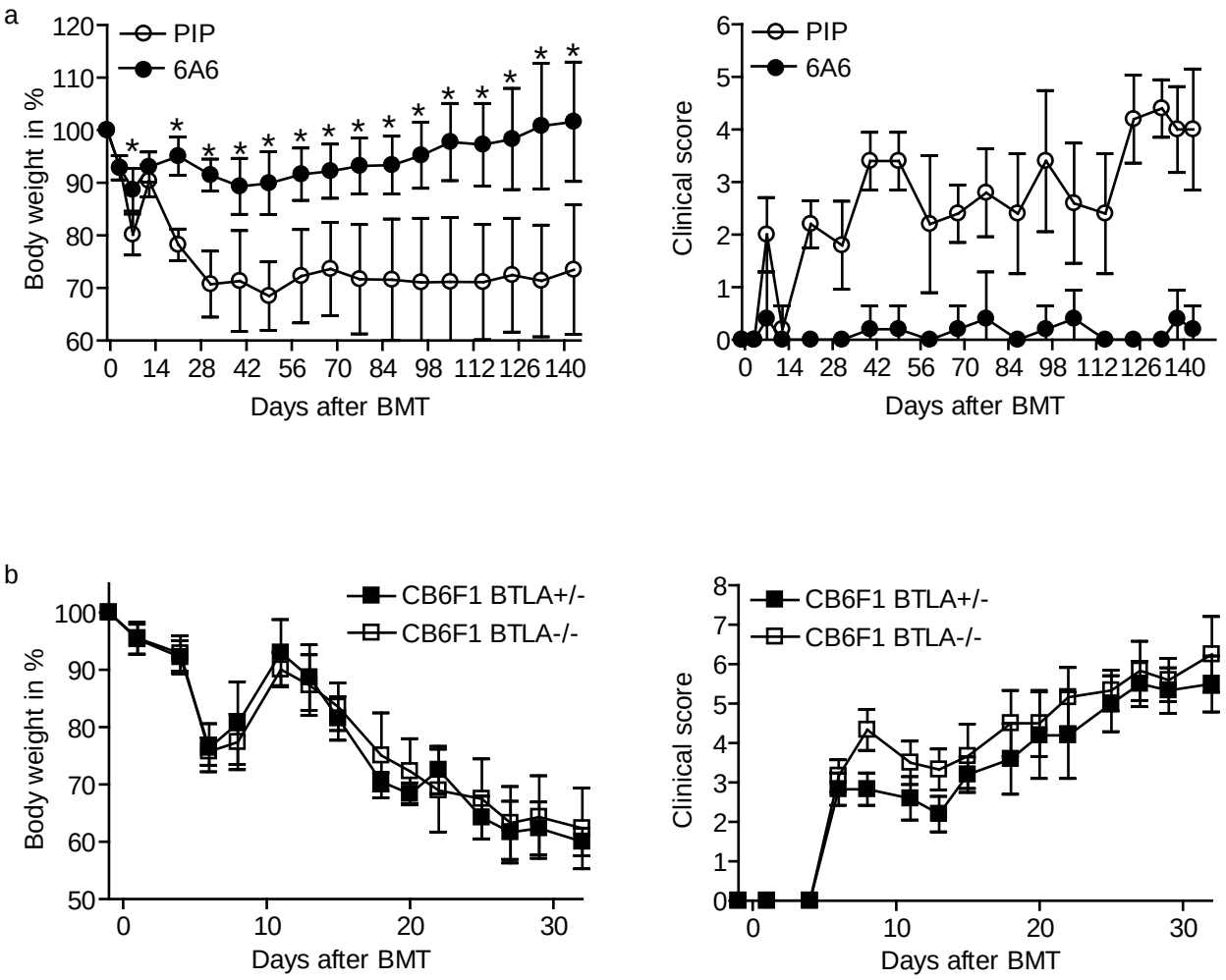

Supplemental Figure 2

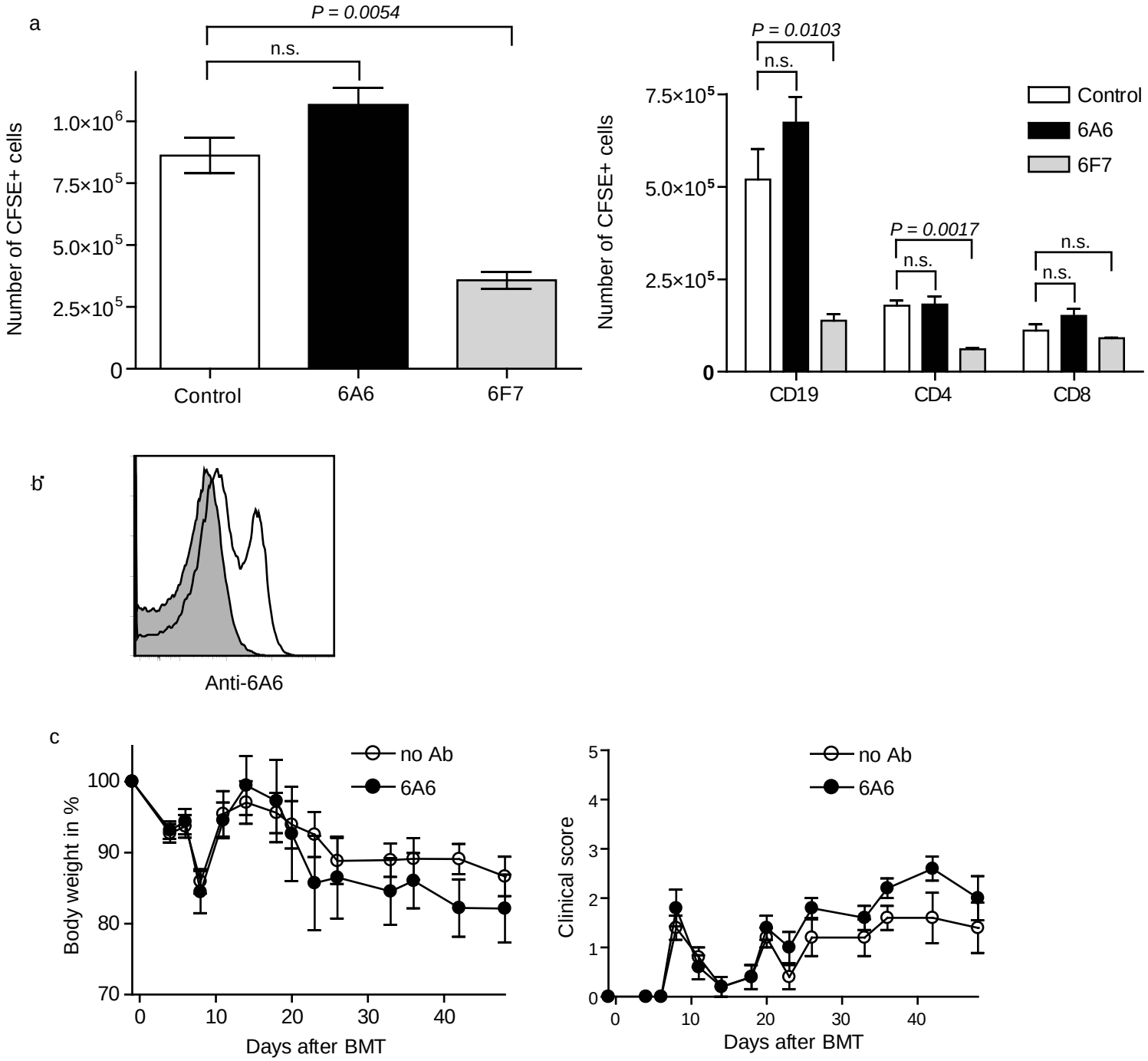

Supplemental Figure 3

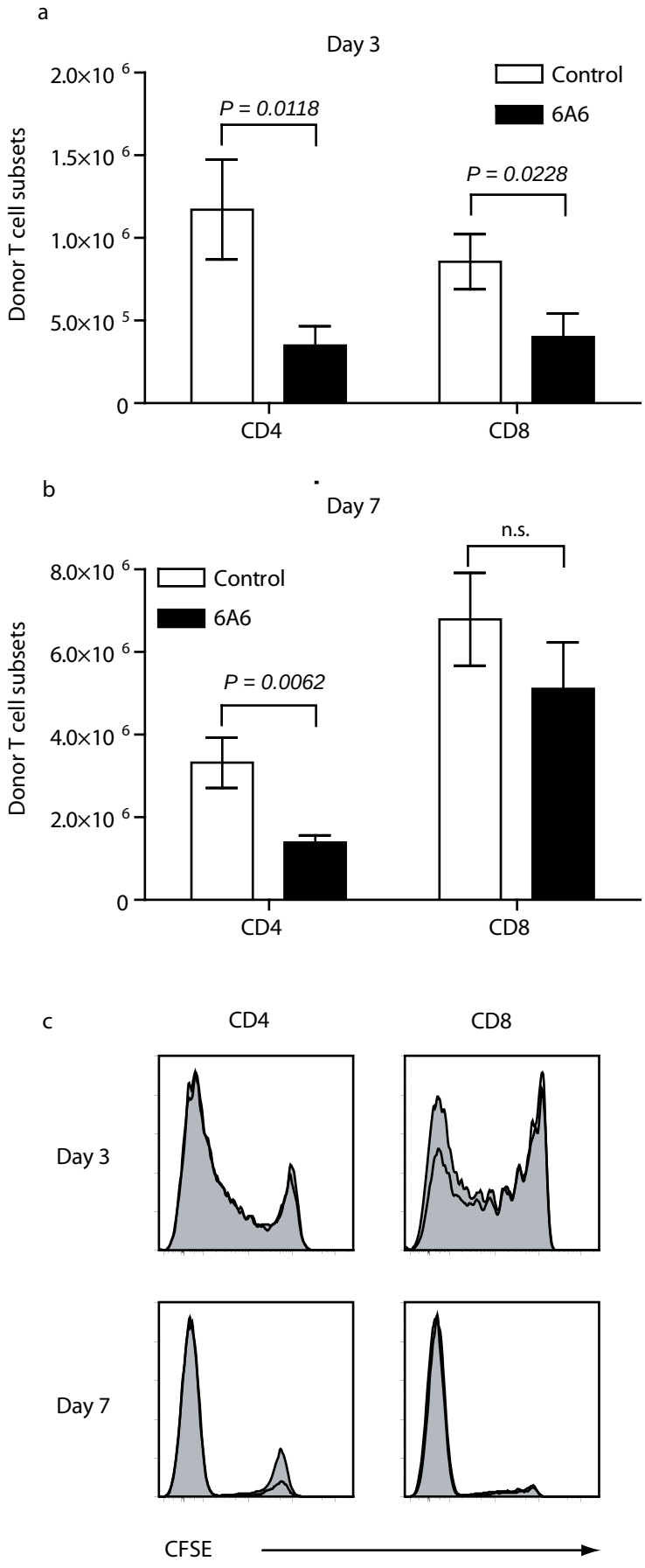

Supplemental Figure 4

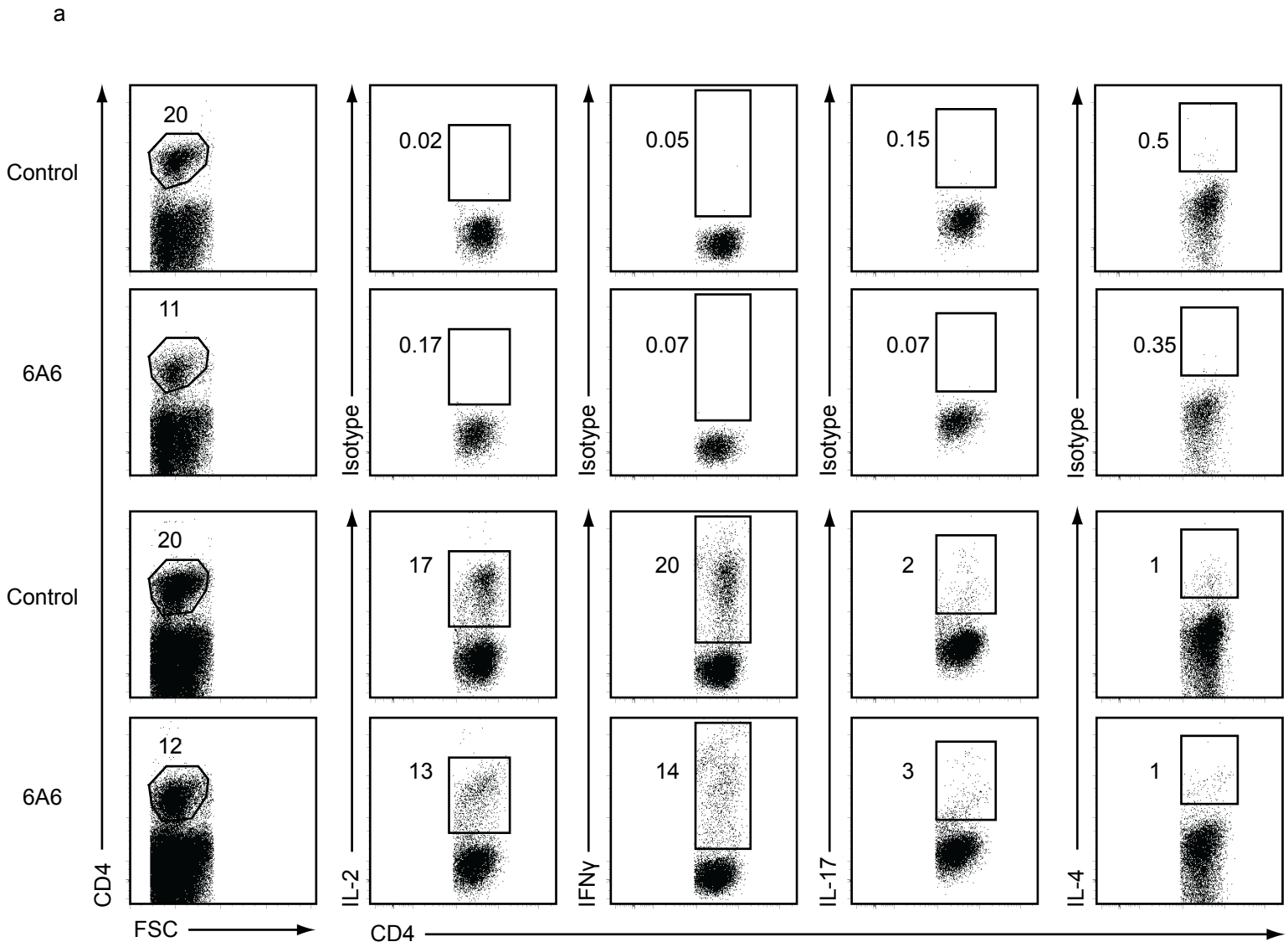

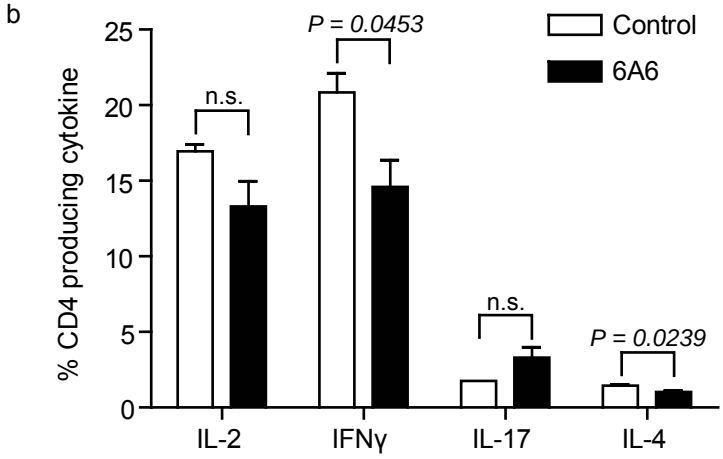

Supplemental Figure 5

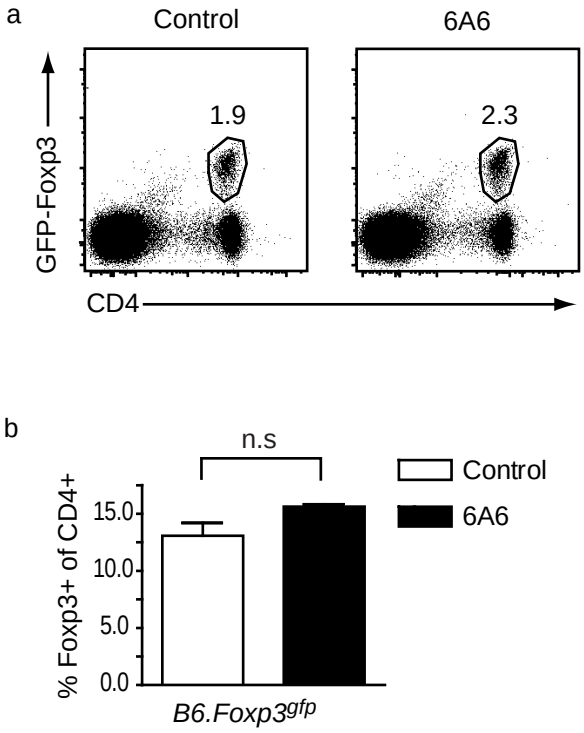

JEM

JEM Home> 2010 Archive > 22 November > Albring et al. 207 (12): 2551

Published November 15, 2010 // JEM vol. 207 no. 12 2551-2559
The Rockefeller University Press, doi: 10.1084/jem.20102017

Brief Definitive Report

Targeting of B and T lymphocyte associated (BTLA) prevents graft-versus-host disease without global immunosuppression

Jörn C. Albring[1,2], Michelle M. Sandau[1], Aaron S. Rapaport[1], Brian T. Edelson[1], Ansuman Satpathy[1], Mona Mashayekhi[1], Stephanie K. Lathrop[3], Chyi-Song Hsieh[3], Matthias Stelljes[4], Marco Colonna[1], Theresa L. Murphy[1], and Kenneth M. Murphy[1,2]

+ Author Affiliations

+ Author Notes

CORRESPONDENCE Kenneth M. Murphy: kmurphy@wustl.edu

ABSTRACT Back to Top

Graft-versus-host disease (GVHD) causes significant morbidity and mortality in allogeneic hematopoietic stem cell transplantation (aHSCT), preventing its broader application to non–life-threatening diseases. We show that a single administration of a nondepleting monoclonal antibody specific for the coinhibitory immunoglobulin receptor, B and T lymphocyte associated (BTLA), permanently prevented GVHD when administered at the time of aHSCT. Once GVHD was established, anti-BTLA treatment was unable to reverse disease, suggesting that its mechanism occurs early after aHSCT. Anti-BTLA treatment prevented GVHD independently of its ligand, the costimulatory tumor necrosis factor receptor herpesvirus entry mediator (HVEM), and required BTLA expression by donor-derived T cells. Furthermore, anti-BTLA treatment led to the relative inhibition of $CD4^+$ forkhead box $P3^-$ ($Foxp3^-$) effector T cell (T eff cell) expansion compared with precommitted naturally occurring donor-derived $CD4^+$ $Foxp3^+$ regulatory T cell (T reg cell) and allowed for graft-versus-tumor (GVT) effects as well as robust responses to pathogens. These results suggest that BTLA agonism rebalances T cell expansion in lymphopenic hosts after aHSCT, thereby preventing GVHD without global immunosuppression. Thus, targeting BTLA with a monoclonal antibody at the initiation of aHSCT therapy might reduce limitations imposed by histocompatibility and allow broader application to treatment of non–life-threatening diseases.

Replacement of an abnormal lymphohematopoietic system by allogeneic hematopoietic stem cell transplantation (aHSCT) from a healthy donor is an effective treatment for many disorders of the hematopoietic system (Sykes and Nikolic, 2005; Copelan, 2006). Induction of a mixed hematopoietic donor-host chimerism can induce long-lasting tolerance to foreign tissues without the need for life-long

immunosuppressive therapy (Kawai et al., 2008). aHSCT therapy has been improved by better donor identification (Petersdorf et al., 2004), more tolerable conditioning regimens (McSweeney et al., 2001), and enhanced supportive care. However, significant treatment-related morbidity and mortality from chemotherapy, radiotherapy, infections, and graft-versus-host disease (GVHD) remain significant clinical problems. Therefore, aHSCT is commonly indicated only for treatment of conditions where other treatment options are far inferior or lacking.

Costimulatory molecules of the CD28 and TNF families regulate GVHD, with inhibitory and activating receptors either decreasing or increasing its severity (Tamada et al., 2000; Blazar et al., 2003; Xu et al., 2007). B and T lymphocyte associated (BTLA) is an inhibitory immunoglobulin superfamily receptor, whose ligand is the TNF receptor herpesvirus entry mediator (HVEM) and which has only been examined in a nonirradiated model of chronic allostimulation without classical GVHD where donor cells lacking BTLA failed to persist (Hurchla et al., 2007). The role of BTLA in aHSCT using irradiated recipients, in which clinical symptoms and pathology similar to human GVHD develop, has not been examined.

RESULTS AND DISCUSSION

Back to Top

To determine the role of BTLA in the development of GVHD, we first examined WT and BTLA$^{-/-}$ donor mice (Watanabe et al., 2003) using a nonlethal parent-into-irradiated F1 model of aHSCT (Stelljes et al., 2008). In this model, GVHD results from partial MHC mismatch between H-2^{b} haplotype donor cells and lethally irradiated H-2$^{b/d}$ haplotype recipients. BM and splenocytes from WT or BTLA$^{-/-}$ mice on the C57BL/6 background were transferred into lethally irradiated CB6F1 recipients (Fig. 1 a). Transplantation of WT donor cells into CB6F1 recipients caused body weight loss of ~30% and clinical scores (Cooke et al., 1996) of ~3 that persisted for >40 d. BTLA$^{-/-}$ and WT donor cells caused similar GVHD, suggesting that BTLA does not normally regulate GVHD in this model. To test whether BTLA expressed by recipient mice might regulate GVHD in this model, we used BTLA$^{-/-}$ CB6F1 hosts as recipients of BTLA$^{-/-}$ BM and splenocytes (Fig. S1 a). BTLA$^{-/-}$ donor cells induced similar GVHD in BTLA$^{+/-}$ and BTLA$^{-/-}$ hosts, which is comparable to GVHD by WT donor cells (Fig. 1 a). Collectively, these data suggest that BTLA does not normally regulate GVHD.

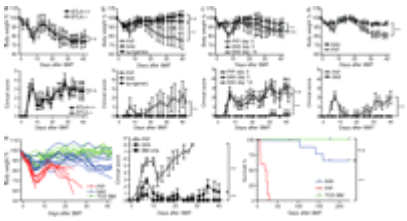

View larger version:

In this page In a new window

Download as PowerPoint Slide

Figure 1.

Anti-BTLA treatment permanently prevents GVHD. (a) Lethally irradiated CB6F1 mice received BMC and splenocytes from C57BL/6 WT (closed squares, *n* = 5) or BTLA$^{-/-}$ (open squares, *n* = 5) donors. (b) Lethally irradiated CB6F1 mice received BMC and splenocytes from syngeneic donors (closed squares, *n* = 10), C57BL/6 mice and antibodies PIP (open circles, *n* = 15), or 6A6 (closed circles, *n* = 15). Shown are cumulative data from three independent experiments. (c) Lethally irradiated CB6F1 mice received BMC and splenocytes from C57BL/6 mice plus control antibody PIP (open circles, *n* = 5) or 6A6 (closed circles, *n* = 5) on the day of BMT or 6A6 14 d after BMT (open squares, *n* = 5). (d) Lethally irradiated CB6F1 mice received BMC and splenocytes from C57BL/6 HVEM$^{-/-}$ mice and control antibody PIP (open circles, *n* = 5) or 6A6 (closed circles, *n* = 5). (e) Lethally irradiated BALB/c mice received TCD-BM alone (green lines and closed squares, *n* = 10) or in combination with splenocytes from C57BL/6 mice and control antibody PIP (red lines and open circles, *n* = 10) or 6A6 (blue lines and closed circles, *n* = 10) on the day of BMT. Shown are cumulative data from two independent experiments. Weight and clinical score data shown are mean ± SD. Data are representative of two independent experiments with five mice per group or cumulative data from independent experiments as indicated. P-values of >0.05 are considered not significant (n.s). ***, P < 0.001.

Because BTLA generates inhibitory signals and functions in autoimmunity (Watanabe et al., 2003), malaria infection (Lepenies et al., 2007), and intestinal inflammation (Steinberg et al., 2008), we wondered whether harnessing the inhibitory effects of BTLA on the immune response by forced engagement would attenuate GVHD. To test this, we compared the effects of an agonistic nondepleting anti-BTLA monoclonal antibody (Hurchla et al., 2005; Lepenies et al., 2007), 6A6, administered at the time of aHSCT (Fig. 1 b) with an isotype control antibody, PIP, that recognizes bacterial GST (Gronowski et al., 1999). Mice treated with PIP showed similar progression of GVHD (Fig. 1, a and b), with clinical scores between 3 and 4 persisting for >140 d (Fig. S1 b). GVHD was associated with thickening of the lamina propria and muscularis, with severe inflammation and ulceration of the colon (Stelljes et al., 2008; Fig. S1 c, bottom). In contrast, a single treatment of 10 µg/g body weight of 6A6, given at the time of aHSCT, prevented GVHD completely, with weight loss and GVHD similar to the syngeneic control group (Fig. 1 b) for 140 d after aHSCT (Fig. S1 b). Furthermore, 6A6-treated mice had no histological evidence of GVHD in the colon (Fig. S1 c, top). Thus, a single administration of anti-BTLA antibody eliminates weight loss, histological changes, and clinical signs of GVHD.

We next asked if 6A6 acted by simply depleting donor cells that express BTLA. As a positive control, we included a depleting murine anti-BTLA antibody, 6F7 (Hurchla et al., 2005; Truong et al., 2009). CFSE-labeled donor cells were transferred into WT recipients that also received PIP, 6A6, or 6F7 antibody. 2 d after transfer, we found similar numbers of $CFSE^+$ cells in mice that received either PIP or 6A6 antibody (Fig. S1 d, left) and no significant differences between numbers of $CD19^+$, $CD4^+$, or $CD8^+$ lymphocytes (Fig. S1 d, right). Treatment with 6F7 caused a significant depletion of $CFSE^+$ lymphocytes, particularly from the $CD19^+$ cell population (Fig. S1 d). Furthermore, surface-bound 6A6 was detectable on live donor-derived cells in vivo up to 7 d after transfer (Fig. S1 e). In addition, 6A6 treatment was unable to prevent GVHD caused when $BTLA^{-/-}$ donors were used as a source of BM for aHSCT (Fig. S1 f). Thus, 6A6 does not deplete lymphocytes (Hurchla et al., 2007; Lepenies et al., 2007) but requires the expression of BTLA on donor cells to prevent GVHD.

Next, we asked if 6A6 could reverse established GVHD. We compared immediate with delayed administration of 6A6 (Fig. 1 c). Again, immediate 6A6 administration prevented GVHD. In contrast, there was no statistical difference in weight loss or clinical scores between mice that received 6A6 14 d after aHSCT and with mice that received PIP (Fig. 1 c).

6A6 binds to a region of BTLA that is involved in interactions with HVEM (Hurchla et al., 2005). Thus, 6A6 might prevent GVHD by preventing HVEM and BTLA interactions, thus blocking costimulatory signaling to donor cells (Xu et al., 2007). Although our data indicated that host BTLA is not involved (Fig. S1 a), we wished to test this possibility independently. Transfer of $HVEM^{-/-}$ donor cells caused induction of GVHD when administered with PIP (Fig. 1 d). The severity of GVHD caused by $HVEM^{-/-}$ donor cells was somewhat less than that caused by WT donor cells (Fig. 1 b), consistent with a study which found that HVEM and LIGHT are costimulatory in promoting GVHD (Xu et al., 2007). However, 6A6 also prevented GVHD caused by $HVEM^{-/-}$ donor cells (Fig. 1 d). These results indicate that 6A6 prevents GVHD in a manner that is independent of HVEM, suggesting it acts directly through BTLA.

Because the parent-into-irradiated F1 model of aHSCT does not result in lethal GVHD, we wished to test the potency of the anti-BTLA treatment in a model of complete MHC mismatch ($H\text{-}2^b$ into $H\text{-}2^d$) that results in lethal GVHD in untreated mice (Lu et al., 2001; Edinger et al., 2003b). Control mice developed severe GVHD with pronounced weight loss and clinical scores of >6 (Fig. 1 e, left and middle) and died within 30 d after aHSCT from severe GVHD (Fig. 1 e, right). Although mice that received the anti-BTLA treatment were not fully

protected from GVHD, with clinical scores ranging from 1 to 3 (Fig. 1 e, middle) and slightly more weight loss than the control group that had received T cell–depleted BM cells (BMCs [TCD-BMs]) alone (Fig. 1 e, left), 70% of recipients treated with 6A6 survived for >200 d after aHSCT.

Although the precise molecular targets of BTLA signaling are still obscure (Gavrieli and Murphy, 2006; Wu et al., 2007), BTLA engagement by HVEM can inhibit T cell proliferation in vitro (Sedy et al., 2005) and promote tolerance induction in vivo (Liu et al., 2009). Therefore, we asked if anti-BTLA treatment alters donor T cell proliferation or IL-2 production in vivo. CFSE-labeled donor splenocytes were transferred into CB6F1 recipients that were treated with PIP, 6A6, or 6F7. Donor T cell proliferation was assessed after aHSCT and, by 3 d after aHSCT, reduced CFSE levels suggested that proliferation had occurred (Fig. 2 e). $CD4^+$ T cells had reduced proliferation after treatment with 6A6 and 6F7 antibodies 3 d after aHSCT (Fig. 2 e, middle), and the total accumulation of donor $CD4^+$ T cells was significantly reduced compared with control ($P < 0.0018$ and $P < 0.0083$; Fig. 2 b). In contrast, $CD8^+$ T cell proliferation and accumulation were not significantly affected by 6A6 treatment ($P < 0.8489$; Fig. 2, a and e, left). As 6F7 treatment leads to partial depletion of cells, we also assessed the level of annexin V binding, which is an indicator of early apoptosis. Mice treated with 6F7, but not PIP or 6A6, showed increased binding of annexin V on $CD4^+$ and $CD8^+$ T cells 7 d after aHSCT, which was not observed on day 3 (Fig. S1 g).

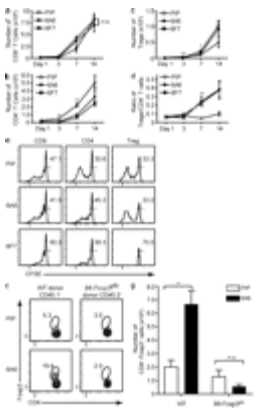

View larger version:
In this page In a new window
Download as PowerPoint Slide

Figure 2.
Anti-BTLA treatment allows for the expansion of preexisting donor-derived T reg cells by inhibiting T eff cell proliferation. (a–e) Lethally irradiated CB6F1 mice received a CFSE-labeled graft from B6.SJL donors and were treated with control antibody PIP (open circles), 6A6 (closed circles), or 6F7 (closed squares; $n = 3$ per group). The number of $CD8^+$ T cells (a), $CD4^+Foxp3^-$ (b), and $CD4^+$ $Foxp3^+$ (c) was calculated from absolute numbers of live splenocytes, and the percentage of the lymphocyte population was assayed by flow cytometry. (d) The ratio of total $CD4^+Foxp3^+/CD4^+Foxp3^-$ cells was calculated at the indicated time points by dividing the number of T reg cells in c by the number of T eff cells in b. (e) CFSE intensity of $CD8^+$, $CD4^+Foxp3^-$, and $CD4^+Foxp3^+$, 3 d after aHSCT with PIP, 6A6, or 6F7 treatment. (f and g) Lethally irradiated CB6F1 mice received aHSCT from B6.SJL mice along with purified $CD4^+$ Foxp3-negative T cells from *B6.Foxp3^{gfp}* mice with control antibody (PIP) or 6A6 ($n = 5$ per group). After 7 d, splenocytes were assayed by flow cytometry to determine the relative frequency of $CD4^+Foxp3^+$ cells among $CD4^+$ cells (f) or the absolute number of $CD4^+Foxp3^+$ T reg cells (g). Statistical comparisons in a–d are between the PIP- and 6A6-treated groups at the indicated time point, and the data are displayed as mean ± SEM. Shown are representative data from two independent experiments with three to five mice per group. P-values of >0.05 are considered not significant (n.s). *, $0.01 < P < 0.05$; **, $0.001 < P < 0.01$.

Although accumulation of $CD4^+$ T cells was lower in 6A6-treated than in PIP-treated mice, the production of IL-2 7 d after aHSCT was not statistically different (Fig. S2, a and b). A small but significant reduction in IFN-γ and IL-4, but not IL-17, production was observed in 6A6-treated mice compared with controls (Fig. S2, a and b). In summary, 6A6 administered at the time of aHSCT reduced the proliferation and accumulation of donor-derived $CD4^+Foxp3^-$ effector T cells (T eff cells) without inducing anergy, inhibiting IL-2 production or causing major alterations in cytokines.

These effects were suggestive of the actions of $CD4^+Foxp3^+$ regulatory T cells (T reg cells) expressing the transcription factor forkhead box P3 (Foxp3; Hori et al., 2003). T reg cells have recently been reported to play a significant role in regulating GVHD (Taylor et al., 2002; Edinger et al., 2003b), and there are ongoing clinical trials aimed directly at the use of T reg cells as an intervention in human GVHD (NCI clinical trial NCT00725062).

To determine whether 6A6 treatment influences T reg cells, we measured the accumulation and proliferation of donor-derived T eff cells after aHSCT (Fig. 2, c and e, right). In PIP-treated recipients that developed GVHD, significantly fewer T reg cell were detected 7 d ($P < 0.0393$) after aHSCT when compared with recipients that received either anti-BTLA treatment 6A6 or 6F7 (Fig. 2 c). Therefore, anti-BTLA treatment inhibits the proliferation of T eff cells yet allows the accumulation of T reg cells, resulting in an increased T reg/T eff cell ratio ($P > 0.0028$; Fig. 2 d). This result is in agreement with the demonstration that T reg cells maintain low levels of BTLA after activation, in contrast to conventional T cells which up-regulate BTLA expression upon activation (Fig. S2 c; Hurchla et al., 2005). Thus, 6A6 treatment increases the numbers and the frequency of donor-derived T reg cells after aHSCT.

6A6 treatment could increase T reg cell frequency either by inducing Foxp3 expression in naive donor $CD4^+$ T cells (Chen et al., 2003) or by causing in vivo expansion of preexisting donor T reg cells relative to T eff cells. To distinguish these alternatives, we used *B6.Foxp3^{gfp}* reporter mice (Fontenot et al., 2005). We performed mixed aHSCT with WT and *Foxp3^{gfp}* mice as donors, using purified GFP-negative cells from *Foxp3^{gfp}* mice to remove preexisting T reg cells from the donor population. In this mixed aHSCT setting, 6A6 treatment similarly decreased the accumulation of T eff cells in both populations, but T reg cells expanded only from preexisting T reg cells (Fig. 2, f and g; and Fig. S2, e and f). Therefore, the donor T reg/T eff cell ratio increased only among the WT donor T cells and not in the *Foxp3^{gfp}* donor T cells, as assessed by intracellular staining for endogenous Foxp3 (Fig. 2 f and Fig. S2 g). In addition, donor-derived $CD4^+$ T cells, which were originally isolated from *B6.Foxp3^{gfp}* mice as negative for GFP expression, remained negative for Foxp3 as assessed by the Foxp3-GFP reporter (Fig. S2 e, right).

To further characterize the conditions necessary for the expansion of T reg cells, we evaluated what effects anti-BTLA treatment had on T reg cells in the steady state and whether the presence of alloantigen or HVEM on host tissue is required. When unmanipulated *B6.Foxp3^{gfp}* mice received 6A6, the frequency of T eff cells, T reg cells, or the resulting ratio did not change (Fig. S3, a–d). Similarly, although syngeneic aHSCT of CB6F1 resulted in a small decrease of T eff cells 7 d after transplant, no major accumulation of T reg cells and no increased T reg/T eff cell ratio was observed (Fig. S3, e–h). When $HVEM^{-/-}$ donors and MHC-mismatched $HVEM^{-/-}$ recipients were used, the ratio of T reg/T eff cells increased by inhibiting the accumulation of T eff cells (Fig. S3, i–l) as observed before (Fig. 2, d and g). Collectively, these results suggest that 6A6 has no effect in the steady state, does not involve HVEM, and requires allostimulation to increase the T reg/T eff cell ratio.

Because BTLA is expressed on both T eff and T reg cells, we tested whether the increased T reg/T eff cell ratio was the result of a decrease in T eff cell expansion, an increased proliferation of T reg cells, or both by performing a mixed aHSCT using congenically marked WT $BTLA^{+/+}$ and $BTLA^{-/-}$ donors. In this setting, the frequency of T reg cell within the $CD4^+BTLA^{-/-}$ population did not change in the presence of 6A6 (7.9 ± 2 vs. 7.3 ± 2%; Fig. 3, a and c), whereas the T reg cell frequency within the $CD4^+$ WT population increased more than threefold in the presence of 6A6 (48 ± 10 vs. 14.4 ± 5.5%; Fig. 3, a and b).

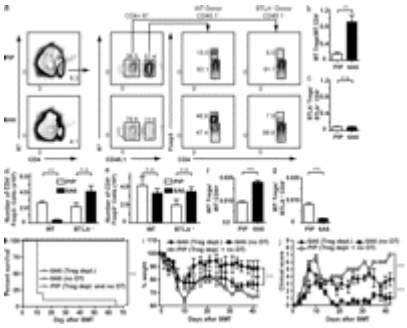

View larger version:
In this page In a new window
Download as PowerPoint Slide

Figure 3.

Direct engagement of BTLA on T eff cells leads to an increased frequency of CD4$^+$Foxp3$^+$ cells. Lethally irradiated CB6F1 mice received a 1:1 mixed aHSCT with WT-B6.SJL and B6 BTLA$^{-/-}$ donor cells (a–e) with either control antibody (PIP) or 6A6 (*n* = 5 per group). After 7 d, splenocytes were analyzed by flow cytometry. (a) Shown are FACS plots to identify donor cells as H-2K^{d-} and CD4$^+$ (left). Intracellular Foxp3 was detected among CD4$^+$ T cells (right) gated on WT-B6.SJL (CD4$^+$CD45.1$^+$ H-2K^{d-}) or B6 BTLA$^{+/+}$ (CD4$^+$CD45.1$^-$ H-2K^{d-}) donor cell populations as indicated. Numbers represent the percentage of cells within the indicated gates. The ratios of the number of WT T reg/WT T eff cells (b) and KO T reg/KO T eff cells (c) are shown, as well as the total number of T eff cells (d) and T reg cells (e) from the indicated donors after treatment with control antibody (PIP, open bars) or 6A6 (closed bars). (f and g) Lethally irradiated BALB/c mice received a 1:1 mixture of purified WT-B6.SJL and BTLA$^{-/-}$ CD4$^+$ cells and T reg cells from *B6.Foxp3^{gfp}* mice, with either control antibody PIP or 6A6 (*n* = 3–4 per group). After 7 d, splenocytes were analyzed by flow cytometry to determine the ratio of WT T reg/WT T eff cells (f) or WT T reg/BTLA$^{-/-}$ T eff cells (g). Data are displayed as mean ± SEM. Shown are representative data from two independent experiments. (h–j) Recipient BALB/c mice received TCD-BM and splenocytes from T reg cell ablated or unmanipulated Foxp3^{DTR} mice and PIP or 6A6 as indicated. Survival curves (h), weight curves (i), and clinical scores (j) are shown for 6A6-treated mice that received a graft from either untreated (no DT) Foxp3^{DTR} donors (dashed line or filled squares; *n* = 5) or a graft from DT-treated (T reg depl.) Foxp3^{DTR} donors (solid line or filled circles; *n* = 5) and PIP-treated mice that received a graft from DT-treated or untreated (T reg depl. and no DT) Foxp3^{DTR} donors (dotted line or open circles; *n* = 10). Data are shown as mean ± SD from two independent experiments. P-values of >0.05 are considered not significant (n.s). **, 0.001 < P < 0.01; ***, P < 0.001.

Importantly, 6A6 treatment decreased T eff cell numbers more than fivefold from 2.6 × 10^5 ± 4.6 × 10^4 cells in the control group to 3.9 × 10^4 ± 1.4 × 10^4 (P < 0.0001; Fig. 3 d), indicating that WT-BTLA$^{+/+}$ T eff cells are the main target of the anti-BTLA treatment. WT and BTLA$^{-/-}$ T reg cells do not expand significantly in the presence of BTLA$^{-/-}$ T eff cells (Fig. 3 e), confirming our observation that T reg cells expand only when T eff cells express BTLA and are inhibited by 6A6. To exclude any indirect effects on host tissues, we cotransferred purified populations of WT T reg cells together with WT or BTLA$^{-/-}$ T eff cells into BALB/c recipients, which express an allele of BTLA not recognized by 6A6 (Fig. 3, f and g; and Fig. S4; Hurchla et al., 2005). The WT T reg/WT T eff cell ratio increased after 6A6 treatement (P < 0.0004; Fig. 3 f) as observed before (Fig. 2 g and Fig. 3 b). In contrast, when BTLA$^{-/-}$ T eff cells were present the WT T reg/BTLA$^{-/-}$ T eff cell ratio did not increase (Fig. 3 g), indicating that the expansion of T reg cells is caused by 6A6 reducing the expansion of T eff cells. In this setting, the WT T reg/BTLA$^{-/-}$ T eff cell ratio even decreased (Fig. 3 g and Fig. S4 i), suggesting that low expression levels of BTLA on T reg cells inhibits their expansion when proliferation of BTLA$^{-/-}$ T eff cells is not restricted.

To ask whether the inhibition of T eff cells had an effect on GVHD in the absence of T reg cells, we used C57BL/6 Foxp3^{DTR} mice as donors in the lethal model of GVHD. Pretreatment with diphtheria toxin reduced T reg cells by >95% in Foxp3^{DTR} donors. 90% of control animals died within 14 d of aHSCT, irrespective of whether or not the BM graft contained T reg cells (Fig. 3 h). All mice that were treated with the 6A6 antibody survived beyond day 70 (Fig. 3 h). Mice that received a graft with T reg cells and 6A6 eventually recovered to ~90% of their starting weight (Fig. 3 i) and developed low-grade GVHD with scores ranging from 1 to 3, as seen before (Fig. 1 e). Mice that received a T reg cell–depleted graft and 6A6, however, recovered only 70–

80% of their starting weight and had more severe GVHD scores ranging from 3 to 5 (Fig. 3 j). These data highlight that forced inhibition of T eff cells through BTLA (Fig. 3 d) is sufficient to prevent lethality. Nonetheless, the relative expansion of T reg cells (Fig. 3, b and f) bears biological significance, as they are required to protect the host from clinical GVHD (Fig. 3, i and j).

Because engagement of BTLA by 6A6 inhibited T eff cell proliferation, we wondered whether this treatment allowed for antigen-specific responses to tumors and pathogens. First, we examined whether graft-versus-tumor (GVT) activity was maintained after 6A6 treatment (Fig. 4, a–c). We used a model of minimal residual disease after aHSCT that utilizes bioluminescence imaging (BLI) of luciferase-expressing A20-Luc leukemia cells (H-2^d) in vivo (Edinger et al., 2003a). In this model, GVT activity requires cytolytic activity of T cells to control the tumor (Edinger et al., 2003b). Transplantation of A20-Luc leukemia cells with TCD-BM alone resulted in progressive tumor growth (Fig. 4, a and b). In mice that had received a T cell–containing graft with or without the 6A6 antibody, however, tumor was never detectable by BLI, suggesting that GVT effects were intact. Although all control mice died before day 45 of severe GVHD, 90% of 6A6-treated mice survived beyond day 90 (Fig. 4 c). To exclude any antibody-mediated anti-tumor effects, we confirmed that the 6A6 antibody does not bind to A20 cells, which was expected because of their BALB/c origin (Fig. S2 d). To document initial tumor engraftment, we quantified the total tumor number A20-GFP cells in the BM by flow cytometry 7 d after aHSCT (Fig. S3 m).

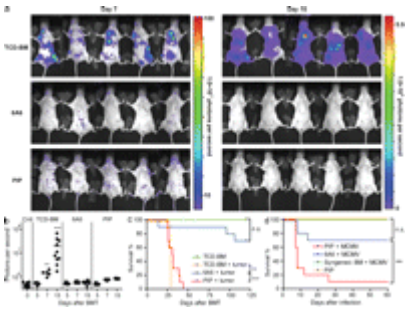

View larger version:
In this page In a new window
Download as PowerPoint Slide

Figure 4.
Anti-BTLA treatment does not lead to global immunosuppression. (a) Representative images of A20-Luc tumor cell localization 7 d (left) and 15 d (right) after aHSCT in lethally irradiated BALB/c mice that had received A20-Luc lymphoma cells with TCD-BM alone (*n* = 10) or together with splenocytes from C57BL/6 mice and control antibody PIP (*n* = 10) or 6A6 (*n* = 10). (b) Shown are units of photons per second for individual animals from panel a for days 5 (*n* = 5), 7 (*n* = 5), and 15 (*n* = 10) after aHSCT, as well as unmanipulated BALB/c mice (day 0, *n* = 12) for comparison. Asterisks indicate statistically significant differences between TCD-BM and 6A6 groups. Shown are cumulative data from two independent experiments, with each point representing the BLI signal from an individual mouse. Horizontal lines represent the mean BLI signal. Vertical lines serve to separate experimental groups. (c) Survival data of mice from a and from mice that received TCD-BM alone without tumor for comparison. Shown are cumulative data from two independent experiments. (d) CB6F1 BMC and splenocytes from syngeneic (green line; *n* = 10) or C57BL/6 donors and antibodies PIP (red line; *n* = 10) or 6A6 (blue line; *n* = 10) were infected with MCMV 4 wk after aHSCT and were monitored for survival. PIP-treated uninfected mice (orange line, n = 10) served as controls. Shown are cumulative data from two independent experiments. Data are shown as mean ± SD from two independent experiments. P-values of >0.05 are considered not significant (n.s). **, 0.001 < P < 0.01; ***, P < 0.001.

We next examined immune responses to murine CMV (MCMV; Nguyen et al., 2008) 4 wk after aHSCT. All animals that had undergone syngeneic aHSCT survived for >60 d after infection (Fig. 4 d). Of the mice in the allogeneic group that had received the PIP antibody, 70% died within 10 d of infection compared with 20% of the 6A6-treated mice. Thus, although 6A6 treatment prevents GVHD, it allows for resistance to MCMV, unlike PIP-treated control recipients.

To test the immune response against bacterial infection, animals were infected with the intracellular bacterium *Listeria monocytogenes*. 3 d after infection, animals that had received the PIP antibody had either higher (P = 0.0005 for liver and P = 0.1816 for spleen) or lower *L. monocytogenes* organ burdens (P = 0.0227 for liver and P = 0.0059 for spleen; Fig. S3, n–p), as has been described previously (Miura et al., 2000). In contrast, anti-BTLA–treated mice controlled infection similarly to both control groups, indicating an intact innate immune response (Fig. S3, n–p). These preliminary results suggest that 6A6-treated mice were similarly resistant to *L. monocytogenes* infection to unmanipulated mice.

In summary, this study demonstrates that the anti-BTLA antibody 6A6 administered at the time of aHSCT prevents GVHD without the need for additional immunosuppressive therapy. The mechanism of action is through direct engagement of BTLA on donor T cells, selectively inhibiting T eff cells and allowing the relative expansion of naturally occurring T reg cells. Once established, this new balance of T eff cells is sufficient to prevent GVHD permanently while allowing for intact responses to viral and bacterial pathogens, as well as GVT effects. Thus, BTLA may represent a novel therapeutic target in prevention of human GVHD. Increasing the safety of aHSCT could potentially allow its application more widely as a tolerogenic therapy in treatment of autoimmune disorders or solid organ transplantation, for which it is currently performed only experimentally (Sykes and Nikolic, 2005; Kawai et al., 2008).

MATERIALS AND METHODS

Back to Top

Mice and BM transplantation.

B6.SJL-Ptprca Pep3b/BoyJ (B6.SJL), C57BL/6, and C57BL/6 × BALB/c F1 (CB6F1) mice were obtained from The Jackson Laboratory or bred in our facility. *BTLA*$^{-/-}$ (Watanabe et al., 2003), *Hvem*$^{-/-}$ (Wang et al., 2005), *Foxp3*^{gfp} (Fontenot et al., 2005), and *Foxp3*^{DTR} (Kim et al., 2007) mice were backcrossed to C57BL/6 for at least nine generations. HVEM$^{-/-}$ H2-K$^{b/d}$ or H2-K$^{d/d}$ were obtained by crossing HVEM$^{-/-}$ mice on a B6 (H2-K$^{b/b}$) background to BALB/c (H2-K$^{d/d}$) mice. The resulting HVEM$^{+/-}$ H2-K$^{d/b}$ F1 mice were intercrossed to obtain HVEM$^{-/-}$ H2-K$^{b/d}$ or H2-K$^{d/d}$ F2 recipients. Mice were 12–18 wk old and sex matched for all experiments. Mice were bred and maintained in our specific pathogen–free animal facility according to institutional guidelines with protocols approved by the Animal Studies Committee of Washington University.

Cell transplantation and assessment of GVHD.

Mice received transplants according to a standard protocol as previously described (Stelljes et al., 2008). In brief, BMCs were harvested by flushing tibia and femurs of donor mice. For the nonlethal parent-into-F1 model of GVHD, CB6F1 (H-2$^{b/d}$) recipients were lethally irradiated with 9 Gy total body irradiation using a ^{137}Cs source at a dose rate of ~70 cGy/min and reconstituted with 2 × 10^7 BMCs and 10^7 splenocytes from syngeneic (H-2$^{b/d}$) or parental C57BL/6 donors (H-2^b). For the lethal model of GVHD, BALB/c (H-2^d) recipients were lethally irradiated with 8 Gy total body irradiation using a ^{137}Cs source at a dose rate of ~70 cGy/min and reconstituted with 2 × 10^7 TCD-BM alone or an additional 10^7 splenocytes from allogeneic C57BL/6 donors (H-2^b). To obtain TCD-BM, cells were depleted of CD4$^+$ and CD8$^+$ cells by magnetic depletion (Miltenyi Biotec) according to the manufacturer's recommendation. In experiments where a T reg cell–depleted graft from *Foxp3*^{DTR} donors was used, recipients received an intraperitoneal injection of 20 µg diphtheria toxin on the day of BMT. GVHD was monitored by calculating the loss in total body weight. Body weights were measured before transplantation and three times a week after transplantation. Clinical GVHD intensity was scored by assessing weight loss, posture, activity, fur texture, and skin integrity (Cooke et al., 1996). Histopathologic analyses of the bowel were performed on hematoxylin and eosin–stained tissue.

Administration of antibody.

In some experiments, mice received at the time of aHSCT, unless otherwise noted, a single intraperitoneal injection of 10–20 µg/g body weight of anti-BTLA antibodies 6A6 and 6F7, whose properties we have previously published in detail (Hurchla et al., 2005). In brief, the IgG hamster monoclonal antibody 6A6 is specific for the C57BL/6 allele of BTLA and does not deplete BTLA-expressing cells in vivo (Hurchla et al., 2007; Lepenies et al., 2007). The IgG1κ mouse monoclonal anti-BTLA antibody 6F7 recognizes all known alleles of BTLA (Hurchla et al., 2005) and has been shown to deplete BTLA-expressing cells in vivo. The IgG1 hamster monoclonal anti-GST antibody PIP (Gronowski et al., 1999) was used as an isotype control.

Cell purification and depletion.

To obtain purified populations of $CD4^+$ $Foxp3^{gfp}$-negative cells or $CD4^+$ $Foxp3^{gfp}$-positive cells in the indicated experiments, $Foxp3^{gfp}$ splenocytes were stained with $CD4^+$ and the desired population was purified by cell sorting on the MoFlo cytometer (Dako). Purification of C57BL/6 $CD4^+$ and $BTLA^{-/-}$ $CD4^+$ cells was obtained from splenocytes that were depleted of $CD8^+$ and $B220^+$ cells by magnetic depletion (Miltenyi Biotech) according to the manufacturer's recommendation. *Foxp3*^{DTR} mice received intraperitoneal injections for 2 d of 20 µg diphtheria toxin per day before harvesting BM and splenocytes for aHSCT.

CFSE labeling and flow cytometry.

Cells were labeled with CFSE (Sigma-Aldrich) by being incubated for 8 min at 25°C with 1 µM CFSE at a density of 40×10^6 cells per ml in PBS. Labeling was quenched by incubation of cells for 1 min with an equal volume of FCS and cells were washed twice with media containing 10% (vol/vol) FCS. 50×10^6 total cells per mouse were injected intravenously. Single cell suspensions from spleens were analyzed by flow cytometry using the following antibodies for detection: K^d-FITC (SF1-1.1), CD4-PECy7, APC, PerCPCy5.5, v450 (RM4-5) and PE (GK1.5), CD8-v450 (53–6.7), anti–Armenian and Syrian hamster IgG cocktail-PE, CD19-APC (1D3), and annexin V–PE (BD); and CD45.1-PECy7 and APC (A20), CD45.2-APC-eFluor780 (104), CD8-APC Alexa Fluor 750 (53–6.7), CD4-APC Alexa Fluor 750 (RM4-5), BTLA-bio (6F7), and SA-v450 (eBioscience). Intracellular Foxp3 was detected using the Mouse Regulatory T cell staining kit (eBioscience) with Foxp3-PE or APC (FJK-16s). For intracellular cytokine staining, splenocytes were first restimulated with PMA/ionomycin for 4 h and were stained with antibodies to surface markers, followed by fixation with 2% formaldehyde for 15 min at room temperature. Cells were then washed once in 0.05% saponin and stained with anti-cytokine antibodies (anti-IL-17 FITC, IL-2 PE, IFN-γ PE-Cy7, and IL-4 APC) in 0.5% saponin. All flow cytometry data were collected on a FACSCanto II (BD) and were analyzed with FlowJo software (Tree Star, Inc.).

Tumor model and assessment of GVT effects.

As a tumor challenge, 2×10^4 A20-Luc or A20-GFP where administered intravenously together with the donor graft as indicated. Imaging was done as previously described (Rehemtulla et al., 2000; Edinger et al., 2003a). In brief, D-Luciferin (Biosynth AG) was reconstituted in 0.9% sodium chloride (Baxter) to a concentration of 15 mg/ml, filtered (0.2 µm), and frozen at −80°C until use. Mice were given intraperitoneal injections at a dose of 150 mg/kg and allowed to remain active in the cage for 5 min to allow circulation of luciferin. Using the Xenogen IVIS 200 system (Caliper Life Sciences) with attached anesthesia chamber, the animals were then anesthetized with 2% isoflurane for 5 min and subsequently transferred to the imaging chamber where they continued to receive a regulated flow of isoflurane through the manifold's nose cones. The Living Image software program (Caliper Life Sciences) was used to obtain and analyze data. For all experiments, a 60-s exposure time was used. To detect A20-GFP in the BM, single cell suspensions from both femurs were analyzed by flow cytometry using the antibody CD19-APC (1D3; BD). Cells that expressed high levels of CD19 and GFP were considered to be A20-GFP cells.

Cell lines.

The BALB/c B cell lymphoma cell line A20 was obtained from the American Type Culture Collection. To generate luciferase-expressing A20 cells (A20-Luc), a 1995-bp HindIII–BamHI fragment from pGL4.23 [luc2/minP] vector (Promega) containing a minimal promoter, a Luc2 coding sequence, and a SV40 late poly (A) signal was cloned into the HindIII and BamHI sites of the pcDNA3.1$^+$ mammalian expression vector (Invitrogen) to generate pcDNA3.1$^+$-Luc2. For stable transfections, 10 × 10^6 A20 cells/ml in complete IMDM supplemented with 10% fetal calf serum and with 30 µg/ml PvuI-linearized pcDNA3.1$^+$-Luc2 were electroporated at room temperature in 0.4-ml aliquots in 0.4-cm cuvettes in a Gene Pulser (Bio-Rad Laboratories) at 240 V and 960 mF. After electroporation, cells were cultured for 24 h in IMDM supplemented with 10% fetal calf serum and then selected in the presence of 800 µg/ml geneticin. To generate GFP-expressing A20 cells, a retroviral reporter vector (Ranganath et al., 1998) was used that contains the coding sequence of herpes simplex virus 1 thymidine kinase, followed by an internal ribosomal entry site and GFP (HSV1-TK-IRES-GFP-RV). The retroviral vector was packaged in Phoenix A cells. Before infection, the A20 cell line was stimulated with 5 µg/ml LPS (Sigma-Aldrich) for 24 h. For infection, cells were cultured in retroviral supernatant supplemented with 8 µg/ml polybrene (Sigma-Aldrich) and 5 µg/ml LPS and spun at 930 rcf for 1 h before being cultured at 37°C for 24 h. 72 h after infection, cells were sorted for high GFP expression on a FACSAria II (BD) and stable GFP expression of >95% was confirmed several times by flow cytometry at later time points.

Models of infectious disease.

For MCMV infection, mice were infected with Smith strain MCMV 4 wk after aHSCT. Virus preparation and administration was performed as described previously (Krug et al., 2004). In brief, a salivary gland stock of MCMV was prepared from BALB/c mice, with a titer of 6.75 × 10^6 PFU/ml. Mice were infected intraperitoneally with a low dose of virus (10^4 PFU/mouse) and then monitored for survival. For *L. monocytogenes* infection, mice were infected intravenously with 2.5 × 10^4 *L. monocytogenes* (strain EGD; gift from E.R. Unanue, Washington University School of Medicine, St. Louis, MO) 3 mo after aHSCT. To determine organ *L. monocytogenes* burden at day 3 after infection, spleens and livers were homogenized in PBS plus 0.05% Triton X-100. Serial dilutions of homogenate were plated on brain heart infusion agar, and bacterial CFUs were assessed after overnight growth at 37°C. Small portions of spleen and liver were also fixed in 10% formalin and stained with hematoxylin and eosin.

Statistical analysis.

A Student's unpaired two-tailed *t* test with a 95% confidence interval was used for statistical analyses of body weight data, clinical scores, and cell numbers. For analyses of survival data the log-rank test was used. A Mann-Whitney unpaired two-tailed Student's *t* test with a 95% confidence interval was used for statistical analyses of bioluminescence data in Fig. 4. Statistical analyses were done using Prism 4 (GraphPad Software, Inc.). FACS data are expressed as means ± SEM. All other data are presented as means ± SD. All experiments have been repeated at least once with three to five mice per group, unless stated otherwise.

Online supplemental material.

Fig. S1 demonstrates that BTLA expression by recipient tissue does not promote GVHD and 6A6 antibody does not deplete lymphocytes. Fig. S2 shows that 6A6 treatment does not lead to donor T eff cell anergy and expands preexisting T reg cells. Fig. S3 shows that 6A6 inhibition of T eff cells and expansion of T reg cells requires allostimulation but not HVEM expression by donor or host. Fig. S4 shows that 6A6 alters the T reg cell/effector CD4$^+$ T cell ratio by directly inhibiting BTLA-expressing T cells. Online supplemental material is available at http://www.jem.org/cgi/content/full/jem.20102017/DC1.

ACKNOWLEDGMENTS Back to Top

The authors thank T.S. Stappenbeck for help with histology and T.R. Bradstreet for help with *L. monocytogenes* experiments.

K.M. Murphy is a Howard Hughes Medical Institute investigator. This work was supported in part by the National Institutes of Health (AI076427-02) and the Department of Defense (W81XWH-09-1-0185). J.C. Albring was supported by a German Research Foundation Grant (AL 1038/1-1). M.M. Sandau was supported by a Ruth L. Kirschstein National Reasearch Service Award (NIH # 5F32AI080062-02) and by the Irvington Institute Fellowship Program of the Cancer Research Institute. B.T. Edelson was supported by the Burroughs Wellcome Fund Career Award for Medical Scientists.

The authors have no conflicting financial interests.

FOOTNOTES Back to Top

Abbreviations used:

aHSCT	allogeneic hematopoietic stem cell transplantation
BLI	bioluminescence imaging
BMC	BM cell
BTLA	B and T lymphocyte associated
Foxp3	forkhead box P3
GVHD	graft-versus-host disease
GVT	graft versus tumor
HVEM	herpesvirus entry mediator
MCMV	murine CMV
TCD-BM	T cell–depleted BMC
T eff cell	$CD4^+Foxp3^-$ effector T cell
T reg cell	$CD4^+Foxp3^+$ regulatory T cell

Submitted: 24 September 2010

Accepted: 29 October 2010

REFERENCES Back to Top

Blazar, B.R., B.M. Carreno, A. Panoskaltsis-Mortari, L. Carter, Y. Iwai, H. Yagita, H. Nishimura, P.A. Taylor. 2003. Blockade of programmed death-1 engagement accelerates graft-versus-host disease lethality by an IFN-gamma-dependent mechanism. *J. Immunol.* 171:1272–1277. Abstract/FREE Full Text

Chen, W., W. Jin, N. Hardegen, K.J. Lei, L. Li, N. Marinos, G. McGrady, S.M. Wahl. 2003. Conversion of peripheral $CD4^+CD25^-$ naive T cells to $CD4^+CD25^+$ regulatory T cells by TGF-β induction of transcription factor Foxp3. *J. Exp. Med.* 198:1875–1886. doi:10.1084/jem.20030152 Abstract/FREE Full Text

Cooke, K.R., L. Kobzik, T.R. Martin, J. Brewer, J. Delmonte Jr, J.M. Crawford, J.L.M. Ferrara. 1996. An experimental model of idiopathic pneumonia syndrome after bone marrow transplantation: I. The roles of minor H antigens and endotoxin. *Blood.* 88:3230–3239. Abstract/FREE Full Text

Copelan, E.A.2006. Hematopoietic stem-cell transplantation. *N. Engl. J. Med.* 354:1813–1826. doi:10.1056/NEJMra052638 CrossRef Medline

Edinger, M., Y.A. Cao, M.R. Verneris, M.H. Bachmann, C.H. Contag, R.S. Negrin. 2003a. Revealing lymphoma growth and the efficacy of immune cell therapies using in vivo bioluminescence imaging. *Blood.* 101:640–648. doi:10.1182/blood-2002-06-1751 Abstract/FREE Full Text

Edinger, M., P. Hoffmann, J. Ermann, K. Drago, C.G. Fathman, S. Strober, R.S. Negrin. 2003b. CD4+CD25+ regulatory T cells preserve graft-versus-tumor activity while inhibiting graft-versus-host disease after bone marrow transplantation. *Nat. Med.* 9:1144–1150. doi:10.1038/nm915 CrossRef Medline

Fontenot, J.D., J.P. Rasmussen, L.M. Williams, J.L. Dooley, A.G. Farr, A.Y. Rudensky. 2005. Regulatory T cell lineage specification by the forkhead transcription factor foxp3. *Immunity.* 22:329–341. doi:10.1016/j.immuni.2005.01.016 CrossRef Medline

Gavrieli, M., K.M. Murphy. 2006. Association of Grb-2 and PI3K p85 with phosphotyrosile peptides derived from BTLA. *Biochem. Biophys. Res. Commun.* 345:1440–1445. doi:10.1016/j.bbrc.2006.05.036 CrossRef Medline

Gronowski, A.M., D.M. Hilbert, K.C.F. Sheehan, G. Garotta, R.D. Schreiber. 1999. Baculovirus stimulates antiviral effects in mammalian cells. *J. Virol.* 73:9944–9951. Abstract/FREE Full Text

Hori, S., T. Nomura, S. Sakaguchi. 2003. Control of regulatory T cell development by the transcription factor Foxp3. *Science.* 299:1057–1061. doi:10.1126/science.1079490 Abstract/FREE Full Text

Hurchla, M.A., J.R. Sedy, M. Gavrieli, M. Gavrielli, C.G. Drake, T.L. Murphy, K.M. Murphy. 2005. B and T lymphocyte attenuator exhibits structural and expression polymorphisms and is highly induced in anergic CD4+ T cells. *J. Immunol.* 174:3377–3385. Abstract/FREE Full Text

Hurchla, M.A., J.R. Sedy, K.M. Murphy. 2007. Unexpected role of B and T lymphocyte attenuator in sustaining cell survival during chronic allostimulation. *J. Immunol.* 178:6073–6082. Abstract/FREE Full Text

Kawai, T., A.B. Cosimi, T.R. Spitzer, N. Tolkoff-Rubin, M. Suthanthiran, S.L. Saidman, J. Shaffer, F.I. Preffer, R.C. Ding, V. Sharma, et al. 2008. HLA-mismatched renal transplantation without maintenance immunosuppression. *N. Engl. J. Med.* 358:353–361. doi:10.1056/NEJMoa071074 CrossRef Medline

Kim, J.M., J.P. Rasmussen, A.Y. Rudensky. 2007. Regulatory T cells prevent catastrophic autoimmunity throughout the lifespan of mice. *Nat. Immunol.* 8:191–197. doi:10.1038/ni1428 CrossRef Medline

Krug, A., A.R. French, W. Barchet, J.A.A. Fischer, A. Dzionek, J.T. Pingel, M.M. Orihuela, S. Akira, W.M. Yokoyama, M. Colonna. 2004. TLR9-dependent recognition of MCMV by IPC and DC generates coordinated cytokine responses that activate antiviral NK cell function. *Immunity.* 21:107–119. doi:10.1016/j.immuni.2004.06.007 CrossRef Medline

Lepenies, B., K. Pfeffer, M.A. Hurchla, T.L. Murphy, K.M. Murphy, J. Oetzel, B. Fleischer, T. Jacobs. 2007. Ligation of B and T lymphocyte attenuator prevents the genesis of experimental cerebral malaria. *J. Immunol.* 179:4093–4100. Abstract/FREE Full Text

Liu, X.K., M. Alexiou, N. Martin-Orozco, Y. Chung, R.I. Nurieva, L. Ma, Q. Tian, G. Kollias, S. Lu, D. Graf, C. Dong. 2009. Cutting edge: A critical role of B and T lymphocyte attenuator in peripheral T cell tolerance induction. *J. Immunol.* 182:4516–4520. doi:10.4049/jimmunol.0803161 Abstract/FREE Full Text

Lu, Y., S. Sakamaki, H. Kuroda, T. Kusakabe, Y. Konuma, T. Akiyama, A. Fujimi, N. Takemoto, K. Nishiie, T. Matsunaga, et al. 2001. Prevention of lethal acute graft-versus-host disease in mice by oral administration of T helper 1 inhibitor, TAK-603. *Blood.* 97:1123–1130. doi:10.1182/blood.V97.4.1123 Abstract/FREE Full Text

McSweeney, P.A., D. Niederwieser, J.A. Shizuru, B.M. Sandmaier, A.J. Molina, D.G. Maloney, T.R. Chauncey, T.A. Gooley, U. Hegenbart, R.A. Nash, et al. 2001. Hematopoietic cell transplantation in older patients with hematologic malignancies: replacing high-dose cytotoxic therapy with graft-versus-tumor effects. *Blood.* 97:3390–3400. doi:10.1182/blood.V97.11.3390 Abstract/FREE Full Text

Miura, T., D. Mizuki, S. Sasaki, S. Hasegawa, H. Sashinami, A. Nakane. 2000. Host resistance to *Listeria monocytogenes* infection is enhanced but resistance to *Staphylococcus aureus* infection is reduced in acute graft-

versus-host disease in mice. *Infect. Immun.* 68:4340–4343. doi:10.1128/IAI.68.7.4340-4343.2000 Abstract/FREE Full Text

Nguyen, V.H., S. Shashidhar, D.S. Chang, L. Ho, N. Kambham, M. Bachmann, J.M. Brown, R.S. Negrin. 2008. The impact of regulatory T cells on T-cell immunity following hematopoietic cell transplantation. *Blood.* 111:945–953. doi:10.1182/blood-2007-07-103895 Abstract/FREE Full Text

Petersdorf, E.W., C. Anasetti, P.J. Martin, T. Gooley, J. Radich, M. Malkki, A. Woolfrey, A. Smith, E. Mickelson, J.A. Hansen. 2004. Limits of HLA mismatching in unrelated hematopoietic cell transplantation. *Blood.* 104:2976–2980. doi:10.1182/blood-2004-04-1674 Abstract/FREE Full Text

Ranganath, S., W. Ouyang, D. Bhattarcharya, W.C. Sha, A. Grupe, G. Peltz, K.M. Murphy. 1998. GATA-3-dependent enhancer activity in IL-4 gene regulation. *J. Immunol.* 161:3822–3826. Abstract/FREE Full Text

Rehemtulla, A., L.D. Stegman, S.J. Cardozo, S. Gupta, D.E. Hall, C.H. Contag, B.D. Ross. 2000. Rapid and quantitative assessment of cancer treatment response using in vivo bioluminescence imaging. *Neoplasia.* 2:491–495. doi:10.1038/sj.neo.7900121 CrossRef Medline

Sedy, J.R., M. Gavrieli, K.G. Potter, M.A. Hurchla, R.C. Lindsley, K. Hildner, S. Scheu, K. Pfeffer, C.F. Ware, T.L. Murphy, K.M. Murphy. 2005. B and T lymphocyte attenuator regulates T cell activation through interaction with herpesvirus entry mediator. *Nat. Immunol.* 6:90–98. doi:10.1038/ni1144 CrossRef Medline

Steinberg, M.W., O. Turovskaya, R.B. Shaikh, G. Kim, D.F. McCole, K. Pfeffer, K.M. Murphy, C.F. Ware, M. Kronenberg. 2008. A crucial role for HVEM and BTLA in preventing intestinal inflammation. *J. Exp. Med.* 205:1463–1476. doi:10.1084/jem.20071160 Abstract/FREE Full Text

Stelljes, M., S. Hermann, J. Albring, G. Köhler, M. Löffler, C. Franzius, C. Poremba, V. Schlösser, S. Volkmann, C. Opitz, et al. 2008. Clinical molecular imaging in intestinal graft-versus-host disease: mapping of disease activity, prediction, and monitoring of treatment efficiency by positron emission tomography. *Blood.* 111:2909–2918. doi:10.1182/blood-2007-10-119164 Abstract/FREE Full Text

Sykes, M., B. Nikolic. 2005. Treatment of severe autoimmune disease by stem-cell transplantation. *Nature.* 435:620–627. doi:10.1038/nature03728 CrossRef Medline

Tamada, K., K. Shimozaki, A.I. Chapoval, G. Zhu, G. Sica, D. Flies, T. Boone, H. Hsu, Y.X. Fu, S. Nagata, et al. 2000. Modulation of T-cell-mediated immunity in tumor and graft-versus-host disease models through the LIGHT co-stimulatory pathway. *Nat. Med.* 6:283–289. doi:10.1038/73136 CrossRef Medline

Taylor, P.A., C.J. Lees, B.R. Blazar. 2002. The infusion of ex vivo activated and expanded CD4(+)CD25(+) immune regulatory cells inhibits graft-versus-host disease lethality. *Blood.* 99:3493–3499. doi:10.1182/blood.V99.10.3493 Abstract/FREE Full Text

Truong, W., W.W. Hancock, J.C. Plester, S. Merani, D.C. Rayner, G. Thangavelu, K.M. Murphy, C.C. Anderson, A.M. Shapiro. 2009. BTLA targeting modulates lymphocyte phenotype, function, and numbers and attenuates disease in nonobese diabetic mice. *J. Leukoc. Biol.* 86:41–51. doi:10.1189/jlb.1107753 Abstract/FREE Full Text

Wang, Y., S.K. Subudhi, R.A. Anders, J. Lo, Y. Sun, S. Blink, Y. Wang, J. Wang, X. Liu, K. Mink, et al. 2005. The role of herpesvirus entry mediator as a negative regulator of T cell-mediated responses. *J. Clin. Invest.* 115:711–717. CrossRef Medline

Watanabe, N., M. Gavrieli, J.R. Sedy, J. Yang, F. Fallarino, S.K. Loftin, M.A. Hurchla, N. Zimmerman, J. Sim, X. Zang, et al. 2003. BTLA is a lymphocyte inhibitory receptor with similarities to CTLA-4 and PD-1. *Nat. Immunol.* 4:670–679. doi:10.1038/ni944 CrossRef Medline

Wu, T.H., Y. Zhen, C. Zeng, H.F. Yi, Y. Zhao. 2007. B and T lymphocyte attenuator interacts with CD3zeta and inhibits tyrosine phosphorylation of TCRzeta complex during T-cell activation. *Immunol. Cell Biol.* 85:590–595. doi:10.1038/sj.icb.7100087 Medline

Xu, Y., A.S. Flies, D.B. Flies, G. Zhu, S. Anand, S.J. Flies, H. Xu, R.A. Anders, W.W. Hancock, L. Chen, K. Tamada. 2007. Selective targeting of the LIGHT-HVEM costimulatory system for the treatment of graft-versus-host disease. *Blood.* 109:4097–4104. doi:10.1182/blood-2006-09-047332 Abstract/FREE Full Text

The Journal of Immunology

Unexpected Role of B and T Lymphocyte Attenuator in Sustaining Cell Survival during Chronic Allostimulation

Michelle A. Hurchla, John R. Sedy and Kenneth M. Murphy

J. Immunol. 2007;178;6073-6082
http://www.jimmunol.org/cgi/content/full/178/10/6073

The Journal of Immunology is published twice each month by The American Association of Immunologists, Inc., 9650 Rockville Pike, Bethesda, MD 20814-3994.

Print ISSN: 0022-1767 Online ISSN: 1550-6606.

Unexpected Role of B and T Lymphocyte Attenuator in Sustaining Cell Survival during Chronic Allostimulation

Michelle A. Hurchla,* John R. Sedy,* and Kenneth M. Murphy[1]*†

B and T lymphocyte attenuator (BTLA; CD272) can deliver inhibitory signals to B and T cells upon binding its ligand herpesvirus entry mediator. Because CD28, CTLA-4, programmed death-1, and ICOS regulate the development of acute graft-vs-host disease (GVHD), we wished to assess if BTLA also played a role in this T cell-mediated response. In the nonirradiated parental-into-F_1 model of acute GVHD, $BTLA^{+/+}$ and $BTLA^{-/-}$ donor lymphocytes showed equivalent engraftment and expansion during the first week of the alloresponse. Unexpectedly, $BTLA^{-/-}$ donor T cells failed to sustain GVHD, showing a decline in surviving donor cell numbers beginning at day 9 and greatly reduced by day 11. Similarly, inhibition of BTLA-herpesvirus entry mediator engagement by in vivo administration of a blocking anti-BTLA Ab also caused reduced survival of donor cells. Microarray analysis revealed several genes that were differentially expressed by $BTLA^{-/-}$ and $BTLA^{+/+}$ donor $CD4^+$ T cells preceding the decline in $BTLA^{-/-}$ donor T cells. Several genes influencing Th cell polarization were differentially expressed by $BTLA^{+/+}$ and $BTLA^{-/-}$ donor cells. Additionally, the re-expression of the IL-7Rα subunit that occurs in $BTLA^{+/+}$ donor cells after 1 wk of in vivo allostimulation was not observed in $BTLA^{-/-}$ donor $CD4^+$ cells. The striking loss of $BTLA^{-/-}$ T cells in this model indicates a role for BTLA activity in sustaining $CD4^+$ T cell survival under the conditions of chronic stimulation in the nonirradiated parental-into-F_1 GVHD. ***The Journal of Immunology,*** **2007, 178: 6073–6082.**

B and T lymphocyte attenuator (BTLA)[2] is a lymphoid-specific cell surface receptor that is expressed by B cells, T cells, dendritic cells, macrophages, and NK cells in C57BL/6 mice (1–4). BTLA shows both structural and expression polymorphisms in mice, with BALB/c and C57BL/6 alleles differing at 10 aa within the extracellular region, and the BALB/c allele lacking expression by macrophages or NK cells (2). Functional analysis has suggested that BTLA exerts inhibitory actions, indicating a role more similar to CTLA-4 and programmed death-1 (PD-1) than to activating receptors of the CD28/B7 family (1, 4).

BTLA represses Ag-driven T cell proliferation upon binding its ligand, herpesvirus entry mediator (HVEM) (5), a member of the TNFR superfamily, expressed mainly by T lymphocytes and immature dendritic cells (6). An agonist Ab to murine BTLA inhibits IL-2 secretion and T cell proliferation in vitro, further suggesting an inhibitory role for BTLA (4). Phosphorylation of BTLA leads to recruitment of Src homology domain 2-containing protein tyrosine phosphatases (SHP-1 and SHP-2) to two tyrosine motifs in the cytoplasmic domain of mouse and human BTLA (3, 5). Human BTLA possesses an additional tyrosine residue that may also participate in inhibitory signaling (7). BTLA expression is increased on in vivo-anergized T cells, but not on $CD25^+$ T regulatory cells, in contrast to CTLA-4 and PD-1, suggesting it may have a distinct role in modulating immune responses (2). Notably, mouse and human BTLA contain a conserved intracellular tyrosine motif suggestive of a Grb-2 recruitment site (1, 3), which can interact with Grb-2 and the p85 subunit of PI3K in vitro (8). Although the function of this region has not been established, it suggests that BTLA may have the capability to function in a costimulatory or prosurvival manner.

The effects of BTLA-HVEM interactions may also be influenced by the interactions of HVEM with its additional ligands, tumor necrosis family members LIGHT (TNFSF14) and lymphotoxin (LT)α (9). In contrast to the inhibitory nature of BTLA-HVEM interactions, HVEM-LIGHT binding exerts a costimulatory effect on T cell activation (10–12). This regulatory network is increasingly complex because HVEM has the potential to bind BTLA and LIGHT simultaneously (13–15). Consequently, the balance between costimulatory and inhibitory signals may be regulated by a complex including BTLA, HVEM, and LIGHT.

Graft-vs-host disease (GVHD) is an immune response against alloantigens, such as foreign MHC molecules (reviewed in Refs. 16 and 17). In the parental-into-F_1 model of GVHD, parental T cells react against alloantigens of the F_1 host, whereas F_1 host T cells are tolerant to parental cells (18, 19). The type of GVHD that develops in nonirradiated, immunocompetent F_1 recipients is dependent on the strain of parental donor cells transferred (18). In the most widely reported version of this model, transfer of C57BL/6 (H-2^b) splenocytes into a nonirradiated, immunocompetent C57BL/6 × DBA/2 F_1 (B6D2F_1; H-$2^{b/d}$) host induces acute GVHD (aGVHD), characterized by a Th1 cytokine driven, cell-mediated response against host tissues (18, 20). Donor T cells exert cytotoxic effects through Fas-Fas ligand interactions, perforin, and inflammatory cytokines (21–23). In contrast, transfer of DBA/2 (H-2^d) splenocytes into B6D2F_1 hosts results in a chronic form of GVHD (cGVHD), characterized by production of Th2 cytokines and activation of host B cells, resulting in

*Department of Pathology and Center for Immunology and †Howard Hughes Medical Institute, Washington University School of Medicine, St. Louis, MO 63110

Received for publication October 2, 2006. Accepted for publication March 7, 2007.

The costs of publication of this article were defrayed in part by the payment of page charges. This article must therefore be hereby marked *advertisement* in accordance with 18 U.S.C. Section 1734 solely to indicate this fact.

[1] Address correspondence and reprint requests to Dr. Kenneth M. Murphy, Department of Pathology, Washington University School of Medicine, 660 South Euclid Avenue, St. Louis, MO 63110. E-mail address: murphy@pathology.wustl.edu

[2] Abbreviations used in this paper: BTLA, B and T lymphocyte attenuator; 7-AAD, 7-aminoactinomycin; GVHD, graft-vs-host disease; aGVHD, acute GVHD; cGVHD, chronic form of GVHD; HVEM, herpesvirus entry mediator; LIGHT, homologous to lymphotoxins, exhibits inducible expression, and competes with HSV glycoprotein D for HVEM, a receptor expressed by T lymphocytes; LT, lymphotoxin; PD-1, programmed death-1.

autoantibody development and a systemic lupus erythematosus-like syndrome (24, 25).

In this study, a related parental-into-F_1 model of GVHD was examined. In this model, transfer of C57BL/6 donor cells into C57BL/6 × BALB/c F_1 ($CB6F_1$; H-$2^{b/d}$) yields aGVHD, whereas BALB/c donor cells produce chronic GVHD (26). Although GVHD induced in $CB6F_1$ mice is generally similar to that in $B6D2F_1$, as described above, strain-dependent differences have been identified. BALB/c-into-$CB6F_1$ resulted in chronic GVHD that was comparable to that of DBA/2-into-$B6D2F_1$ (26). The aGVHD resulting from C57BL/6-into-$CB6F_1$, characterized by donor cell expansion and antihost CTL activity, was similar to that in C57BL/6-into-$B6D2F_1$ during the first 3 wk following transfer (26). After 3 wk, while C57BL/6 donor cells continued to expand in $B6D2F_1$ hosts, the percentage of parental cells progressively decreased in $CB6F_1$ hosts (26). By 12 wk, the C57BL/6-into-$CB6F_1$ mice had transitioned to cGVHD, with an absence of antihost CTL activity and the development of autoantibodies (26). In this study, we analyze the 2 wk following transfer of C57BL/6-into-$CB6F_1$, a point at which only aGVHD parameters are observed.

Costimulatory signals have been demonstrated to be essential to the development of disease in a variety of GVHD models. Blocking B7/CD28 costimulatory interactions with mAbs to B7-1 and B7-2 (27, 28), CTLA-4Ig, a soluble competitive inhibitor of CD28 (29–31), or by using *CD28*$^{-/-}$ splenocytes (32) inhibited donor T cell activation and disease development. Blockade of ICOS signaling strongly suppressed Th2-driven cGVHD disease yet augmented donor T cell expansion in Th1-driven aGVHD (33). Several studies have established that inhibitory receptors slow the development of GVHD. Blocking Abs against CTLA-4 (34) or PD-1 (35) accelerated GVHD following bone marrow transplant. CTLA-4 and PD-1 do not appear fully redundant in their regulation of GVHD because an additive increase in disease severity occurs when both pathways are inhibited (35).

In this study, we use the nonirradiated parental-into-F_1 model of GVHD to examine the function of BTLA in regulating alloresponses. We anticipated that *BTLA*$^{-/-}$ parental cells would have augmented alloreactivity, similar to that seen in the absence of inhibitory signals such as CTLA-4 or PD-1. Unexpectedly, we observed that *BTLA*$^{-/-}$ donor splenocytes are unable to sustain this GVHD response. Although *BTLA*$^{-/-}$ lymphocytes react to host alloantigens and expand in an early effector response, this response is not sustained. In comparison to *BTLA*$^{+/+}$ donor cells, *BTLA*$^{-/-}$ donor T cells undergo a rapid contraction in vivo beginning on day 10, which is accompanied by resolution of GVHD pathology. DNA microarray analysis indicates that $CD4^+$ *BTLA*$^{-/-}$ donor cells have altered expression of several important genes that may influence the effector response or survival of T cells, including IL-7Rα (36–38), IL-18Rα (39), and IL-4 (reviewed in Ref. 40). These results suggest that BTLA may act not only as an inhibitor as shown previously (1, 2, 4, 5) but, under some conditions, may participate in providing signals that promote the immune responses.

Materials and Methods

Reagents

The following Abs used for FACS analysis were from BD Pharmingen: CD4-PE-Cy7 (RM4-5), CD8-PE or allophycocyanin (53-6.7), B220-allophycocyanin (RA3-6B2), H-$2K^d$-FITC or PE (SF1-1.1), H-$2K^b$-FITC or PE (AF6-88.5), IL-15Rβ-PE (TM-β1), IL-6Rα-PE (D7715A7), IFN-γRα-biotin (GR20), BrdU-FITC, annexin V-allophycocyanin, and streptavidin-allophycocyanin. IL-7Rα-FITC (A7R34) and BTLA-PE (6F7, pan-allele specific) were obtained from eBioscience. IL-18Rα-biotin (polyclonal) and goat IgG-biotin were obtained from R&D Systems. Four-color analysis was performed on a FACSCalibur (BD Biosciences) and analyzed using FlowJo (Tree Star). For in vivo blockade, endotoxin-free anti-BTLA (6A6, C57BL/6-allele specific) was purified from hybridoma supernatants according to standard procedures (2). Isotype control hamster IgG was obtained from Jackson ImmunoResearch Laboratories.

Mice

C57BL/6, BALB/c, and C57BL/6 × BALB/c F_1 ($CB6F_1$) mice were bred in our facility. *Btla*$^{-/-}$ mice were backcrossed to C57BL/6 or BALB/c for at least nine generations (1). In some experiments, *BTLA*$^{+/-}$ × *BTLA*$^{+/-}$ (generation 9) littermate mice were used as donors, and the *BTLA* genotypes of mice were determined by surface staining of $B220^+$ peripheral blood cells with 6F7-PE (anti-BTLA). All donor and host mice were 8–12 wk of age and sex matched. Syngeneic $CB6F_1$ mice were used as control donors.

Induction of GVHD

Unless otherwise stated, single-cell suspensions of pooled donor splenocytes were subjected to RBC lysis and suspended in sterile, endotoxin-free HBSS. aGVHD was induced as previously described in Ref. 33, except that 5×10^7 C57BL/6 donor cells (which we found to yield similar results as the reported 6×10^7 cells) were injected via the lateral tail vein into normal, nonirradiated $CB6F_1$ host mice. Control mice received donor cells from syngeneic $CB6F_1$ mice. To induce cGVHD, 8×10^7 pooled BALB/c donor splenocyte were transferred into $CB6F_1$ mice. At indicated time points, splenocytes from each GVHD-induced mouse were analyzed separately.

ELISA for anti-DNA Abs

Serum autoantibodies specific for ssDNA and dsDNA were detected by ELISA. After precoating with 0.01% poly-L-lysine, ELISA plates were coated with 3 μg/ml single-stranded calf thymus DNA (Sigma-Aldrich) or 2.5 μg/ml double-stranded calf thymus DNA (Sigma-Aldrich) in PBS. Nonspecific binding was blocked by incubating with 10% FCS. Serial dilutions of each experimental serum were plated and developed with anti-mouse-IgG-HRP (Southern Biotechnology Associates). Serum from an MRL/*lpr* mouse was used as a positive control for autoantibodies. The OD reading for MRL/*lpr* serum was set to an arbitrary unit of 1, and the level of autoantibody in serum from experimental mice was expressed relative to this value.

In vivo treatment with anti-BTLA mAb

Experimental mice were injected i.p. with 100 μg of purified 6A6 (monoclonal anti-BL/6 BTLA) (2) or control hamster-IgG (Jackson ImmunoResearch Laboratories) at the time of GVHD induction (day 0) or again on day 3 and 6 following transfer, as indicated.

Assessment of proliferation by CFSE dilution and BrdU incorporation

To assess cell division during the initiation of GVHD, donor cells were labeled with 1 μM CFSE (Molecular Probes) before transfer, as in Ref. 5. To assess proliferation at later stages of the response, in vivo 5-BrdU (BD Pharmingen) labeling and FACS staining were conducted according to the manufacturer's suggested protocol (BrdU Flow kit; BD Pharmingen). Briefly, 18 h before harvest, mice were injected i.p. with 1 mg of BrdU in PBS. BrdU incorporation was assessed by FACS staining of fixed and permeabilized cells with anti-BrdU-FITC.

CFSE-based cytotoxicity assay

This FACS-based CTL assay was conducted as reported by Jedema et al. (41), with alterations noted below. Briefly, allogeneic P815 (H-$2K^d$) or syngeneic EL4 (H-$2K^b$) target cells were labeled with 1 μM CFSE. Target cells were suspended in medium at 1×10^5 cells/ml and 100 μl/well plated in round-bottom 96-well plates. Whole splenocytes from GVHD-induced mice, subjected only to RBC lysis, served as effector cells and were plated at the indicated E:T ratios. Plates were incubated for 4 h at 37°C. Wells were harvested, and 7-aminoactinomycin (7-AAD) was added just before FACS analysis. Lysed targets were determined by the percentage of $CFSE^+$ cells that were 7-AAD^+ (Molecular Probes). Nonspecific lysis was assessed in wells without effector cells added. Splenocytes from naive $CB6F_1$ served as a syngeneic control.

Microarray analysis

On days 9 and 10 following GVHD induction, the $CD4^+$ donor-derived population was sorted from pooled splenocytes of several experimental

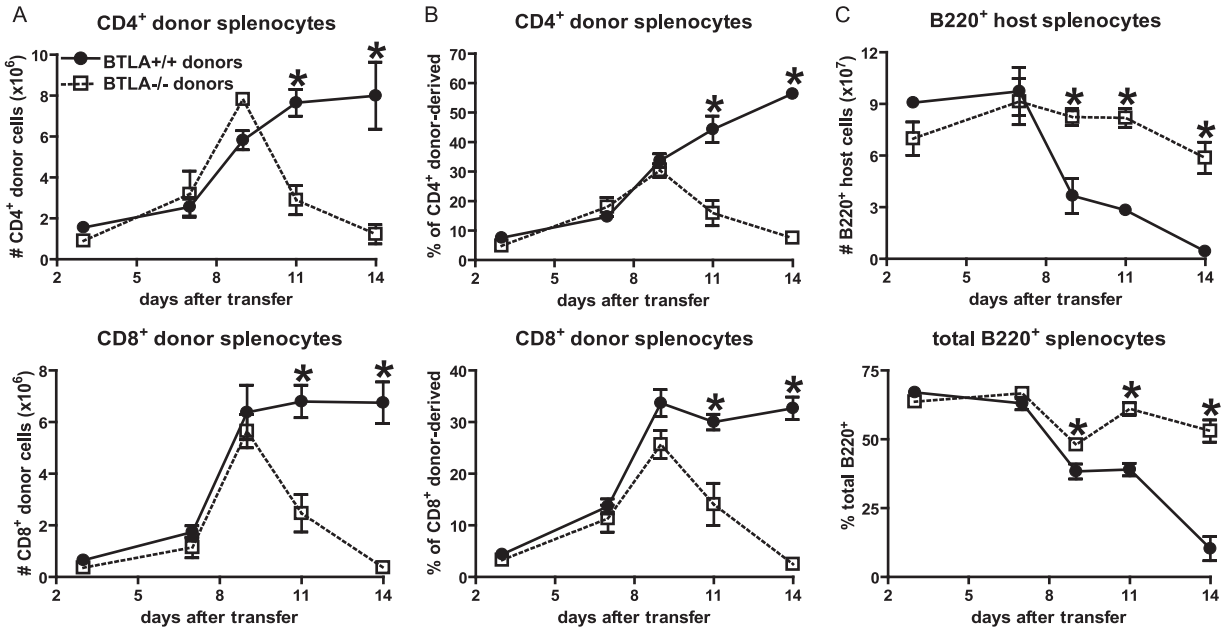

FIGURE 1. C57BL/6 *BTLA*$^{-/-}$ donor T lymphocytes fail to persist long term in CB6F$_1$ hosts. A total of 5×10^7 donor splenocytes from C57BL/6 *BTLA*$^{+/+}$ (H-2^b, ●) or C57BL/6 *BTLA*$^{-/-}$ (H-2^b, □) mice 5 were transferred into CB6F$_1$ (H-2$^{b/d}$) hosts. Spleens were harvested at days 3, 7, 9, 11, and 14 after transfer and analyzed by FACS to establish the kinetics of donor-host chimerism. Donor-derived cells were distinguished by the absence of H-2K^d. *A*, The absolute number of live donor CD4$^+$ (*top panel*) and CD8$^+$ (*bottom panel*) splenocytes were calculated at each time point. *B*, The percentage of splenic CD4$^+$ (*top panel*) or CD8$^+$ (*bottom panel*) compartments that were donor derived is shown at each time point. *C*, *BTLA*$^{-/-}$ donor cells fail to elicit a strong antihost response, as demonstrated by maintenance of the host B cell compartment. The absolute number of live B220$^+$ host splenocytes (*top panel*) and the total percentage of B220$^+$ splenocytes (*bottom panel*) are shown at each time point. Average values were calculated from three mice per group at each time point with error bars indicating SEM. Asterisks indicate time points at which Student's *t* tests indicate significant differences of $p < 0.05$ between *BTLA*$^{+/+}$ and *BTLA*$^{-/-}$ donors. Data are representative of five independent experiments.

mice that had received *BTLA*$^{+/+}$ or *BTLA*$^{-/-}$ and stained with anti-H-2K^d-FITC, anti-BTLA-PE, and anti-CD4-allophycocyanin. Post-sort analysis showed >95% purity of the sorted populations. RNA was extracted with the RNeasy kit (Qiagen). Biotinylated cRNA target was generated using the Two-Cycle cDNA synthesis kit (Affymetrix). Each cRNA was hybridized to the Affymetrix Mouse Genome 430 2.0 array. Data were analyzed using dCHIP (www.dchip.org).

Results

BTLA is required for maintenance of donor lymphocytes in the parental-into-F$_1$ GVHD model

To investigate the functions of BTLA during an in vivo allogeneic immune response stimulated by MHC mismatch, we compared the actions of *BTLA*$^{+/+}$ and *BTLA*$^{-/-}$ cells in a model of parental-into-F$_1$-induced aGVHD. Transfer of C57BL/6 (H-2K^b) *BTLA*$^{+/+}$ splenocytes into unirradiated CB6F$_1$ (H-2$^{b/d}$) hosts elicited a progressive expansion of donor CD4$^+$ and CD8$^+$ lymphocytes characteristic of aGVHD, as expected (Fig. 1, *A* and *B*). However, transfer of *BTLA*$^{-/-}$ cells was unable to sustain donor cell expansion over the course of a 14-day response (Fig. 1, *A* and *B*). To characterize the kinetics of this response, the absolute number (Fig. 1*A*) and percentage (Fig. 1*B*) of donor T cells in the spleens of GVHD-induced mice were assessed by FACS on days 3, 7, 9, 11, and 14 after transfer. Mice receiving either *BTLA*$^{+/+}$ and *BTLA*$^{-/-}$ donor cells showed expansion of donor T cells during the initial 9 days following GVHD induction (Fig. 1, *A* and *B*). However, *BTLA*$^{-/-}$ donor cells began to decline in numbers after day 10, in contrast to the progressive increase in *BTLA*$^{+/+}$ donor CD4$^+$ and CD8$^+$ T cells (Fig. 1, *A* and *B*). To investigate whether BTLA expressed by host cells was important in controlling GVHD, donor cells were also transferred into *BTLA*$^{-/-}$ CB6F$_1$ hosts. Again, *BTLA*$^{+/+}$ T cells continually expanded in *BTLA*$^{-/-}$ recipients, whereas *BTLA*$^{-/-}$ T cells showed a rapid contraction by days 11 and 14, suggesting that BTLA expressed by the host is not required for maintenance of GVHD by donor cells (data not shown).

The inability of *BTLA*$^{-/-}$ donor lymphocytes to sustain aGVHD was also demonstrated by the absence of an antihost cytotoxic response, apparent from the lack of depletion of the host B220$^+$ population (Fig. 1*C*). On day 14, spleens from mice receiving *BTLA*$^{+/+}$ cells were <10% B220$^+$, indicating cytolysis of host B cells, as expected. In contrast, mice receiving *BTLA*$^{-/-}$ cells retained a normal number of B cells, ~60% of splenocytes.

To determine whether *BTLA*$^{-/-}$ donor lymphocytes were engrafting and expanding, we transferred and analyzed CFSE-labeled donor cells (Fig. 2). CD4$^+$ and CD8$^+$ T cells from *BTLA*$^{+/+}$ and *BTLA*$^{-/-}$ donors showed similar percentages and numbers of cells that had undergone division after 3 days (Fig. 2). These results indicate that later disappearance of *BTLA*$^{-/-}$ donor cells is not due to a failure in initial activation by host alloantigens. We also used *BTLA*$^{+/+}$, *BTLA*$^{+/-}$, and *BTLA*$^{-/-}$ littermates generated from an intercross of C57BL/6 *BTLA*$^{+/-}$ mice as donor cells to test for any minor histocompatibility mismatch with CB6F$_1$ host mice. Again, only the *BTLA*$^{-/-}$ donor cells failed to survive at day 14, whereas both *BTLA*$^{+/+}$ and *BTLA*$^{+/-}$ donor cells expanded to occupy 60–70% of the CD4$^+$ and CD8$^+$ compartments (Fig. 3), suggesting that the findings were due to the absence of donor cell BTLA expression rather than a result of transplant incompatibility.

We also evaluated a model of cGVHD characterized by gradual development of a Th2 cytokine-induced, autoantibody-mediated disease (24, 25). Transfer of BALB/c *BTLA*$^{+/+}$ donor splenocytes into CB6F$_1$ hosts induced expansion of CD4$^+$ and CD8$^+$ donor T cells (although to a lower extent than seen in aGVHD, as expected (26)), the development of anti-dsDNA and anti-ssDNA Abs and activation of host-derived B cells as measured by CD69 induction

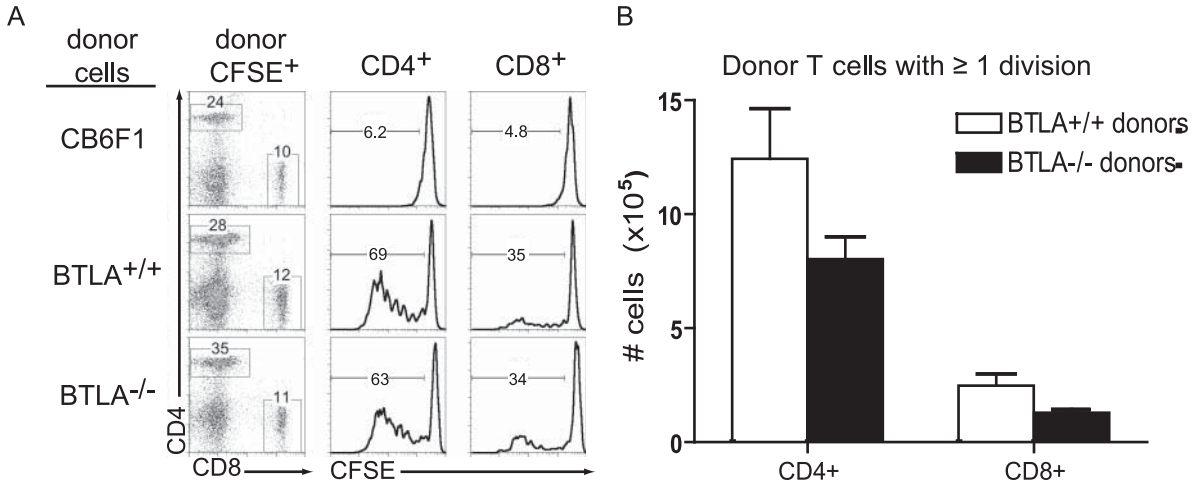

FIGURE 2. *BTLA*$^{-/-}$ donor cells engraft and divide during the initiation stage of GVHD. A total of 5×10^7 CFSE-labeled $CB6F_1$, C57BL/6 *BTLA*$^{+/+}$, or *BTLA*$^{-/-}$ splenocytes were transferred to $CB6F_1$ host mice. Splenocytes were harvested 3 days posttransfer and gated on live, CFSE$^+$ donor lymphocytes by FACS. *A*, Donor cells were divided into CD4$^+$ and CD8$^+$ populations (first column), and the percentage of the donor CD4$^+$ (second column) and CD8$^+$ (third column) populations that had undergone one or more divisions was assessed by CFSE dilution. Histogram gates indicate the percentage of each population undergoing one or more divisions. *B*, Following the gating scheme above, the absolute number of donor cells that had undergone one or more divisions was calculated. Bar graphs show an average of three mice, with error bars indicating SEM (*BTLA*$^{+/+}$ donors, □; *BTLA*$^{-/-}$ donors, ■). Student's *t* tests did not show significant differences between *BTLA*$^{+/+}$ and *BTLA*$^{-/-}$ donor cells (CD4$^+$, $p = 0.143$; CD8$^+$, $p = 0.084$). Data are representative of two independent experiments.

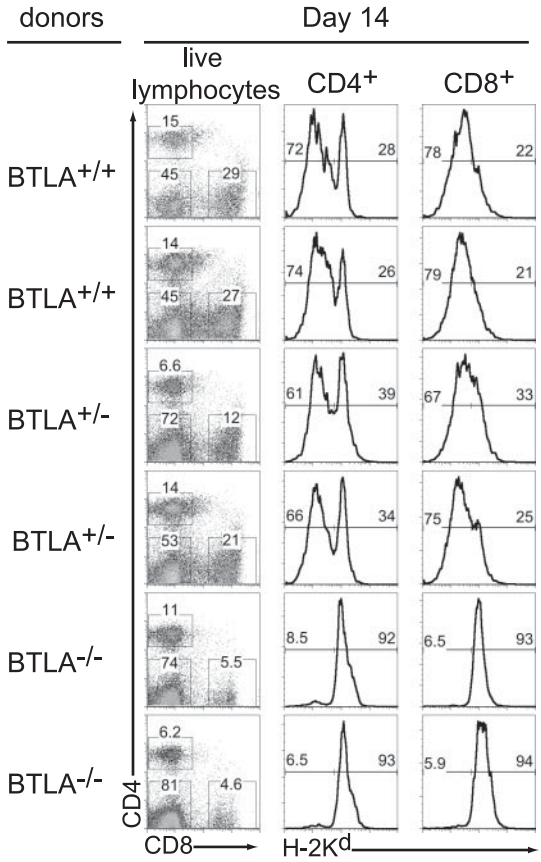

FIGURE 3. Failed survival of *BTLA*$^{-/-}$ donor cells cannot be attributed to a minor histocompatibility mismatch. *BTLA*$^{+/+}$, *BTLA*$^{+/-}$, or *BTLA*$^{-/-}$ littermates from a *BTLA*$^{+/-}$ × *BTLA*$^{+/-}$ breeding (generation 9 backcross to C57BL/6) were used as donor splenocytes. Donor mice were tail bled and BTLA genotyped confirmed by FACS staining of B220$^+$ cells before transfer (data not shown). Donor splenocytes (5×10^7) from a single mouse were transferred into a $CB6F_1$ host and harvested on day 14. The percentage of donor-derived cells (H-2K^d negative) in the CD4$^+$ (second column) and CD8$^+$ (third column) populations are indicated by the *left gate* on each histogram. The H-2K^d-positive population (*right gates*) indicates host cells.

(Fig. 4), as expected for BALB/c donors (25, 42). Kinetic analysis revealed that BALB/c *BTLA*$^{-/-}$ donor T lymphocytes expand equivalently to *BTLA*$^{+/+}$ cells during the initial 10 days following transfer (Fig. 4*A*). However, similar to the transfer of C57BL/6 donor cells, BALB/c *BTLA*$^{-/-}$ donor CD4$^+$ and CD8$^+$ cells rapidly contract by day 12 of the response (Fig. 4*A*). Transfer of BALB/c *BTLA*$^{-/-}$ donor splenocytes also failed to show the induction of anti-DNA autoantibodies characteristic of cGVHD (Fig. 4*B*). Additionally, host B cells from mice receiving *BTLA*$^{-/-}$ donor cells were not activated, as measured by a failure to up-regulate CD69 (Fig. 4*C*). Thus, BALB/c *BTLA*$^{-/-}$ donor cells show a similar defect in sustaining cGVHD as was found for C57BL/6 BTLA$^{-/-}$ donor cells in sustaining aGVHD.

BTLA blockade by Ab treatment prevents maintenance of BTLA$^{+/+}$ *donor lymphocyte in aGVHD*

The 6A6 mAb is specific for the C57BL/6 allele of BTLA and blocks binding to its ligand HVEM (2). Administration of 6A6 at the time of transfer of *BTLA*$^{+/+}$ donor cells resulted in a loss of donor lymphocytes by day 14 of the response, similar to the transfer of *BTLA*$^{-/-}$ cells (Fig. 5). To ensure that the abrogation of donor cell expansion was not due to opsonization and rapid host clearance of BTLA-expressing donor cells by the Ab, we examined the kinetics the GVH response in the presence of 6A6 administration. (Fig. 5). Expansion of C57BL/6 *BTLA*$^{+/+}$ donor cells in recipients treated with isotype control or anti-BTLA Ab was equivalent at days 3 and 8 following transfer (Fig. 5). By day 14, few donor CD4$^+$ and CD8$^+$ lymphocytes were present in mice that had received anti-BTLA Abs (Fig. 5). A single Ab treatment at the time of transfer was sufficient to cause the loss of donor cells, as additional Ab administration at days 3 and 6 had no additional effect (data not shown). The observation that blocking BTLA/HVEM interactions through Ab treatment yields the loss of donor cells similar to transfer of *BTLA*$^{-/-}$ splenocytes suggests that the interaction of BTLA with its ligand HVEM is necessary to support the survival of donor lymphocytes in aGVHD.

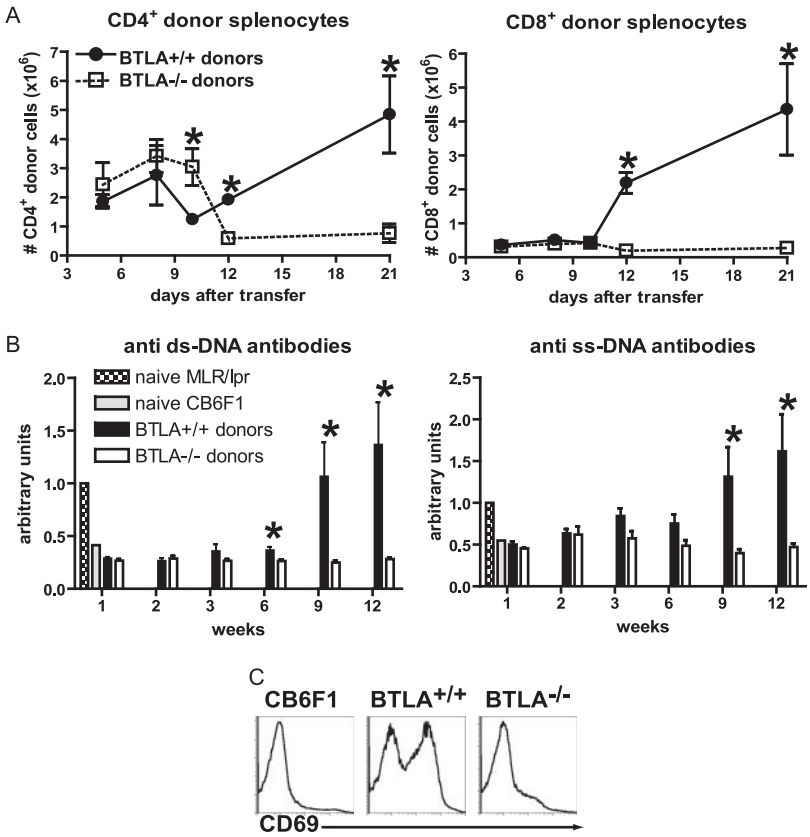

FIGURE 4. Transfer of BALB/c *BTLA*$^{-/-}$ donor cells fails to elicit a chronic GVHD response. Chronic GVHD was induced by adoptively transferring 8×10^7 BALB/c *BTLA*$^{+/+}$ or *BTLA*$^{-/-}$ donor splenocytes into $CB6F_1$ hosts. *A*, Spleens from mice receiving *BTLA*$^{+/+}$ (●, H-2H^d) or *BTLA*$^{-/-}$ (□, H-2K^d) donor cells were harvested at days 5, 8, 10, 12, and 21 after transfer and analyzed by FACS as in Fig. 1, except that donor cells were H-2K^b negative. The absolute number of live donor CD4$^+$ (*left panel*) and CD8$^+$ (*right panel*) splenocytes was calculated at each time point. Average values were calculated from three mice per group at each time point with error bars indicating SEM. Asterisks indicate time points at which Student's *t* tests indicate significant differences of $p < 0.05$ between *BTLA*$^{+/+}$ and *BTLA*$^{-/-}$ donor cells. *B*, Serum was obtained from GVHD-induced mice at the indicated time points and assessed by ELISA for development of anti-dsDNA (*left graph*) or anti-ssDNA (*right graph*) Abs. Naive MRL/*lpr* mouse serum (▩) was used as a positive control for autoantibodies, whereas naive $CB6F_1$ serum (▨) was used as a negative control. The amount of autoantibody in MRL/*lpr* serum was set to an arbitrary value of 1, and the amount of anti-DNA Ab in serum from mice receiving *BTLA*$^{+/+}$ cells (■) or *BTLA*$^{-/-}$ cells (□) was calculated relative to MRL/*lpr* serum. The average of four mice per group is shown, with error bars indicating SEM. Asterisks indicate points at which Student's *t* tests indicate significant differences of $p < 0.05$. *C*, Transfer of *BTLA*$^{-/-}$ donor cells fails to induce activation of host B cells. Splenocytes were harvested on day 11 after GVHD induction. The expression level of the activation marker CD69 on host B cells (B220$^+$, H-2K^b positive) is shown. Data are representative of two independent experiments.

BTLA$^{-/-}$ *donor cells demonstrate reduced BrdU incorporation and antihost CTL activity before contraction*

Contraction of *BTLA*$^{-/-}$ donor cells could be a result either of decreased proliferation or increased cell death. Therefore, we examined these parameters at days 9 and 10, a time just before the onset of rapid contraction, using BrdU labeling, markers of apoptosis, and assays for cytolytic activity (Fig. 6). At day 9, the percentage of *BTLA*$^{-/-}$ donor T cells that had incorporated BrdU

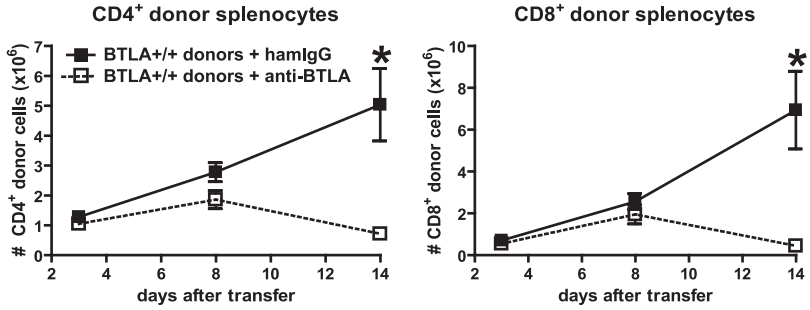

FIGURE 5. Anti-BTLA Ab treatment at the initiation of GVHD inhibits the long-term survival of *BTLA*$^{+/+}$ donor lymphocytes. C57BL/6 *BTLA*$^{+/+}$ splenocytes (5×10^7) were transferred into $CB6F_1$ hosts. A total of 100 μg of hamster IgG (isotype control, ■) or anti-BTLA Ab (6A6, □) was administered i.p. to host mice concurrent with donor cell transfer (day 0). Splenocytes were harvested after 3, 8, and 14 days and analyzed for donor/host chimerism as in Fig. 1. Absolute numbers of donor CD4$^+$ (*left graph*) and CD8$^+$ (*right graph*) were calculated at each time point. Average values are shown for three mice per group at each time point with error bars indicating SEM. Asterisks indicate points at which Student's *t* tests indicate significant differences of $p < 0.05$ between isotype- and 6A6-treated mice. Data are representative of three independent experiments.

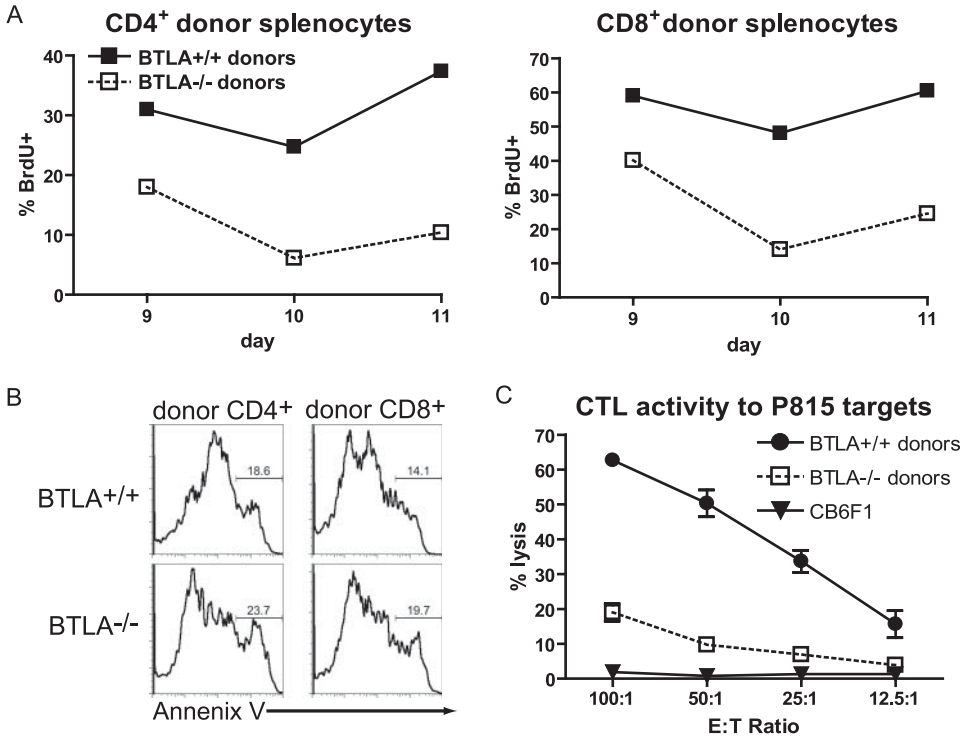

FIGURE 6. *BTLA*$^{-/-}$ donor cells incorporate less BrdU but do not exhibit increased apoptosis before contraction. GVHD was induced by transferring 5×10^7 *BTLA*$^{+/+}$ C57BL/6 (■) or *BTLA*$^{-/-}$ (□) splenocytes into $CB6F_1$ hosts. *A*, Splenocytes were harvested at days 9, 10, and 11 following transfer. Eighteen hours before harvest, mice were injected i.p. with 1 mg of BrdU to observe cellular proliferation. Splenocytes were subjected to FACS staining to identify the percentage of donor CD4$^+$ (*left graph*) and CD8$^+$ (*right graph*) cells incorporating BrdU. Data at each time point is representative of the average of two mice per group. *B*, The percentage of annexin V-positive donor CD4$^+$ (*left panels*) or CD8$^+$ (*right panels*) splenocytes from mice receiving *BTLA*$^{+/+}$ (*upper panels*) or *BTLA*$^{-/-}$ (*lower panels*) splenocytes was assessed at day 9 by FACS. Gates indicate the percentage of annexin V-positive cells. Data are representative of two mice per group. *C*, At day 10, unfractionated splenocytes from GVHD-induced mice were analyzed for CTL activity against allogeneic (H-2K^d) P815 cells. Effector splenocytes were incubated with CFSE-labeled targets at the indicated ratios for 4 h. A vitality dye (7-AAD) was added, and the percentage of target cells lysed (CFSE$^+$7-AAD$^+$) was determined by FACS. CTL activity was not observed toward syngeneic (H-2K^b) EL4 cell targets (data not shown). The mean ± SEM of three mice per group is shown.

is approximately two-thirds of the percentage of BrdU$^+$*BTLA*$^{+/+}$ donors (Fig. 6*A*). On day 10, BrdU incorporation by *BTLA*$^{-/-}$ donor cells is further reduced to approximately one-third the level of *BTLA*$^{+/+}$ donors (Fig. 6*A*). *BTLA*$^{-/-}$ donor CD4$^+$ and CD8$^+$ T cells showed a similar degree of reduced BrdU incorporation. However, we did not observe a detectable difference in the degree of annexin V staining, a marker of apoptotic cells, of CD4$^+$ or CD8$^+$ *BTLA*$^{-/-}$ and *BTLA*$^{+/+}$ donor cells at day 9 (Fig. 6*B*). Analysis of cytolytic activity at day 10 showed that *BTLA*$^{-/-}$ donor cells had a greatly reduced capacity to kill allogeneic P815 (H-2K^d) cells in vitro compared with *BTLA*$^{+/+}$ donor cells (Fig. 6*C*). This result agrees with our finding of normal levels of host B220$^+$ cells persisting in mice receiving *BTLA*$^{-/-}$ donor cells (Fig. 1*C*). Overall, these results suggest that the failure of *BTLA*$^{-/-}$ donor cells to sustain GVHD is due to a progressive decrease in donor cell proliferation, survival, and insufficient antihost CTL activity.

Differential gene expression of BTLA$^{+/+}$ *and BTLA*$^{-/-}$ *donor CD4*$^+$ *cells during GVHD*

We performed DNA microarray studies to characterize the potential molecular mechanism accounting for the contraction of *BTLA*$^{-/-}$ donor populations during GVHD. GVHD was induced by transferring either C57BL/6 *BTLA*$^{+/+}$ or *BTLA*$^{-/-}$ donor cells into $CB6F_1$ recipients, and donor CD4$^+$ lymphocytes were harvested 9 and 10 days after transfer. We selected these times for analysis because they directly precede the decline in *BTLA*$^{-/-}$ donor cells and may reveal cellular changes leading to their loss. Consistent with comparable annexin V staining on *BTLA*$^{+/+}$ and *BTLA*$^{-/-}$ donor cells (Fig. 6*B*), no differential expression of either pro- or antiapoptotic genes (including BCL-2, BCL-x_L, and Bad)

Table I. *Global gene analysis reveals genes induced and inhibited in BTLA*$^{+/+}$ *and BTLA*$^{-/-}$*CD4*$^+$ *donor cells 9 days after acute GVHD induction*[a]

Gene	Day 9 Fold change	Day 9 BTLA$^{+/+}$	Day 9 BTLA$^{-/-}$
Genes induced in BTLA$^{+/+}$ CD4$^+$ donors			
BTLA[b]	40.99	4321	112
IL-7Rα[b]	3.16	1020	323
IL-18Rβ[b]	2.76	488	176
CXCR6[b]	2.32	4046	1742
IL-18Rα[b]	1.70	3042	1785
Genes inhibited in BTLA$^{+/+}$ CD4$^+$ donors			
IL-4[c]	3.4	87	297
IL-1R antagonist[c]	2.5	97	244
IL-1R1[c]	2.0	276	138
NFATc1[c]	1.96	2760	1407
Bcl-3[c]	1.81	467	258
IL-6Rα[c]	1.61	114	185

[a] RNA was harvested from donor CD4$^+$ lymphocytes sorted from the spleens of GVHD mice at day 9 following GVHD induction. Data were analyzed using dCHIP, with the relative expression values and fold changes reported for immune-related genes demonstrating differential expression at each time point.
[b] Genes with higher expression in *BTLA*$^{+/+}$ as compared with *BTLA*$^{-/-}$.
[c] Genes with higher expression in *BTLA*$^{-/-}$ cells as compared with *BTLA*$^{+/+}$.

Table II. *Global gene analysis reveals genes induced and inhibited in BTLA$^{+/+}$ and BTLA$^{-/-}$CD4$^+$ donor cells 10 days after acute GVHD induction*[a]

Gene	Day 10 Fold change	BTLA$^{+/+}$	BTLA$^{-/-}$
Genes induced in BTLA$^{+/+}$ CD4$^+$ donors			
BTLA[b]	16.89	2634	155
T1/ST2[b]	11.13	1569	141
IL-18Rα[b]	7.33	3420	466
CXCR6[b]	6.87	2316	337
Granzyme B[b]	6.86	2199	320
CCL2 (MIP-2α)[b]	5.53	1195	216
IL-18Rβ[b]	4.91	305	62
CCR2[b]	3.72	1068	286
TNFSF7 (CD70)[b]	3.59	226	63
IFNγR1[b]	3.39	2363	696
CD86[b]	3.09	341	110
CCL3 (MIP-1α)[b]	2.99	1011	338
TNFSF25 (DR3)[b]	2.35	1161	495
CCL4 (MIP-1β)[b]	2.20	515	234
CCL5 (RATNES)[b]	2.04	426	208
IL-7Rα[b]	1.88	853	454
Genes inhibited in BTLA$^{+/+}$ CD4$^+$ donors			
IL-4[c]	10.45	81	847
IL-1R1[c]	9.57	85	821
CD109[c]	9.51	46	443
CXCR5[c]	4.81	627	3020
IL-6α[c]	4.03	171	689
gp130[c]	3.60	93	335
GADD45[c]	3.54	66	236
IL-1R antagonist[c]	3.37	119	403
IL-13Rα[c]	2.79	71	200
LIGHT[c]	2.52	221	557
ITK[c]	2.50	1465	3665
BcoR[c]	2.38	434	1034
TNFSF8 (CD30L)[c]	2.15	998	2149
IL-16[c]	2.09	526	1099

[a] RNA was harvested from donor CD4$^+$ lymphocytes sorted from the spleens of GVHD mice at day 10 following GVHD induction. Data were analyzed using dCHIP, with the relative expression values and fold changes reported for immune-related genes demonstrating differential expression at each time point.
[b] Genes with higher expression in *BTLA*$^{+/+}$ as compared with *BTLA*$^{-/-}$ cells.
[c] Genes with higher expression in *BTLA*$^{-/-}$ cells as compared with *BTLA*$^{+/+}$.

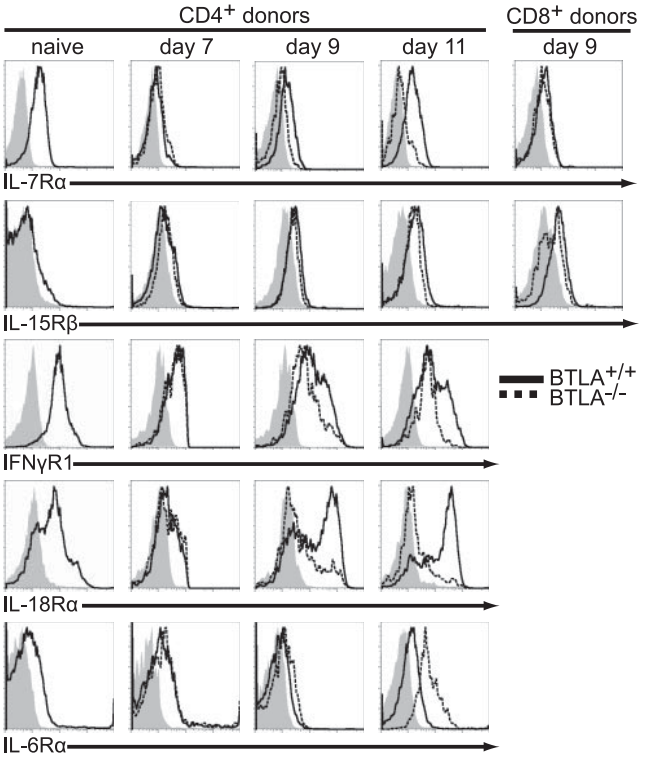

FIGURE 7. Differential gene expression of *BTLA*$^{+/+}$ and *BTLA*$^{-/-}$ donor CD4$^+$ cells during GVHD. C57BL/6 *BTLA*$^{+/+}$ splenocytes (5×10^7) were transferred into CB6F$_1$ hosts. Splenocytes were harvested on days 9 and 10. The surface levels of various receptors are compared with *BTLA*$^{+/+}$ (solid lines) and *BTLA*$^{-/-}$ (dashed lines) CD4$^+$ donor cells. Isotype control staining of a mixture of *BTLA*$^{+/+}$ and *BTLA*$^{-/-}$ splenocytes is shown (shaded regions). The first column indicates the receptor level on naive *BTLA*$^{+/+}$ C57BL/6 cells. Expression levels of all receptors are similar between *BTLA*$^{+/+}$ and *BTLA*$^{-/-}$ cells at day 7. IL-7Rα, IL-18Rα, and IFN-γR1 levels are increased on *BTLA*$^{+/+}$ compared with *BTLA*$^{-/-}$ donor cells at days 9 and 11. IL-6Rα expression is higher on BTLA$^{-/-}$ donor cells at day 11, whereas IL-15Rβ levels remain equivalent between *BTLA*$^{+/+}$ and *BTLA*$^{-/-}$ cells throughout. Expression of IL-15Rβ, but not IL-7Rα, was lower on CD8$^+$*BTLA*$^{-/-}$ donor cells than *BTLA*$^{+/+}$ donor cells at day 9 (*right column*).

was seen by DNA microarray (Tables I and II). We identified several immune specific genes that were differentially expressed by *BTLA*$^{+/+}$ and *BTLA*$^{-/-}$ donor CD4$^+$ populations at day 9 (Table I) and day 10 (Table II). These included IL-7Rα, IL-18Rα, IL-6Rα, and IFN-γR1 (Fig. 7).

IL-7Rα (CD127) showed 3.2- and 1.8-fold higher expression in *BTLA*$^{+/+}$ compared with *BTLA*$^{-/-}$CD4$^+$ T cells on days 9 and 10, respectively (Table I). On day 10, T1/ST2, an IL-1R family member (43), was expressed 11.1-fold higher in *BTLA*$^{+/+}$CD4$^+$ donor cells compared with *BTLA*$^{-/-}$ cells (Table II). IL-18Rα showed a 1.7-fold higher expression at day 9 and a 7.3-fold higher expression at day 10 in *BTLA*$^{+/+}$ donor cells. IFN-γR1 (CD119) expression was 3.3-fold higher in the *BTLA*$^{+/+}$ donor CD4$^+$ population than the *BTLA*$^{-/-}$ donors at day 10 (Table II). Some genes were expressed more highly by *BTLA*$^{-/-}$CD4$^+$ donor cells compared with *BTLA*$^{+/+}$CD4$^+$ donor cells. IL-4 expression was 3.4-fold higher in *BTLA*$^{-/-}$ cells at day 9 (Table I), which increased to a 10.4-fold higher expression on day 10 (Table II). IL-6Rα had 1.6-fold higher expression in *BTLA*$^{-/-}$ cells at day 9 and 4-fold higher expression at day 10 (Table I).

We verified some of these differences by FACS analysis (Fig. 7). IL-7Rα surface expression on *BTLA*$^{+/+}$CD4$^+$ donor cells increased progressively over time, ultimately returning to levels similar to that of naive CD4$^+$ cells, whereas *BTLA*$^{-/-}$ donor cells failed to re-express the receptor (Fig. 7). In contrast, the expression of IL-7Rα on CD8$^+$*BTLA*$^{-/-}$ donor cells was equivalent to that of *BTLA*$^{+/+}$ donors at day 9. Although the IL-15Rβ-chain (CD122) remained equivalently expressed by both *BTLA*$^{+/+}$ and *BTLA*$^{-/-}$CD4$^+$ donor cells populations at all time points, CD8$^+$*BTLA*$^{-/-}$ donor cells expressed decreased levels of IL-15Rβ at day 9 (Fig. 7). The IL-18Rα was expressed equivalently at day 7 but later increased on *BTLA*$^{+/+}$ donor CD4$^+$ cells and decreased on *BTLA*$^{-/-}$ donor cells (Fig. 7). IFN-γR1 expression remained unchanged on *BTLA*$^{-/-}$CD4$^+$ donor cells but was increased on *BTLA*$^{+/+}$CD4$^+$ donor cells at days 9 and 11 (Fig. 7). IL-6Rα was expressed equivalently between *BTLA*$^{+/+}$ and BTLA$^{-/-}$ cells at day 7 but was up-regulated on only *BTLA*$^{-/-}$ donors at day 11 (Fig. 7).

Discussion

The major finding of this study is the unexpected stimulatory, rather than inhibitory, role of BTLA in an in vivo model of chronic allostimulation. In the parental-into-F$_1$ nonirradiated GVHD model, we found that *BTLA*$^{-/-}$ donor cells were unable to sustain

GVHD pathology, as opposed to the expected augmentation of disease. These data suggest that BTLA, acting either as a receptor or as a ligand for HVEM, has prosurvival activity in this in vivo model of sustained alloresponse. Although the initial activation and expansion of $BTLA^{-/-}$ and $BTLA^{+/+}$ donor cells was similar, $BTLA^{-/-}$ donor cell numbers began to decrease at day 10, eventually disappearing (Fig. 1). Thus, under this model of chronic allostimulation, BTLA is acting in a prosurvival manner and is clearly necessary for the maintenance, rather than the initiation, of the effector T cell response.

BTLA was initially identified as having inhibitory actions on T cell proliferation and cytokine production in vitro (1, 44). Inhibitory actions observed in vivo in models of experimental allergic encephalomyelitis (1) and allergic airway inflammation (45) support these observations. Engagement of BTLA on murine $CD4^+$ T cells by the BTLA ligand HVEM expressed on APCs (5) or by a HVEM-Fc fusion protein (13) also caused a reduction in early T cell proliferation. A chimeric receptor containing the extracellular domain of CD28 fused to the human BTLA cytoplasmic tail was able to potently inhibit IL-2 production by primary human CD4 T cells, again indicating inhibitory actions for BTLA (7). Finally, a recent report describing increased homeostatic expansion of $BTLA^{-/-}$ T cells in lymphopenic hosts and increased numbers of $CD8^+$ central memory cells in $BTLA^{-/-}$ and $HVEM^{-/-}$ mice further demonstrates the inhibitory activity of BTLA (46).

However, not all reported actions of BTLA have been inhibitory. Two different systems of cardiac transplantation (47) were used to evaluate the role of BTLA in allograft rejection (48). In the first system, partially MHC mismatched allografts, differing at a single class II MHC locus, are tolerated for long periods by wild-type recipient mice. These allografts were rapidly rejected, rather than tolerated, by $BTLA^{-/-}$ or $HVEM^{-/-}$ recipients, consistent with an inhibitory action of BTLA in the recipient immune response (48). In the second system, fully MHC mismatched, with differences at both class I and class II MHC loci, cardiac allografts are rapidly rejected by wild-type mice. These allografts showed slightly prolonged survival in $BTLA^{-/-}$ recipients (48). Although the basis for this difference was not established, these results suggested a positive action of BTLA in the recipient immune response.

In addition to ITIM and immunoreceptor tyrosine-based switch motif inhibitory motifs (1), the cytoplasmic domains of human and mouse BTLA contain other conserved tyrosine-containing motifs that may be relevant to signaling, such as sites that may recruit Grb-2 (7, 8). In one study, mutation of all cytoplasmic tyrosine residues was required to abolish the inhibitory actions of a chimeric signaling protein containing the human BTLA cytoplasmic domain (7). Another study indicated that the one Grb-2 recruitment motif in murine BTLA may interact with both Grb-2 and the p85 subunit of PI3K (8). While indirect evidence, a peptide containing the conserved phosphorylated Grb-2 recruitment region of the BTLA cytoplasmic domain had the ability to interact with PI3K, suggesting that BTLA may sometimes have a positive, rather than inhibitory, action (8). However, neither of these studies examined the in vivo role of these conserved signaling motifs.

To analyze the role of BTLA in immune regulation in vivo, we have surveyed various models of pathogen infections, induced and spontaneous autoimmunity, and various transplantation systems. As part of this survey, we examined the nonirradiated parental-into-F_1 GVHD system (18), expecting to observe augmented immune responses against host cells in the absence of BTLA's inhibitory actions. This nonirradiated GVHD model is distinct from other models of GVHD models that use host irradiation and bone marrow transplantation to more closely mimic GVHD that arises in clinical settings using myeloablative conditioning (reviewed in Ref. 17). Indeed, each model system contributes unique factors that complicate the analysis of the allogeneic response. Irradiation causes epithelial damage and extensive inflammatory cytokine production that exacerbate GVHD (16), whereas the nonirradiated model is complicated by an intact host immune system that may respond to inflammatory stimuli and contribute an antigraft response (49). Consequently, different mechanisms may account for the pathology in the irradiated and nonirradiated systems, and distinct roles for perforin (50, 51) and IFN-γ (52, 53) have been revealed in each model.

Global gene expression analysis of $BTLA^{+/+}$ and $BTLA^{-/-}$ donor cells harvested from hosts on days 9 and 10 revealed several genes with differential expression (Table I). Many of the differentially expressed genes are known to function during allogeneic responses. Polarization of donor $CD4^+$ T cells toward the Th1 phenotype is important for development of aGVHD (54–56). Interestingly, genes associated with Th2 cells were increased in $BTLA^{-/-}$ $CD4^+$ donors cells, whereas genes associated with Th1 cells were decreased in $BTLA^{-/-}$ $CD4^+$ donors. For example, IL-4 was increased in $BTLA^{-/-}$ $CD4^+$ donors (Table I) and is Th2 specific (40), whereas IL-18Rα and CXCR6 were decreased in $BTLA^{-/-}$ $CD4^+$ donors cells and are Th1 specific (39, 57, 58). Thus, the inability of $BTLA^{-/-}$ donor cells to mount a sustained effector response to allogeneic stimulation may be due to altered $CD4^+$ T cell polarization.

We also found that IL-7Rα failed to become highly expressed on $BTLA^{-/-}$ cells to the same extent as $BTLA^{+/+}$ donor $CD4^+$ cells. IL-7 is critical for homeostatic survival of naive T cells (59) and regulates the transition of $CD4^+$ effector T cells to long-lived and memory T cells (36–38). It was also recently reported that persistence of GVHD in an irradiated model system involved the development of alloreactive $CD4^+$ or $CD8^+$ memory T cells whose survival required the cytokines IL-2, IL-7, and IL-15 despite chronic allostimulation (60, 61). Conceivably, failure of $BTLA^{-/-}$ $CD4^+$ cells to re-express IL-7Rα in the nonirradiated GVHD model could prevent necessary survival signaling such as BCL-2 (62) or PI3K (63), causing the contraction observed after day 10 in vivo.

HVEM activity was shown recently to be required for manifestation of disease in a similar parental-into-F_1 nonirradiated model of GVHD (64). $HVEM^{-/-}$ and $LIGHT^{-/-}$ donor T cells showed decreased survival and reduced antihost CTL activity compared with wild type donor cells 7–10 days following transfer (64). Previously, blockade of LIGHT using soluble LTβR-Ig or anti-LIGHT Ab was found to reduced severity of GVHD in this system (12). Notably, cotransfer of WT and $LIGHT^{-/-}$ T cells showed that wild-type donor cells had a significant survival advantage after 11 days (64).

That study (64), taken together with the results reported here, indicate that HVEM, LIGHT, and BTLA all have similar actions on promoting donor cell survival in the parental-into-F_1 model of GVHD. We have independently confirmed that $HVEM^{-/-}$ donor cells show reduced survival in this model (data not shown), as reported previously (64). If HVEM signaling, activated by LIGHT or LTα, delivers a prosurvival signal required for donor cell maintenance, then our results suggest that BTLA may be playing some role in augmenting this signaling pathway. Thus, sustaining a chronic alloresponse may require a complex involving BTLA, LIGHT, and HVEM. In the absence of BTLA, the LIGHT-HVEM complex may either induce an apoptotic signal or be insufficient to maintain cell expansion and survival. In summary, our data identify a condition in which BTLA unexpectedly promotes, rather than inhibits, an immune response. We do not know whether this

action is mediated by BTLA signaling or by BTLA acting as a ligand for HVEM, with HVEM mediating the prosurvival signals. Distinguishing between these and other possibilities will likely require extensive additional analysis and involve mutations of both BTLA and HVEM.

Disclosures

The authors have no financial conflict of interest.

References

1. Watanabe, N., M. Gavrieli, J. R. Sedy, J. Yang, F. Fallarino, S. K. Loftin, M. A. Hurchla, N. Zimmerman, J. Sim, X. Zang, et al. 2003. BTLA is a lymphocyte inhibitory receptor with similarities to CTLA-4 and PD-1. *Nat. Immunol.* 4: 670–679.
2. Hurchla, M. A., J. R. Sedy, M. Gavrielli, C. G. Drake, T. L. Murphy, and K. M. Murphy. 2005. B and T lymphocyte attenuator exhibits structural and expression polymorphisms and is highly induced in anergic $CD4^+$ T cells. *J. Immunol.* 174: 3377–3385.
3. Gavrieli, M., N. Watanabe, S. K. Loftin, T. L. Murphy, and K. M. Murphy. 2003. Characterization of phosphotyrosine binding motifs in the cytoplasmic domain of B and T lymphocyte attenuator required for association with protein tyrosine phosphatases SHP-1 and SHP-2. *Biochem. Biophys. Res. Commun.* 312: 1236–1243.
4. Krieg, C., P. Han, R. Stone, O. D. Goularte, and J. Kaye. 2005. Functional analysis of B and T lymphocyte attenuator engagement on $CD4^+$ and $CD8^+$ T cells. *J. Immunol.* 175: 6420–6427.
5. Sedy, J. R., M. Gavrieli, K. G. Potter, M. A. Hurchla, R. C. Lindsley, K. Hildner, S. Scheu, K. Pfeffer, C. F. Ware, T. L. Murphy, and K. M. Murphy. 2005. B and T lymphocyte attenuator regulates T cell activation through interaction with herpesvirus entry mediator. *Nat. Immunol.* 6: 90–98.
6. Croft, M. 2005. The evolving crosstalk between co-stimulatory and co-inhibitory receptors: HVEM-BTLA. *Trends Immunol.* 26: 292–294.
7. Chemnitz, J. M., A. R. Lanfranco, I. Braunstein, and J. L. Riley. 2006. B and T lymphocyte attenuator-mediated signal transduction provides a potent inhibitory signal to primary human CD4 T cells that can be initiated by multiple phosphotyrosine motifs. *J. Immunol.* 176: 6603–6614.
8. Gavrieli, M., and K. M. Murphy. 2006. Association of Grb-2 and PI3K p85 with phosphotyrosile peptides derived from BTLA. *Biochem. Biophys. Res. Commun.* 345: 1440–1445.
9. Mauri, D. N., R. Ebner, R. I. Montgomery, K. D. Kochel, T. C. Cheung, G. L. Yu, S. Ruben, M. Murphy, R. J. Eisenberg, G. H. Cohen, et al. 1998. LIGHT, a new member of the TNF superfamily, and lymphotoxin α are ligands for herpesvirus entry mediator. *Immunity* 8: 21–30.
10. Scheu, S., J. Alferink, T. Potzel, W. Barchet, U. Kalinke, and K. Pfeffer. 2002. Targeted disruption of LIGHT causes defects in costimulatory T cell activation and reveals cooperation with lymphotoxin β in mesenteric lymph node genesis. *J. Exp. Med.* 195: 1613–1624.
11. Tamada, K., K. Shimozaki, A. I. Chapoval, Y. Zhai, J. Su, S. F. Chen, S. L. Hsieh, S. Nagata, J. Ni, and L. Chen. 2000. LIGHT, a TNF-like molecule, costimulates T cell proliferation and is required for dendritic cell-mediated allogeneic T cell response. *J. Immunol.* 164: 4105–4110.
12. Tamada, K., K. Shimozaki, A. I. Chapoval, G. Zhu, G. Sica, D. Flies, T. Boone, H. Hsu, Y. X. Fu, S. Nagata, et al. 2000. Modulation of T cell-mediated immunity in tumor and graft-versus-host disease models through the LIGHT co-stimulatory pathway. *Nat. Med.* 6: 283–289.
13. Gonzalez, L. C., K. M. Loyet, J. Calemine-Fenaux, V. Chauhan, B. Wranik, W. Ouyang, and D. L. Eaton. 2005. A coreceptor interaction between the CD28 and TNF receptor family members B and T lymphocyte attenuator and herpesvirus entry mediator. *Proc. Natl. Acad. Sci. USA* 102: 1116–1121.
14. Compaan, D. M., L. C. Gonzalez, I. Tom, K. M. Loyet, D. Eaton, and S. G. Hymowitz. 2005. Attenuating lymphocyte activity: the crystal structure of the BTLA-HVEM complex. *J. Biol. Chem.* 280: 39553–39561.
15. Cheung, T. C., I. R. Humphreys, K. G. Potter, P. S. Norris, H. M. Shumway, B. R. Tran, G. Patterson, R. Jean-Jacques, M. Yoon, P. G. Spear, et al. 2005. Evolutionarily divergent herpesviruses modulate T cell activation by targeting the herpesvirus entry mediator cosignaling pathway. *Proc. Natl. Acad. Sci. USA* 102: 13218–13223.
16. Reddy, P., and J. L. Ferrara. 2003. Immunobiology of acute graft-versus-host disease. *Blood Rev.* 17: 187–194.
17. Welniak, L. A., B. R. Blazar, and W. J. Murphy. Immunobiology of allogeneic hematopoietic stem cell transplantation. *Annu. Rev. Immunol.* In press.
18. Shearer, G. M., and R. P. Polisson. 1980. Mutual recognition of parental and F_1 lymphocytes: selective abrogation of cytotoxic potential of F_1 lymphocytes by parental lymphocytes. *J. Exp. Med.* 151: 20–31.
19. Hakim, F. T., S. O. Sharrow, S. Payne, and G. M. Shearer. 1991. Repopulation of host lymphohematopoietic systems by donor cells during graft-versus-host reaction in unirradiated adult F_1 mice injected with parental lymphocytes. *J. Immunol.* 146: 2108–2115.
20. Via, C. S. 1991. Kinetics of T cell activation in acute and chronic forms of murine graft-versus-host disease. *J. Immunol.* 146: 2603–2609.
21. Via, C. S., S. O. Sharrow, and G. M. Shearer. 1987. Role of cytotoxic T lymphocytes in the prevention of lupus-like disease occurring in a murine model of graft-vs-host disease. *J. Immunol.* 139: 1840–1849.
22. Ferrara, J. L. 1993. Cytokine dysregulation as a mechanism of graft versus host disease. *Curr. Opin. Immunol.* 5: 794–799.
23. Iwasaki, T., T. Hamano, K. Saheki, T. Kuroiwa, Y. Kataoka, Y. Takemoto, A. Ogata, J. Fujimoto, and E. Kakishita. 2000. Graft-versus-host-disease-associated donor cell engraftment in an F-1 hybrid model is dependent upon the Fas pathway. *Immunology* 99: 94–100.
24. Gleichmann, E., E. H. Van Elven, and J. P. Van der Veen. 1982. A systemic lupus erythematosus (SLE)-like disease in mice induced by abnormal T-B cell cooperation: preferential formation of autoantibodies characteristic of SLE. *Eur. J. Immunol.* 12: 152–159.
25. Dewit, D., M. Vanmechelen, C. Zanin, J. M. Doutrelepont, T. Velu, C. Gerard, D. Abramowicz, J. P. Scheerlinck, P. Debaetselier, J. Urbain, et al. 1993. Preferential activation of Th2 cells in chronic graft-versus-host reaction. *J. Immunol.* 150: 361–366.
26. Tschetter, J. R., E. Mozes, and G. M. Shearer. 2000. Progression from acute to chronic disease in a murine parent-into-F_1 model of graft-versus-host disease. *J. Immunol.* 165: 5987–5994.
27. Blazar, B. R., A. H. Sharpe, P. A. Taylor, A. PanoskaltsisMortari, G. S. Gray, R. Korngold, and D. A. Vallera. 1996. Infusion of anti-B7.1 (CD80) and anti-B7.2 (CD86) monoclonal antibodies inhibits murine graft-versus-host disease lethality in part via direct effects on $CD4^+$ and $CD8^+$ T cells. *J. Immunol.* 157: 3250–3259.
28. Lang, T. J., P. Nguyen, R. Peach, W. C. Gause, and C. S. Via. 2002. In vivo CD86 blockade inhibits $CD4^+$ T cell activation, whereas CD80 blockade potentiates $CD8^+$ T cell activation and CTL effector function. *J. Immunol.* 168: 3786–3792.
29. Blazar, B. R., P. A. Taylor, P. S. Linsley, and D. A. Vallera. 1994. In vivo blockade of CD28/CTLA4: B7/BB1 interaction with CTLA4-Ig reduces lethal murine graft-versus-host disease across the major histocompatibility complex barrier in mice. *Blood* 83: 3815–3825.
30. Hakim, F. T., R. Cepeda, G. S. Gray, C. H. June, and R. Abe. 1995. Acute graft-versus-host reaction can be aborted by blockade of costimulatory molecules. *J. Immunol.* 155: 1757–1766.
31. Via, C. S., V. Rus, P. Nguyen, P. Linsley, and W. C. Gause. 1996. Differential effect of CTLA4Ig on murine graft-versus-host disease (GVHD) development—CTLA4Ig prevents both acute and chronic GVHD development but reverses only chronic GVHD. *J. Immunol.* 157: 4258–4267.
32. Yu, X. Z., P. J. Martin, and C. Anasetti. 1998. Role of CD28 in acute graft-versus-host disease. *Blood* 92: 2963–2970.
33. Ogawa, S., G. Nagamatsu, M. Watanabe, S. Watanabe, T. Hayashi, S. Horita, K. Nitta, H. Nihei, K. Tezuka, and R. Abe. 2001. Opposing effects of anti-activation-inducible lymphocyte-immunomodulatory molecule/inducible costimulator antibody on the development of acute versus chronic graft-versus-host disease. *J. Immunol.* 167: 5741–5748.
34. Blazar, B. R., P. A. Taylor, A. Panoskaltsis-Mortari, A. H. Sharpe, and D. A. Vallera. 1999. Opposing roles of CD28:B7 and CTLA-4:B7 pathways in regulating in vivo alloresponses in murine recipients of MHC disparate T cells. *J. Immunol.* 162: 6368–6377.
35. Blazar, B. R., B. M. Carreno, A. Panoskaltsis-Mortari, L. Carter, Y. Iwai, H. Yagita, H. Nishimura, and P. A. Taylor. 2003. Blockade of programmed death-1 engagement accelerates graft-versus-host disease lethality by an IFN-γ-dependent mechanism. *J. Immunol.* 171: 1272–1277.
36. Li, J., G. Huston, and S. L. Swain. 2003. IL-7 promotes the transition of CD4 effectors to persistent memory cells. *J. Exp. Med.* 198: 1807–1815.
37. Kondrack, R. M., J. Harbertson, J. T. Tan, M. E. McBreen, C. D. Surh, and L. M. Bradley. 2003. Interleukin-7 regulates the survival and generation of memory CD4 cells. *J. Exp. Med.* 198: 1797–1806.
38. Seddon, B., P. Tomlinson, and R. Zamoyska. 2003. Interleukin-7 and T cell receptor signals regulate homeostasis of CD4 memory cells. *Nat.* 4: 680–686.
39. Hoshino, K., H. Tsutsui, T. Kawai, K. Takeda, K. Nakanishi, Y. Takeda, and S. Akira. 1999. Cutting edge: generation of IL-18 receptor-deficient mice—evidence for IL-1 receptor-related protein as an essential IL-18 binding receptor. *J. Immunol.* 162: 5041–5044.
40. Murphy, K. M., and S. L. Reiner. 2002. The lineage decisions of helper T cells. *Nat. Rev. Immunol.* 2: 933–944.
41. Jedema, I., N. M. van der Werff, R. M. Barge, R. Willemze, and J. H. Falkenburg. 2004. New CFSE-based assay to determine susceptibility to lysis by cytotoxic T cells of leukemic precursor cells within a heterogeneous target cell population. *Blood* 103: 2677–2682.
42. Morris, S. C., R. L. Cheek, P. L. Cohen, and R. A. Eisenberg. 1990. Autoantibodies in chronic graft versus host result from cognate T-B interactions. *J. Exp. Med.* 171: 503–517.
43. Mitcham, J. L., P. Parnet, T. P. Bonnert, K. E. Garka, M. J. Gerhart, J. L. Slack, M. A. Gayle, S. K. Dower, and J. E. Sims. 1996. T1/ST2 signaling establishes it as a member of an expanding interleukin-1 receptor family. *J. Biol. Chem.* 271: 5777–5783.
44. Han, P., O. D. Goularte, K. Rufner, B. Wilkinson, and J. Kaye. 2004. An inhibitory Ig superfamily protein expressed by lymphocytes and APCs is also an early marker of thymocyte positive selection. *J. Immunol.* 172: 5931–5939.
45. Deppong, C., T. I. Juehne, M. Hurchla, L. D. Friend, D. D. Shah, C. M. Rose, T. L. Bricker, L. P. Shornick, E. C. Crouch, T. L. Murphy, et al. 2006. Cutting edge: B and T lymphocyte attenuator and programmed death receptor-1 inhibitory receptors are required for termination of acute allergic airway inflammation. *J. Immunol.* 176: 3909–3913.
46. Krieg, C., O. Boyman, Y. X. Fu, and J. Kaye. 2007. B and T lymphocyte attenuator regulates $CD8^+$ T cell-intrinsic homeostasis and memory cell generation. *Nat. Immunol.* 8: 162–171.

47. Corry, R. J., H. J. Winn, and P. S. Russell. 1973. Primarily vascularized allografts of hearts in mice. The role of H-2D, H-2K, and non-H-2 antigens in rejection. *Transplantation* 16: 343–350.
48. Tao, R., L. Wang, R. Han, T. Wang, Q. Ye, T. Honjo, T. L. Murphy, K. M. Murphy, and W. W. Hancock. 2005. Differential effects of B and T lymphocyte attenuator and programmed death-1 on acceptance of partially versus fully MHC-mismatched cardiac allografts. *J. Immunol.* 175: 5774–5782.
49. Gleichmann, E., and H. Gleichmann. 1985. Pathogenesis of graft-versus-host reactions (GVHR) and GVH-like diseases. *J. Invest. Dermatol.* 85: 115s–120s.
50. Shustov, A., I. Luzina, P. Nguyen, J. C. Papadimitriou, B. Handwerger, K. B. Elkon, and C. S. Via. 2000. Role of perforin in controlling B cell hyperactivity and humoral autoimmunity. *J. Clin. Invest.* 106: R39–R47.
51. Baker, M. B., R. L. Riley, E. R. Podack, and R. B. Levy. 1997. Graft-versus-host-disease-associated lymphoid hypoplasia and B cell dysfunction is dependent upon donor T cell-mediated Fas-ligand function, but not perforin function. *Proc. Natl. Acad. Sci. USA* 94: 1366–1371.
52. Ellison, C. A., J. M. Fischer, K. T. HayGlass, and J. G. Gartner. 1998. Murine graft-versus-host disease in an F_1-hybrid model using IFN-γ gene knockout donors. *J. Immunol.* 161: 631–640.
53. Murphy, W. J., L. A. Welniak, D. D. Taub, R. H. Wiltrout, P. A. Taylor, D. A. Vallera, M. Kopf, H. Young, D. L. Longo, and B. R. Blazar. 1998. Differential effects of the absence of interferon-γ and IL-4 in acute graft-versus-host disease after allogeneic bone marrow transplantation in mice. *J. Clin. Invest.* 102: 1742–1748.
54. Krenger, W., K. M. Snyder, J. C. H. Byon, G. Falzarano, and J. L. M. Ferrara. 1995. Polarized type-2 alloreactive $Cd4^+$ and $Cd8^+$ donor T cells fail to induce experimental acute graft-versus-host disease. *J. Immunol.* 155: 585–593.
55. Fowler, D. H., K. Kurasawa, A. Husebekk, P. A. Cohen, and R. E. Gress. 1994. Cells of Th2 cytokine phenotype prevent LPS-induced lethality during murine graft-versus-host reaction: regulation of cytokines and $CD8^+$ lymphoid engraftment. *J. Immunol.* 152: 1004–1013.
56. Rus, V., A. Svetic, P. Nguyen, W. C. Gause, and C. S. Via. 1995. Kinetics of Th1 and Th2 cytokine production during the early course of acute and chronic murine graft-versus-host disease: regulatory role of donor $CD8^+$ T cells. *J. Immunol.* 155: 2396–2406.
57. Smeltz, R. B., J. Chen, J. Hu-Li, and E. M. Shevach. 2001. Regulation of interleukin (IL)-18 receptor α chain expression on $CD4^+$ T cells during T helper (Th)1/Th2 differentiation: critical downregulatory role of IL-4. *J. Exp. Med.* 194: 143–153.
58. Kim, C. H., E. J. Kunkel, J. Boisvert, B. Johnston, J. J. Campbell, M. C. Genovese, H. B. Greenberg, and E. C. Butcher. 2001. Bonzo/CXCR6 expression defines type 1-polarized T cell subsets with extralymphoid tissue homing potential. *J. Clin. Invest.* 107: 595–601.
59. Tan, J. T., E. Dudl, E. LeRoy, R. Murray, J. Sprent, K. I. Weinberg, and C. D. Surh. 2001. IL-7 is critical for homeostatic proliferation and survival of naive T cells. *Proc. Natl. Acad. Sci. USA* 98: 8732–8737.
60. Zhang, Y., G. Joe, E. Hexner, J. Zhu, and S. G. Emerson. 2005. Alloreactive memory T cells are responsible for the persistence of graft-versus-host disease. *J. Immunol.* 174: 3051–3058.
61. Zhang, Y., G. Joe, E. Hexner, J. Zhu, and S. G. Emerson. 2005. Host-reactive $CD8^+$ memory stem cells in graft-versus-host disease. *Nat. Med.* 11: 1299–1305.
62. Freeden-Jeffry, U., N. Solvason, M. Howard, and R. Murray. 1997. The earliest T lineage-committed cells depend on IL-7 for Bcl-2 expression and normal cell cycle progression. *Immunity* 7: 147–154.
63. Sharfe, N., H. K. Dadi, and C. M. Roifman. 1995. JAK3 protein tyrosine kinase mediates interleukin-7-induced activation of phosphatidylinositol-3′ kinase. *Blood* 86: 2077–2085.
64. Xu, Y., A. S. Flies, D. B. Flies, G. Zhu, S. Anand, S. J. Flies, H. Xu, R. A. Anders, W. W. Hancock, L. Chen, and K. Tamada. Selective targeting of the LIGHT-HVEM co-stimulatory system for the treatment of graft-versus-host disease. *Blood.* In press.

The Journal of Immunology

Unexpected Role of B and T Lymphocyte Attenuator in Sustaining Cell Survival during Chronic Allostimulation

Michelle A. Hurchla, John R. Sedy and Kenneth M. Murphy

J. Immunol. 2007;178;6073-6082
http://www.jimmunol.org/cgi/content/full/178/10/6073

The Journal of Immunology is published twice each month by The American Association of Immunologists, Inc., 9650 Rockville Pike, Bethesda, MD 20814-3994.

Print ISSN: 0022-1767 Online ISSN: 1550-6606.

Unexpected Role of B and T Lymphocyte Attenuator in Sustaining Cell Survival during Chronic Allostimulation

Michelle A. Hurchla,* John R. Sedy,* and Kenneth M. Murphy[1]*†

B and T lymphocyte attenuator (BTLA; CD272) can deliver inhibitory signals to B and T cells upon binding its ligand herpesvirus entry mediator. Because CD28, CTLA-4, programmed death-1, and ICOS regulate the development of acute graft-vs-host disease (GVHD), we wished to assess if BTLA also played a role in this T cell-mediated response. In the nonirradiated parental-into-F_1 model of acute GVHD, *BTLA*$^{+/+}$ and *BTLA*$^{-/-}$ donor lymphocytes showed equivalent engraftment and expansion during the first week of the alloresponse. Unexpectedly, *BTLA*$^{-/-}$ donor T cells failed to sustain GVHD, showing a decline in surviving donor cell numbers beginning at day 9 and greatly reduced by day 11. Similarly, inhibition of BTLA-herpesvirus entry mediator engagement by in vivo administration of a blocking anti-BTLA Ab also caused reduced survival of donor cells. Microarray analysis revealed several genes that were differentially expressed by *BTLA*$^{-/-}$ and *BTLA*$^{+/+}$ donor CD4$^+$ T cells preceding the decline in *BTLA*$^{-/-}$ donor T cells. Several genes influencing Th cell polarization were differentially expressed by *BTLA*$^{+/+}$ and *BTLA*$^{-/-}$ donor cells. Additionally, the re-expression of the IL-7Rα subunit that occurs in *BTLA*$^{+/+}$ donor cells after 1 wk of in vivo allostimulation was not observed in *BTLA*$^{-/-}$ donor CD4$^+$ cells. The striking loss of *BTLA*$^{-/-}$ T cells in this model indicates a role for BTLA activity in sustaining CD4$^+$ T cell survival under the conditions of chronic stimulation in the nonirradiated parental-into-F_1 GVHD. ***The Journal of Immunology,*** **2007, 178: 6073–6082.**

B and T lymphocyte attenuator (BTLA)[2] is a lymphoid-specific cell surface receptor that is expressed by B cells, T cells, dendritic cells, macrophages, and NK cells in C57BL/6 mice (1–4). BTLA shows both structural and expression polymorphisms in mice, with BALB/c and C57BL/6 alleles differing at 10 aa within the extracellular region, and the BALB/c allele lacking expression by macrophages or NK cells (2). Functional analysis has suggested that BTLA exerts inhibitory actions, indicating a role more similar to CTLA-4 and programmed death-1 (PD-1) than to activating receptors of the CD28/B7 family (1, 4).

BTLA represses Ag-driven T cell proliferation upon binding its ligand, herpesvirus entry mediator (HVEM) (5), a member of the TNFR superfamily, expressed mainly by T lymphocytes and immature dendritic cells (6). An agonist Ab to murine BTLA inhibits IL-2 secretion and T cell proliferation in vitro, further suggesting an inhibitory role for BTLA (4). Phosphorylation of BTLA leads to recruitment of Src homology domain 2-containing protein tyrosine phosphatases (SHP-1 and SHP-2) to two tyrosine motifs in the cytoplasmic domain of mouse and human BTLA (3, 5). Human BTLA possesses an additional tyrosine residue that may also participate in inhibitory signaling (7). BTLA expression is increased on in vivo-anergized T cells, but not on CD25$^+$ T regulatory cells, in contrast to CTLA-4 and PD-1, suggesting it may have a distinct role in modulating immune responses (2). Notably, mouse and human BTLA contain a conserved intracellular tyrosine motif suggestive of a Grb-2 recruitment site (1, 3), which can interact with Grb-2 and the p85 subunit of PI3K in vitro (8). Although the function of this region has not been established, it suggests that BTLA may have the capability to function in a costimulatory or prosurvival manner.

The effects of BTLA-HVEM interactions may also be influenced by the interactions of HVEM with its additional ligands, tumor necrosis family members LIGHT (TNFSF14) and lymphotoxin (LT)α (9). In contrast to the inhibitory nature of BTLA-HVEM interactions, HVEM-LIGHT binding exerts a costimulatory effect on T cell activation (10–12). This regulatory network is increasingly complex because HVEM has the potential to bind BTLA and LIGHT simultaneously (13–15). Consequently, the balance between costimulatory and inhibitory signals may be regulated by a complex including BTLA, HVEM, and LIGHT.

Graft-vs-host disease (GVHD) is an immune response against alloantigens, such as foreign MHC molecules (reviewed in Refs. 16 and 17). In the parental-into-F_1 model of GVHD, parental T cells react against alloantigens of the F_1 host, whereas F_1 host T cells are tolerant to parental cells (18, 19). The type of GVHD that develops in nonirradiated, immunocompetent F_1 recipients is dependent on the strain of parental donor cells transferred (18). In the most widely reported version of this model, transfer of C57BL/6 (H-2^b) splenocytes into a nonirradiated, immunocompetent C57BL/6 × DBA/2 F_1 (B6D2F_1; H-2$^{b/d}$) host induces acute GVHD (aGVHD), characterized by a Th1 cytokine driven, cell-mediated response against host tissues (18, 20). Donor T cells exert cytotoxic effects through Fas-Fas ligand interactions, perforin, and inflammatory cytokines (21–23). In contrast, transfer of DBA/2 (H-2^d) splenocytes into B6D2F_1 hosts results in a chronic form of GVHD (cGVHD), characterized by production of Th2 cytokines and activation of host B cells, resulting in

*Department of Pathology and Center for Immunology and †Howard Hughes Medical Institute, Washington University School of Medicine, St. Louis, MO 63110

Received for publication October 2, 2006. Accepted for publication March 7, 2007.

The costs of publication of this article were defrayed in part by the payment of page charges. This article must therefore be hereby marked *advertisement* in accordance with 18 U.S.C. Section 1734 solely to indicate this fact.

[1] Address correspondence and reprint requests to Dr. Kenneth M. Murphy, Department of Pathology, Washington University School of Medicine, 660 South Euclid Avenue, St. Louis, MO 63110. E-mail address: murphy@pathology.wustl.edu

[2] Abbreviations used in this paper: BTLA, B and T lymphocyte attenuator; 7-AAD, 7-aminoactinomycin; GVHD, graft-vs-host disease; aGVHD, acute GVHD; cGVHD, chronic form of GVHD; HVEM, herpesvirus entry mediator; LIGHT, homologous to lymphotoxins, exhibits inducible expression, and competes with HSV glycoprotein D for HVEM, a receptor expressed by T lymphocytes; LT, lymphotoxin; PD-1, programmed death-1.

autoantibody development and a systemic lupus erythematosus-like syndrome (24, 25).

In this study, a related parental-into-F_1 model of GVHD was examined. In this model, transfer of C57BL/6 donor cells into C57BL/6 × BALB/c F_1 ($CB6F_1$; H-$2^{b/d}$) yields aGVHD, whereas BALB/c donor cells produce chronic GVHD (26). Although GVHD induced in $CB6F_1$ mice is generally similar to that in $B6D2F_1$, as described above, strain-dependent differences have been identified. BALB/c-into-$CB6F_1$ resulted in chronic GVHD that was comparable to that of DBA/2-into-$B6D2F_1$ (26). The aGVHD resulting from C57BL/6-into-$CB6F_1$, characterized by donor cell expansion and antihost CTL activity, was similar to that in C57BL/6-into-$B6D2F_1$ during the first 3 wk following transfer (26). After 3 wk, while C57BL/6 donor cells continued to expand in $B6D2F_1$ hosts, the percentage of parental cells progressively decreased in $CB6F_1$ hosts (26). By 12 wk, the C57BL/6-into-$CB6F_1$ mice had transitioned to cGVHD, with an absence of antihost CTL activity and the development of autoantibodies (26). In this study, we analyze the 2 wk following transfer of C57BL/6-into-$CB6F_1$, a point at which only aGVHD parameters are observed.

Costimulatory signals have been demonstrated to be essential to the development of disease in a variety of GVHD models. Blocking B7/CD28 costimulatory interactions with mAbs to B7-1 and B7-2 (27, 28), CTLA-4Ig, a soluble competitive inhibitor of CD28 (29–31), or by using *CD28*$^{-/-}$ splenocytes (32) inhibited donor T cell activation and disease development. Blockade of ICOS signaling strongly suppressed Th2-driven cGVHD disease yet augmented donor T cell expansion in Th1-driven aGVHD (33). Several studies have established that inhibitory receptors slow the development of GVHD. Blocking Abs against CTLA-4 (34) or PD-1 (35) accelerated GVHD following bone marrow transplant. CTLA-4 and PD-1 do not appear fully redundant in their regulation of GVHD because an additive increase in disease severity occurs when both pathways are inhibited (35).

In this study, we use the nonirradiated parental-into-F_1 model of GVHD to examine the function of BTLA in regulating alloresponses. We anticipated that *BTLA*$^{-/-}$ parental cells would have augmented alloreactivity, similar to that seen in the absence of inhibitory signals such as CTLA-4 or PD-1. Unexpectedly, we observed that *BTLA*$^{-/-}$ donor splenocytes are unable to sustain this GVHD response. Although *BTLA*$^{-/-}$ lymphocytes react to host alloantigens and expand in an early effector response, this response is not sustained. In comparison to *BTLA*$^{+/+}$ donor cells, *BTLA*$^{-/-}$ donor T cells undergo a rapid contraction in vivo beginning on day 10, which is accompanied by resolution of GVHD pathology. DNA microarray analysis indicates that $CD4^+$ *BTLA*$^{-/-}$ donor cells have altered expression of several important genes that may influence the effector response or survival of T cells, including IL-7Rα (36–38), IL-18Rα (39), and IL-4 (reviewed in Ref. 40). These results suggest that BTLA may act not only as an inhibitor as shown previously (1, 2, 4, 5) but, under some conditions, may participate in providing signals that promote the immune responses.

Materials and Methods

Reagents

The following Abs used for FACS analysis were from BD Pharmingen: CD4-PE-Cy7 (RM4-5), CD8-PE or allophycocyanin (53-6.7), B220-allophycocyanin (RA3-6B2), H-$2K^d$-FITC or PE (SF1-1.1), H-$2K^b$-FITC or PE (AF6-88.5), IL-15Rβ-PE (TM-β1), IL-6Rα-PE (D7715A7), IFN-γRα-biotin (GR20), BrdU-FITC, annexin V-allophycocyanin, and streptavidin-allophycocyanin. IL-7Rα-FITC (A7R34) and BTLA-PE (6F7, pan-allele specific) were obtained from eBioscience. IL-18Rα-biotin (polyclonal) and goat IgG-biotin were obtained from R&D Systems. Four-color analysis was performed on a FACSCalibur (BD Biosciences) and analyzed using FlowJo (Tree Star). For in vivo blockade, endotoxin-free anti-BTLA (6A6, C57BL/6-allele specific) was purified from hybridoma supernatants according to standard procedures (2). Isotype control hamster IgG was obtained from Jackson ImmunoResearch Laboratories.

Mice

C57BL/6, BALB/c, and C57BL/6 × BALB/c F_1 ($CB6F_1$) mice were bred in our facility. *Btla*$^{-/-}$ mice were backcrossed to C57BL/6 or BALB/c for at least nine generations (1). In some experiments, *BTLA*$^{+/-}$ × *BTLA*$^{+/-}$ (generation 9) littermate mice were used as donors, and the *BTLA* genotypes of mice were determined by surface staining of $B220^+$ peripheral blood cells with 6F7-PE (anti-BTLA). All donor and host mice were 8–12 wk of age and sex matched. Syngeneic $CB6F_1$ mice were used as control donors.

Induction of GVHD

Unless otherwise stated, single-cell suspensions of pooled donor splenocytes were subjected to RBC lysis and suspended in sterile, endotoxin-free HBSS. aGVHD was induced as previously described in Ref. 33, except that 5×10^7 C57BL/6 donor cells (which we found to yield similar results as the reported 6×10^7 cells) were injected via the lateral tail vein into normal, nonirradiated $CB6F_1$ host mice. Control mice received donor cells from syngeneic $CB6F_1$ mice. To induce cGVHD, 8×10^7 pooled BALB/c donor splenocyte were transferred into $CB6F_1$ mice. At indicated time points, splenocytes from each GVHD-induced mouse were analyzed separately.

ELISA for anti-DNA Abs

Serum autoantibodies specific for ssDNA and dsDNA were detected by ELISA. After precoating with 0.01% poly-L-lysine, ELISA plates were coated with 3 μg/ml single-stranded calf thymus DNA (Sigma-Aldrich) or 2.5 μg/ml double-stranded calf thymus DNA (Sigma-Aldrich) in PBS. Nonspecific binding was blocked by incubating with 10% FCS. Serial dilutions of each experimental serum were plated and developed with anti-mouse-IgG-HRP (Southern Biotechnology Associates). Serum from an MRL/*lpr* mouse was used as a positive control for autoantibodies. The OD reading for MRL/*lpr* serum was set to an arbitrary unit of 1, and the level of autoantibody in serum from experimental mice was expressed relative to this value.

In vivo treatment with anti-BTLA mAb

Experimental mice were injected i.p. with 100 μg of purified 6A6 (monoclonal anti-BL/6 BTLA) (2) or control hamster-IgG (Jackson ImmunoResearch Laboratories) at the time of GVHD induction (day 0) or again on day 3 and 6 following transfer, as indicated.

Assessment of proliferation by CFSE dilution and BrdU incorporation

To assess cell division during the initiation of GVHD, donor cells were labeled with 1 μM CFSE (Molecular Probes) before transfer, as in Ref. 5. To assess proliferation at later stages of the response, in vivo 5-BrdU (BD Pharmingen) labeling and FACS staining were conducted according to the manufacturer's suggested protocol (BrdU Flow kit; BD Pharmingen). Briefly, 18 h before harvest, mice were injected i.p. with 1 mg of BrdU in PBS. BrdU incorporation was assessed by FACS staining of fixed and permeabilized cells with anti-BrdU-FITC.

CFSE-based cytotoxicity assay

This FACS-based CTL assay was conducted as reported by Jedema et al. (41), with alterations noted below. Briefly, allogeneic P815 (H-$2K^d$) or syngeneic EL4 (H-$2K^b$) target cells were labeled with 1 μM CFSE. Target cells were suspended in medium at 1×10^5 cells/ml and 100 μl/well plated in round-bottom 96-well plates. Whole splenocytes from GVHD-induced mice, subjected only to RBC lysis, served as effector cells and were plated at the indicated E:T ratios. Plates were incubated for 4 h at 37°C. Wells were harvested, and 7-aminoactinomycin (7-AAD) was added just before FACS analysis. Lysed targets were determined by the percentage of $CFSE^+$ cells that were 7-AAD^+ (Molecular Probes). Nonspecific lysis was assessed in wells without effector cells added. Splenocytes from naive $CB6F_1$ served as a syngeneic control.

Microarray analysis

On days 9 and 10 following GVHD induction, the $CD4^+$ donor-derived population was sorted from pooled splenocytes of several experimental

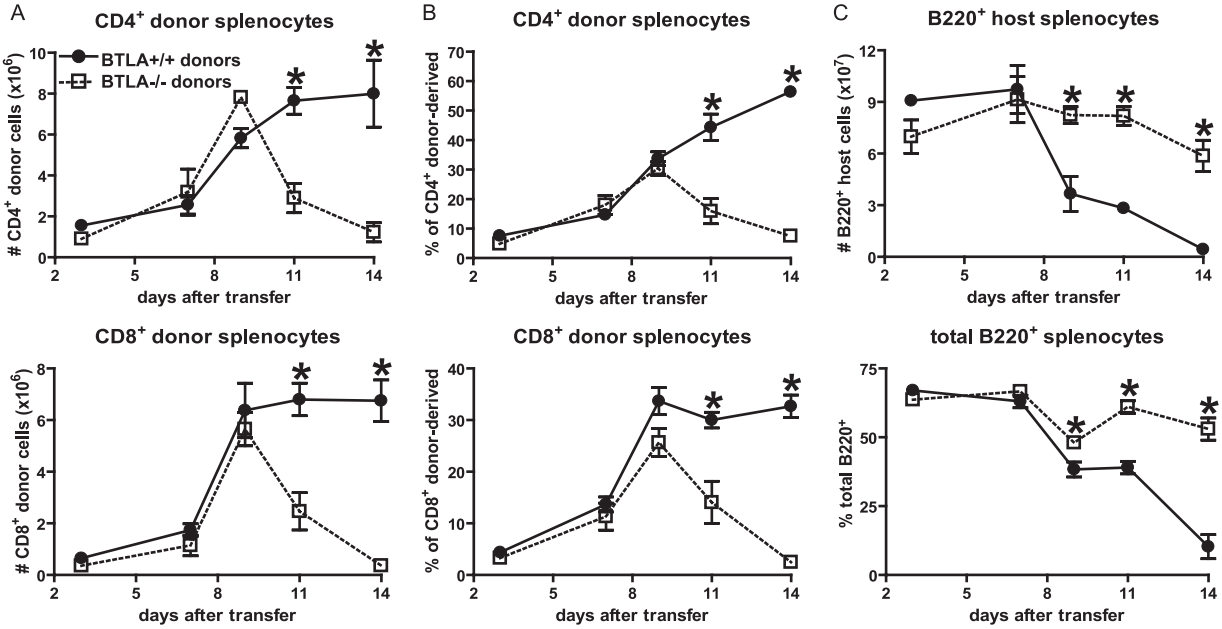

FIGURE 1. C57BL/6 *BTLA*$^{-/-}$ donor T lymphocytes fail to persist long term in CB6F$_1$ hosts. A total of 5×10^7 donor splenocytes from C57BL/6 *BTLA*$^{+/+}$ (H-2^b, ●) or C57BL/6 *BTLA*$^{-/-}$ (H-2^b, □) mice 5 were transferred into CB6F$_1$ (H-2$^{b/d}$) hosts. Spleens were harvested at days 3, 7, 9, 11, and 14 after transfer and analyzed by FACS to establish the kinetics of donor-host chimerism. Donor-derived cells were distinguished by the absence of H-2K^d. *A*, The absolute number of live donor CD4$^+$ (*top panel*) and CD8$^+$ (*bottom panel*) splenocytes were calculated at each time point. *B*, The percentage of splenic CD4$^+$ (*top panel*) or CD8$^+$ (*bottom panel*) compartments that were donor derived is shown at each time point. *C*, *BTLA*$^{-/-}$ donor cells fail to elicit a strong antihost response, as demonstrated by maintenance of the host B cell compartment. The absolute number of live B220$^+$ host splenocytes (*top panel*) and the total percentage of B220$^+$ splenocytes (*bottom panel*) are shown at each time point. Average values were calculated from three mice per group at each time point with error bars indicating SEM. Asterisks indicate time points at which Student's *t* tests indicate significant differences of $p < 0.05$ between *BTLA*$^{+/+}$ and *BTLA*$^{-/-}$ donors. Data are representative of five independent experiments.

mice that had received *BTLA*$^{+/+}$ or *BTLA*$^{-/-}$ and stained with anti-H-2K^d-FITC, anti-BTLA-PE, and anti-CD4-allophycocyanin. Post-sort analysis showed >95% purity of the sorted populations. RNA was extracted with the RNeasy kit (Qiagen). Biotinylated cRNA target was generated using the Two-Cycle cDNA synthesis kit (Affymetrix). Each cRNA was hybridized to the Affymetrix Mouse Genome 430 2.0 array. Data were analyzed using dCHIP (www.dchip.org).

Results

BTLA is required for maintenance of donor lymphocytes in the parental-into-F$_1$ GVHD model

To investigate the functions of BTLA during an in vivo allogeneic immune response stimulated by MHC mismatch, we compared the actions of *BTLA*$^{+/+}$ and *BTLA*$^{-/-}$ cells in a model of parental-into-F$_1$-induced aGVHD. Transfer of C57BL/6 (H-2K^b) *BTLA*$^{+/+}$ splenocytes into unirradiated CB6F$_1$ (H-2$^{b/d}$) hosts elicited a progressive expansion of donor CD4$^+$ and CD8$^+$ lymphocytes characteristic of aGVHD, as expected (Fig. 1, *A* and *B*). However, transfer of *BTLA*$^{-/-}$ cells was unable to sustain donor cell expansion over the course of a 14-day response (Fig. 1, *A* and *B*). To characterize the kinetics of this response, the absolute number (Fig. 1*A*) and percentage (Fig. 1*B*) of donor T cells in the spleens of GVHD-induced mice were assessed by FACS on days 3, 7, 9, 11, and 14 after transfer. Mice receiving either *BTLA*$^{+/+}$ and *BTLA*$^{-/-}$ donor cells showed expansion of donor T cells during the initial 9 days following GVHD induction (Fig. 1, *A* and *B*). However, *BTLA*$^{-/-}$ donor cells began to decline in numbers after day 10, in contrast to the progressive increase in *BTLA*$^{+/+}$ donor CD4$^+$ and CD8$^+$ T cells (Fig. 1, *A* and *B*). To investigate whether BTLA expressed by host cells was important in controlling GVHD, donor cells were also transferred into *BTLA*$^{-/-}$ CB6F$_1$ hosts. Again, *BTLA*$^{+/+}$ T cells continually expanded in *BTLA*$^{-/-}$ recipients, whereas *BTLA*$^{-/-}$ T cells showed a rapid contraction by days 11 and 14, suggesting that BTLA expressed by the host is not required for maintenance of GVHD by donor cells (data not shown).

The inability of *BTLA*$^{-/-}$ donor lymphocytes to sustain aGVHD was also demonstrated by the absence of an antihost cytotoxic response, apparent from the lack of depletion of the host B220$^+$ population (Fig. 1*C*). On day 14, spleens from mice receiving *BTLA*$^{+/+}$ cells were <10% B220$^+$, indicating cytolysis of host B cells, as expected. In contrast, mice receiving *BTLA*$^{-/-}$ cells retained a normal number of B cells, ~60% of splenocytes.

To determine whether *BTLA*$^{-/-}$ donor lymphocytes were engrafting and expanding, we transferred and analyzed CFSE-labeled donor cells (Fig. 2). CD4$^+$ and CD8$^+$ T cells from *BTLA*$^{+/+}$ and *BTLA*$^{-/-}$ donors showed similar percentages and numbers of cells that had undergone division after 3 days (Fig. 2). These results indicate that later disappearance of *BTLA*$^{-/-}$ donor cells is not due to a failure in initial activation by host alloantigens. We also used *BTLA*$^{+/+}$, *BTLA*$^{+/-}$, and *BTLA*$^{-/-}$ littermates generated from an intercross of C57BL/6 *BTLA*$^{+/-}$ mice as donor cells to test for any minor histocompatibility mismatch with CB6F$_1$ host mice. Again, only the *BTLA*$^{-/-}$ donor cells failed to survive at day 14, whereas both *BTLA*$^{+/+}$ and *BTLA*$^{+/-}$ donor cells expanded to occupy 60–70% of the CD4$^+$ and CD8$^+$ compartments (Fig. 3), suggesting that the findings were due to the absence of donor cell BTLA expression rather than a result of transplant incompatibility.

We also evaluated a model of cGVHD characterized by gradual development of a Th2 cytokine-induced, autoantibody-mediated disease (24, 25). Transfer of BALB/c *BTLA*$^{+/+}$ donor splenocytes into CB6F$_1$ hosts induced expansion of CD4$^+$ and CD8$^+$ donor T cells (although to a lower extent than seen in aGVHD, as expected (26)), the development of anti-dsDNA and anti-ssDNA Abs and activation of host-derived B cells as measured by CD69 induction

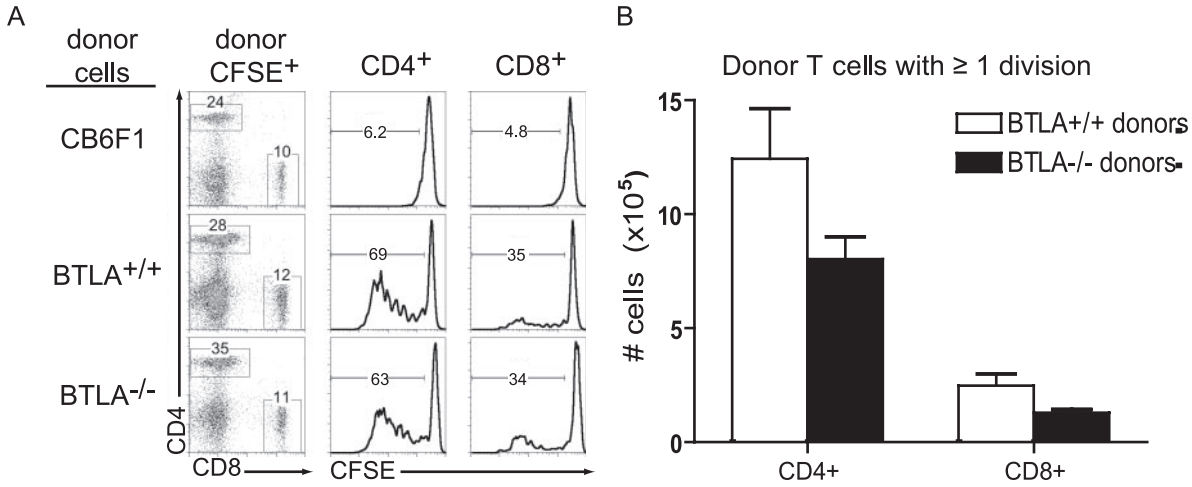

FIGURE 2. *BTLA*$^{-/-}$ donor cells engraft and divide during the initiation stage of GVHD. A total of 5×10^7 CFSE-labeled CB6F$_1$, C57BL/6 *BTLA*$^{+/+}$, or *BTLA*$^{-/-}$ splenocytes were transferred to CB6F$_1$ host mice. Splenocytes were harvested 3 days posttransfer and gated on live, CFSE$^+$ donor lymphocytes by FACS. *A*, Donor cells were divided into CD4$^+$ and CD8$^+$ populations (first column), and the percentage of the donor CD4$^+$ (second column) and CD8$^+$ (third column) populations that had undergone one or more divisions was assessed by CFSE dilution. Histogram gates indicate the percentage of each population undergoing one or more divisions. *B*, Following the gating scheme above, the absolute number of donor cells that had undergone one or more divisions was calculated. Bar graphs show an average of three mice, with error bars indicating SEM (*BTLA*$^{+/+}$ donors, □; *BTLA*$^{-/-}$ donors, ■). Student's *t* tests did not show significant differences between *BTLA*$^{+/+}$ and *BTLA*$^{-/-}$ donor cells (CD4$^+$, $p = 0.143$; CD8$^+$, $p = 0.084$). Data are representative of two independent experiments.

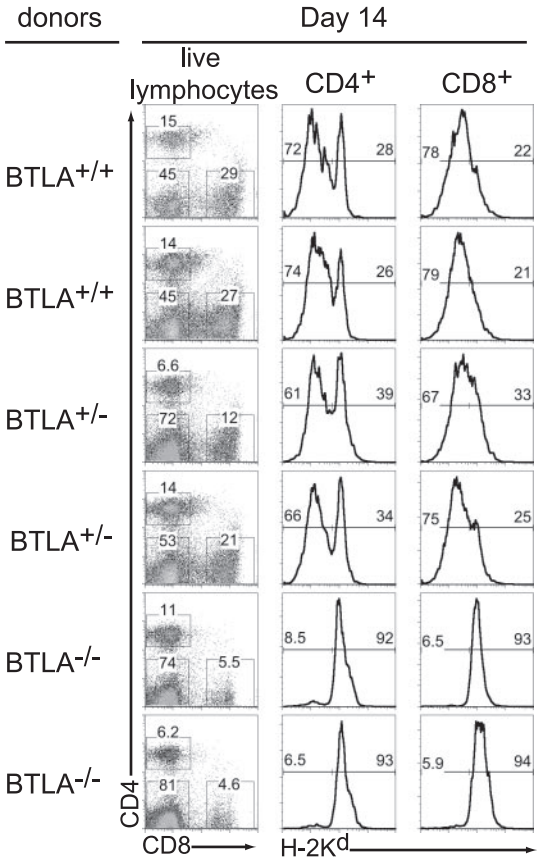

FIGURE 3. Failed survival of *BTLA*$^{-/-}$ donor cells cannot be attributed to a minor histocompatibility mismatch. *BTLA*$^{+/+}$, *BTLA*$^{+/-}$, or *BTLA*$^{-/-}$ littermates from a *BTLA*$^{+/-}$ × *BTLA*$^{+/-}$ breeding (generation 9 backcross to C57BL/6) were used as donor splenocytes. Donor mice were tail bled and BTLA genotyped confirmed by FACS staining of B220$^+$ cells before transfer (data not shown). Donor splenocytes (5×10^7) from a single mouse were transferred into a CB6F$_1$ host and harvested on day 14. The percentage of donor-derived cells (H-2K^d negative) in the CD4$^+$ (second column) and CD8$^+$ (third column) populations are indicated by the *left gate* on each histogram. The H-2K^d-positive population (*right gates*) indicates host cells.

(Fig. 4), as expected for BALB/c donors (25, 42). Kinetic analysis revealed that BALB/c *BTLA*$^{-/-}$ donor T lymphocytes expand equivalently to *BTLA*$^{+/+}$ cells during the initial 10 days following transfer (Fig. 4*A*). However, similar to the transfer of C57BL/6 donor cells, BALB/c *BTLA*$^{-/-}$ donor CD4$^+$ and CD8$^+$ cells rapidly contract by day 12 of the response (Fig. 4*A*). Transfer of BALB/c *BTLA*$^{-/-}$ donor splenocytes also failed to show the induction of anti-DNA autoantibodies characteristic of cGVHD (Fig. 4*B*). Additionally, host B cells from mice receiving *BTLA*$^{-/-}$ donor cells were not activated, as measured by a failure to up-regulate CD69 (Fig. 4*C*). Thus, BALB/c *BTLA*$^{-/-}$ donor cells show a similar defect in sustaining cGVHD as was found for C57BL/6 BTLA$^{-/-}$ donor cells in sustaining aGVHD.

BTLA blockade by Ab treatment prevents maintenance of BTLA$^{+/+}$ *donor lymphocyte in aGVHD*

The 6A6 mAb is specific for the C57BL/6 allele of BTLA and blocks binding to its ligand HVEM (2). Administration of 6A6 at the time of transfer of *BTLA*$^{+/+}$ donor cells resulted in a loss of donor lymphocytes by day 14 of the response, similar to the transfer of *BTLA*$^{-/-}$ cells (Fig. 5). To ensure that the abrogation of donor cell expansion was not due to opsonization and rapid host clearance of BTLA-expressing donor cells by the Ab, we examined the kinetics the GVH response in the presence of 6A6 administration. (Fig. 5). Expansion of C57BL/6 *BTLA*$^{+/+}$ donor cells in recipients treated with isotype control or anti-BTLA Ab was equivalent at days 3 and 8 following transfer (Fig. 5). By day 14, few donor CD4$^+$ and CD8$^+$ lymphocytes were present in mice that had received anti-BTLA Abs (Fig. 5). A single Ab treatment at the time of transfer was sufficient to cause the loss of donor cells, as additional Ab administration at days 3 and 6 had no additional effect (data not shown). The observation that blocking BTLA/HVEM interactions through Ab treatment yields the loss of donor cells similar to transfer of *BTLA*$^{-/-}$ splenocytes suggests that the interaction of BTLA with its ligand HVEM is necessary to support the survival of donor lymphocytes in aGVHD.

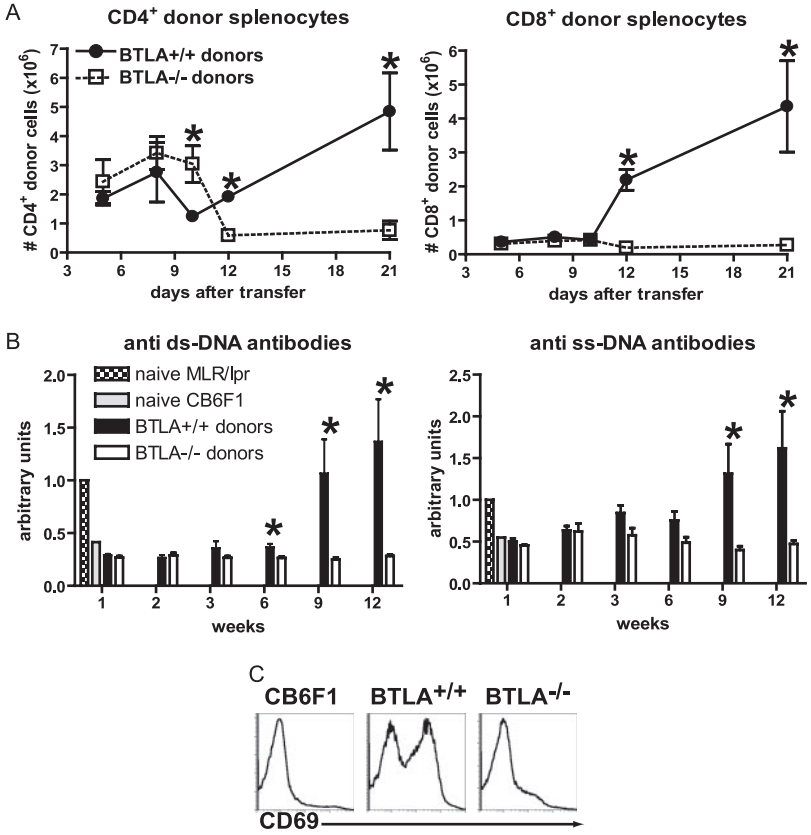

FIGURE 4. Transfer of BALB/c $BTLA^{-/-}$ donor cells fails to elicit a chronic GVHD response. Chronic GVHD was induced by adoptively transferring 8×10^7 BALB/c $BTLA^{+/+}$ or $BTLA^{-/-}$ donor splenocytes into $CB6F_1$ hosts. *A*, Spleens from mice receiving $BTLA^{+/+}$ (●, H-2H^d) or $BTLA^{-/-}$ (□, H-2K^d) donor cells were harvested at days 5, 8, 10, 12, and 21 after transfer and analyzed by FACS as in Fig. 1, except that donor cells were H-2K^b negative. The absolute number of live donor CD4$^+$ (*left panel*) and CD8$^+$ (*right panel*) splenocytes was calculated at each time point. Average values were calculated from three mice per group at each time point with error bars indicating SEM. Asterisks indicate time points at which Student's *t* tests indicate significant differences of $p < 0.05$ between $BTLA^{+/+}$ and $BTLA^{-/-}$ donor cells. *B*, Serum was obtained from GVHD-induced mice at the indicated time points and assessed by ELISA for development of anti-dsDNA (*left graph*) or anti-ssDNA (*right graph*) Abs. Naive MRL/*lpr* mouse serum (▩) was used as a positive control for autoantibodies, whereas naive $CB6F_1$ serum (▨) was used as a negative control. The amount of autoantibody in MRL/*lpr* serum was set to an arbitrary value of 1, and the amount of anti-DNA Ab in serum from mice receiving $BTLA^{+/+}$ cells (■) or $BTLA^{-/-}$ cells (□) was calculated relative to MRL/*lpr* serum. The average of four mice per group is shown, with error bars indicating SEM. Asterisks indicate points at which Student's *t* tests indicate significant differences of $p < 0.05$. *C*, Transfer of $BTLA^{-/-}$ donor cells fails to induce activation of host B cells. Splenocytes were harvested on day 11 after GVHD induction. The expression level of the activation marker CD69 on host B cells (B220$^+$, H-2K^b positive) is shown. Data are representative of two independent experiments.

$BTLA^{-/-}$ donor cells demonstrate reduced BrdU incorporation and antihost CTL activity before contraction

Contraction of $BTLA^{-/-}$ donor cells could be a result either of decreased proliferation or increased cell death. Therefore, we examined these parameters at days 9 and 10, a time just before the onset of rapid contraction, using BrdU labeling, markers of apoptosis, and assays for cytolytic activity (Fig. 6). At day 9, the percentage of $BTLA^{-/-}$ donor T cells that had incorporated BrdU

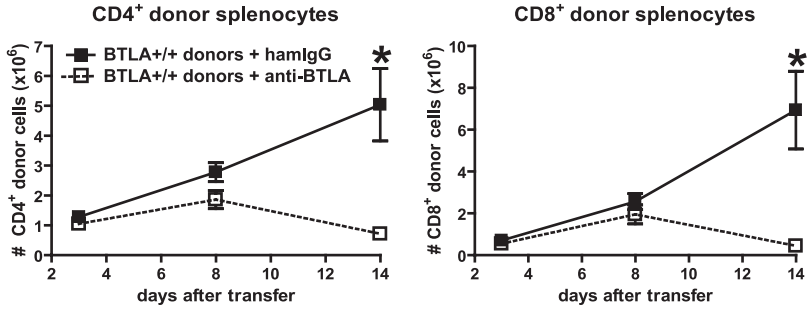

FIGURE 5. Anti-BTLA Ab treatment at the initiation of GVHD inhibits the long-term survival of $BTLA^{+/+}$ donor lymphocytes. C57BL/6 $BTLA^{+/+}$ splenocytes (5×10^7) were transferred into $CB6F_1$ hosts. A total of 100 μg of hamster IgG (isotype control, ■) or anti-BTLA Ab (6A6, □) was administered i.p. to host mice concurrent with donor cell transfer (day 0). Splenocytes were harvested after 3, 8, and 14 days and analyzed for donor/host chimerism as in Fig. 1. Absolute numbers of donor CD4$^+$ (*left graph*) and CD8$^+$ (*right graph*) were calculated at each time point. Average values are shown for three mice per group at each time point with error bars indicating SEM. Asterisks indicate points at which Student's *t* tests indicate significant differences of $p < 0.05$ between isotype- and 6A6-treated mice. Data are representative of three independent experiments.

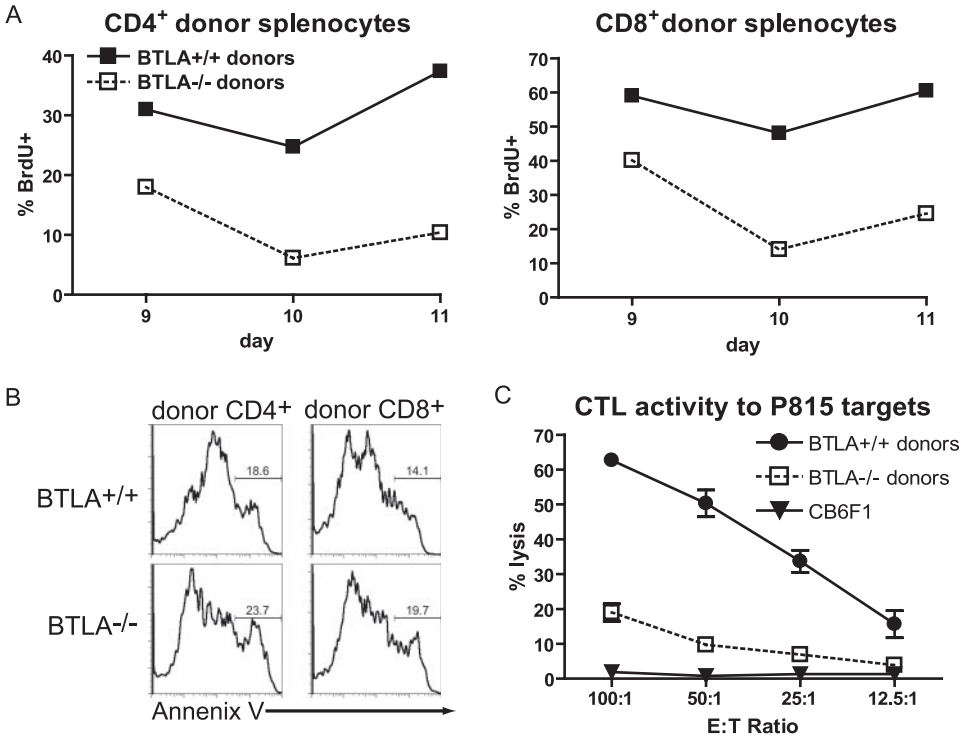

FIGURE 6. *BTLA*$^{-/-}$ donor cells incorporate less BrdU but do not exhibit increased apoptosis before contraction. GVHD was induced by transferring 5×10^7 *BTLA*$^{+/+}$ C57BL/6 (■) or *BTLA*$^{-/-}$ (□) splenocytes into CB6F$_1$ hosts. *A*, Splenocytes were harvested at days 9, 10, and 11 following transfer. Eighteen hours before harvest, mice were injected i.p. with 1 mg of BrdU to observe cellular proliferation. Splenocytes were subjected to FACS staining to identify the percentage of donor CD4$^+$ (*left graph*) and CD8$^+$ (*right graph*) cells incorporating BrdU. Data at each time point is representative of the average of two mice per group. *B*, The percentage of annexin V-positive donor CD4$^+$ (*left panels*) or CD8$^+$ (*right panels*) splenocytes from mice receiving *BTLA*$^{+/+}$ (*upper panels*) or *BTLA*$^{-/-}$ (*lower panels*) splenocytes was assessed at day 9 by FACS. Gates indicate the percentage of annexin V-positive cells. Data are representative of two mice per group. *C*, At day 10, unfractionated splenocytes from GVHD-induced mice were analyzed for CTL activity against allogeneic (H-2K^d) P815 cells. Effector splenocytes were incubated with CFSE-labeled targets at the indicated ratios for 4 h. A vitality dye (7-AAD) was added, and the percentage of target cells lysed (CFSE$^+$7-AAD$^+$) was determined by FACS. CTL activity was not observed toward syngeneic (H-2K^b) EL4 cell targets (data not shown). The mean ± SEM of three mice per group is shown.

is approximately two-thirds of the percentage of BrdU$^+$*BTLA*$^{+/+}$ donors (Fig. 6*A*). On day 10, BrdU incorporation by *BTLA*$^{-/-}$ donor cells is further reduced to approximately one-third the level of *BTLA*$^{+/+}$ donors (Fig. 6*A*). *BTLA*$^{-/-}$ donor CD4$^+$ and CD8$^+$ T cells showed a similar degree of reduced BrdU incorporation. However, we did not observe a detectable difference in the degree of annexin V staining, a marker of apoptotic cells, of CD4$^+$ or CD8$^+$ *BTLA*$^{-/-}$ and *BTLA*$^{+/+}$ donor cells at day 9 (Fig. 6*B*). Analysis of cytolytic activity at day 10 showed that *BTLA*$^{-/-}$ donor cells had a greatly reduced capacity to kill allogeneic P815 (H-2K^d) cells in vitro compared with *BTLA*$^{+/+}$ donor cells (Fig. 6*C*). This result agrees with our finding of normal levels of host B220$^+$ cells persisting in mice receiving *BTLA*$^{-/-}$ donor cells (Fig. 1*C*). Overall, these results suggest that the failure of *BTLA*$^{-/-}$ donor cells to sustain GVHD is due to a progressive decrease in donor cell proliferation, survival, and insufficient antihost CTL activity.

Differential gene expression of BTLA$^{+/+}$ *and BTLA*$^{-/-}$ *donor CD4*$^+$ *cells during GVHD*

We performed DNA microarray studies to characterize the potential molecular mechanism accounting for the contraction of *BTLA*$^{-/-}$ donor populations during GVHD. GVHD was induced by transferring either C57BL/6 *BTLA*$^{+/+}$ or *BTLA*$^{-/-}$ donor cells into CB6F$_1$ recipients, and donor CD4$^+$ lymphocytes were harvested 9 and 10 days after transfer. We selected these times for analysis because they directly precede the decline in *BTLA*$^{-/-}$ donor cells and may reveal cellular changes leading to their loss. Consistent with comparable annexin V staining on *BTLA*$^{+/+}$ and *BTLA*$^{-/-}$ donor cells (Fig. 6*B*), no differential expression of either pro- or antiapoptotic genes (including BCL-2, BCL-x$_L$, and Bad)

Table I. *Global gene analysis reveals genes induced and inhibited in BTLA*$^{+/+}$ *and BTLA*$^{-/-}$*CD4*$^+$ *donor cells 9 days after acute GVHD induction*[a]

Gene	Day 9		
	Fold change	BTLA$^{+/+}$	BTLA$^{-/-}$
Genes induced in BTLA$^{+/+}$ CD4$^+$ donors			
BTLA[b]	40.99	4321	112
IL-7Rα[b]	3.16	1020	323
IL-18Rβ[b]	2.76	488	176
CXCR6[b]	2.32	4046	1742
IL-18Rα[b]	1.70	3042	1785
Genes inhibited in BTLA$^{+/+}$ CD4$^+$ donors			
IL-4[c]	3.4	87	297
IL-1R antagonist[c]	2.5	97	244
IL-1R1[c]	2.0	276	138
NFATc1[c]	1.96	2760	1407
Bcl-3[c]	1.81	467	258
IL-6Rα[c]	1.61	114	185

[a] RNA was harvested from donor CD4$^+$ lymphocytes sorted from the spleens of GVHD mice at day 9 following GVHD induction. Data were analyzed using dCHIP, with the relative expression values and fold changes reported for immune-related genes demonstrating differential expression at each time point.
[b] Genes with higher expression in *BTLA*$^{+/+}$ as compared with *BTLA*$^{-/-}$.
[c] Genes with higher expression in *BTLA*$^{-/-}$ cells as compared with *BTLA*$^{+/+}$.

Table II. *Global gene analysis reveals genes induced and inhibited in $BTLA^{+/+}$ and $BTLA^{-/-}CD4^{+}$ donor cells 10 days after acute GVHD induction*[a]

Gene	Day 10 Fold change	Day 10 $BTLA^{+/+}$	Day 10 $BTLA^{-/-}$
Genes induced in $BTLA^{+/+}$ $CD4^{+}$ donors			
BTLA[b]	16.89	2634	155
T1/ST2[b]	11.13	1569	141
IL-18Rα[b]	7.33	3420	466
CXCR6[b]	6.87	2316	337
Granzyme B[b]	6.86	2199	320
CCL2 (MIP-2α)[b]	5.53	1195	216
IL-18Rβ[b]	4.91	305	62
CCR2[b]	3.72	1068	286
TNFSF7 (CD70)[b]	3.59	226	63
IFNγR1[b]	3.39	2363	696
CD86[b]	3.09	341	110
CCL3 (MIP-1α)[b]	2.99	1011	338
TNFSF25 (DR3)[b]	2.35	1161	495
CCL4 (MIP-1β)[b]	2.20	515	234
CCL5 (RATNES)[b]	2.04	426	208
IL-7Rα[b]	1.88	853	454
Genes inhibited in $BTLA^{+/+}$ $CD4^{+}$ donors			
IL-4[c]	10.45	81	847
IL-1R1[c]	9.57	85	821
CD109[c]	9.51	46	443
CXCR5[c]	4.81	627	3020
IL-6α[c]	4.03	171	689
gp130[c]	3.60	93	335
GADD45[c]	3.54	66	236
IL-1R antagonist[c]	3.37	119	403
IL-13Rα[c]	2.79	71	200
LIGHT[c]	2.52	221	557
ITK[c]	2.50	1465	3665
BcoR[c]	2.38	434	1034
TNFSF8 (CD30L)[c]	2.15	998	2149
IL-16[c]	2.09	526	1099

[a] RNA was harvested from donor $CD4^{+}$ lymphocytes sorted from the spleens of GVHD mice at day 10 following GVHD induction. Data were analyzed using dCHIP, with the relative expression values and fold changes reported for immune-related genes demonstrating differential expression at each time point.
[b] Genes with higher expression in $BTLA^{+/+}$ as compared with $BTLA^{-/-}$ cells.
[c] Genes with higher expression in $BTLA^{-/-}$ cells as compared with $BTLA^{+/+}$.

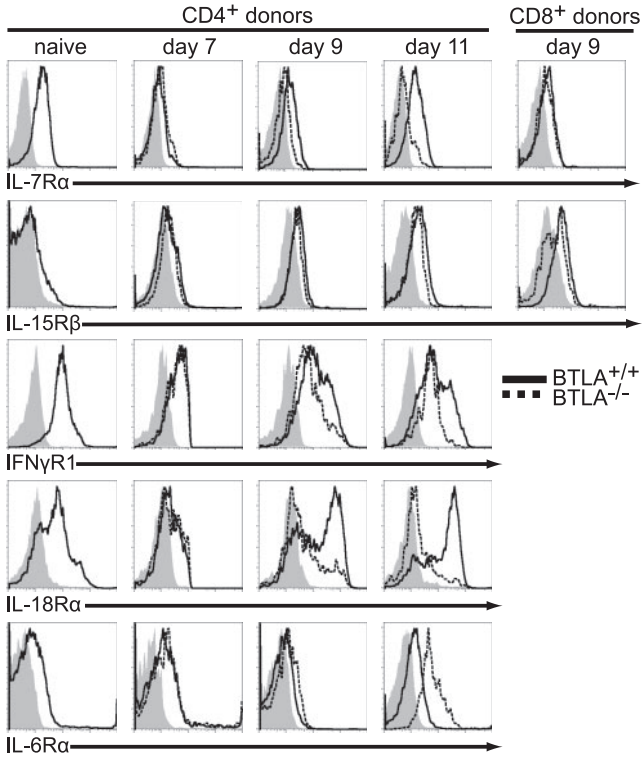

FIGURE 7. Differential gene expression of $BTLA^{+/+}$ and $BTLA^{-/-}$ donor $CD4^{+}$ cells during GVHD. C57BL/6 $BTLA^{+/+}$ splenocytes (5×10^{7}) were transferred into $CB6F_1$ hosts. Splenocytes were harvested on days 9 and 10. The surface levels of various receptors are compared with $BTLA^{+/+}$ (solid lines) and $BTLA^{-/-}$ (dashed lines) $CD4^{+}$ donor cells. Isotype control staining of a mixture of $BTLA^{+/+}$ and $BTLA^{-/-}$ splenocytes is shown (shaded regions). The first column indicates the receptor level on naive $BTLA^{+/+}$ C57BL/6 cells. Expression levels of all receptors are similar between $BTLA^{+/+}$ and $BTLA^{-/-}$ cells at day 7. IL-7Rα, IL-18Rα, and IFN-γR1 levels are increased on $BTLA^{+/+}$ compared with $BTLA^{-/-}$ donor cells at days 9 and 11. IL-6Rα expression is higher on $BTLA^{-/-}$ donor cells at day 11, whereas IL-15Rβ levels remain equivalent between $BTLA^{+/+}$ and $BTLA^{-/-}$ cells throughout. Expression of IL-15Rβ, but not IL-7Rα, was lower on $CD8^{+}BTLA^{-/-}$ donor cells than $BTLA^{+/+}$ donor cells at day 9 (*right column*).

was seen by DNA microarray (Tables I and II). We identified several immune specific genes that were differentially expressed by $BTLA^{+/+}$ and $BTLA^{-/-}$ donor $CD4^{+}$ populations at day 9 (Table I) and day 10 (Table II). These included IL-7Rα, IL-18Rα, IL-6Rα, and IFN-γR1 (Fig. 7).

IL-7Rα (CD127) showed 3.2- and 1.8-fold higher expression in $BTLA^{+/+}$ compared with $BTLA^{-/-}CD4^{+}$ T cells on days 9 and 10, respectively (Table I). On day 10, T1/ST2, an IL-1R family member (43), was expressed 11.1-fold higher in $BTLA^{+/+}CD4^{+}$ donor cells compared with $BTLA^{-/-}$ cells (Table II). IL-18Rα showed a 1.7-fold higher expression at day 9 and a 7.3-fold higher expression at day 10 in $BTLA^{+/+}$ donor cells. IFN-γR1 (CD119) expression was 3.3-fold higher in the $BTLA^{+/+}$ donor $CD4^{+}$ population than the $BTLA^{-/-}$ donors at day 10 (Table II). Some genes were expressed more highly by $BTLA^{-/-}CD4^{+}$ donor cells compared with $BTLA^{+/+}CD4^{+}$ donor cells. IL-4 expression was 3.4-fold higher in $BTLA^{-/-}$ cells at day 9 (Table I), which increased to a 10.4-fold higher expression on day 10 (Table II). IL-6Rα had 1.6-fold higher expression in $BTLA^{-/-}$ cells at day 9 and 4-fold higher expression at day 10 (Table I).

We verified some of these differences by FACS analysis (Fig. 7). IL-7Rα surface expression on $BTLA^{+/+}CD4^{+}$ donor cells increased progressively over time, ultimately returning to levels similar to that of naive $CD4^{+}$ cells, whereas $BTLA^{-/-}$ donor cells failed to re-express the receptor (Fig. 7). In contrast, the expression of IL-7Rα on $CD8^{+}BTLA^{-/-}$ donor cells was equivalent to that of $BTLA^{+/+}$ donors at day 9. Although the IL-15Rβ-chain (CD122) remained equivalently expressed by both $BTLA^{+/+}$ and $BTLA^{-/-}CD4^{+}$ donor cells populations at all time points, $CD8^{+}BTLA^{-/-}$ donor cells expressed decreased levels of IL-15Rβ at day 9 (Fig. 7). The IL-18Rα was expressed equivalently at day 7 but later increased on $BTLA^{+/+}$ donor $CD4^{+}$ cells and decreased on $BTLA^{-/-}$ donor cells (Fig. 7). IFN-γR1 expression remained unchanged on $BTLA^{-/-}CD4^{+}$ donor cells but was increased on $BTLA^{+/+}CD4^{+}$ donor cells at days 9 and 11 (Fig. 7). IL-6Rα was expressed equivalently between $BTLA^{+/+}$ and $BTLA^{-/-}$ cells at day 7 but was up-regulated on only $BTLA^{-/-}$ donors at day 11 (Fig. 7).

Discussion

The major finding of this study is the unexpected stimulatory, rather than inhibitory, role of BTLA in an in vivo model of chronic allostimulation. In the parental-into-F_1 nonirradiated GVHD model, we found that $BTLA^{-/-}$ donor cells were unable to sustain

GVHD pathology, as opposed to the expected augmentation of disease. These data suggest that BTLA, acting either as a receptor or as a ligand for HVEM, has prosurvival activity in this in vivo model of sustained alloresponse. Although the initial activation and expansion of $BTLA^{-/-}$ and $BTLA^{+/+}$ donor cells was similar, $BTLA^{-/-}$ donor cell numbers began to decrease at day 10, eventually disappearing (Fig. 1). Thus, under this model of chronic allostimulation, BTLA is acting in a prosurvival manner and is clearly necessary for the maintenance, rather than the initiation, of the effector T cell response.

BTLA was initially identified as having inhibitory actions on T cell proliferation and cytokine production in vitro (1, 44). Inhibitory actions observed in vivo in models of experimental allergic encephalomyelitis (1) and allergic airway inflammation (45) support these observations. Engagement of BTLA on murine $CD4^+$ T cells by the BTLA ligand HVEM expressed on APCs (5) or by a HVEM-Fc fusion protein (13) also caused a reduction in early T cell proliferation. A chimeric receptor containing the extracellular domain of CD28 fused to the human BTLA cytoplasmic tail was able to potently inhibit IL-2 production by primary human CD4 T cells, again indicating inhibitory actions for BTLA (7). Finally, a recent report describing increased homeostatic expansion of $BTLA^{-/-}$ T cells in lymphopenic hosts and increased numbers of $CD8^+$ central memory cells in $BTLA^{-/-}$ and $HVEM^{-/-}$ mice further demonstrates the inhibitory activity of BTLA (46).

However, not all reported actions of BTLA have been inhibitory. Two different systems of cardiac transplantation (47) were used to evaluate the role of BTLA in allograft rejection (48). In the first system, partially MHC mismatched allografts, differing at a single class II MHC locus, are tolerated for long periods by wild-type recipient mice. These allografts were rapidly rejected, rather than tolerated, by $BTLA^{-/-}$ or $HVEM^{-/-}$ recipients, consistent with an inhibitory action of BTLA in the recipient immune response (48). In the second system, fully MHC mismatched, with differences at both class I and class II MHC loci, cardiac allografts are rapidly rejected by wild-type mice. These allografts showed slightly prolonged survival in $BTLA^{-/-}$ recipients (48). Although the basis for this difference was not established, these results suggested a positive action of BTLA in the recipient immune response.

In addition to ITIM and immunoreceptor tyrosine-based switch motif inhibitory motifs (1), the cytoplasmic domains of human and mouse BTLA contain other conserved tyrosine-containing motifs that may be relevant to signaling, such as sites that may recruit Grb-2 (7, 8). In one study, mutation of all cytoplasmic tyrosine residues was required to abolish the inhibitory actions of a chimeric signaling protein containing the human BTLA cytoplasmic domain (7). Another study indicated that the one Grb-2 recruitment motif in murine BTLA may interact with both Grb-2 and the p85 subunit of PI3K (8). While indirect evidence, a peptide containing the conserved phosphorylated Grb-2 recruitment region of the BTLA cytoplasmic domain had the ability to interact with PI3K, suggesting that BTLA may sometimes have a positive, rather than inhibitory, action (8). However, neither of these studies examined the in vivo role of these conserved signaling motifs.

To analyze the role of BTLA in immune regulation in vivo, we have surveyed various models of pathogen infections, induced and spontaneous autoimmunity, and various transplantation systems. As part of this survey, we examined the nonirradiated parental-into-F_1 GVHD system (18), expecting to observe augmented immune responses against host cells in the absence of BTLA's inhibitory actions. This nonirradiated GVHD model is distinct from other models of GVHD models that use host irradiation and bone marrow transplantation to more closely mimic GVHD that arises in clinical settings using myeloablative conditioning (reviewed in Ref. 17). Indeed, each model system contributes unique factors that complicate the analysis of the allogeneic response. Irradiation causes epithelial damage and extensive inflammatory cytokine production that exacerbate GVHD (16), whereas the nonirradiated model is complicated by an intact host immune system that may respond to inflammatory stimuli and contribute an antigraft response (49). Consequently, different mechanisms may account for the pathology in the irradiated and nonirradiated systems, and distinct roles for perforin (50, 51) and IFN-γ (52, 53) have been revealed in each model.

Global gene expression analysis of $BTLA^{+/+}$ and $BTLA^{-/-}$ donor cells harvested from hosts on days 9 and 10 revealed several genes with differential expression (Table I). Many of the differentially expressed genes are known to function during allogeneic responses. Polarization of donor $CD4^+$ T cells toward the Th1 phenotype is important for development of aGVHD (54–56). Interestingly, genes associated with Th2 cells were increased in $BTLA^{-/-}$ $CD4^+$ donors cells, whereas genes associated with Th1 cells were decreased in $BTLA^{-/-}$ $CD4^+$ donors. For example, IL-4 was increased in $BTLA^{-/-}$ $CD4^+$ donors (Table I) and is Th2 specific (40), whereas IL-18Rα and CXCR6 were decreased in $BTLA^{-/-}$ $CD4^+$ donors cells and are Th1 specific (39, 57, 58). Thus, the inability of $BTLA^{-/-}$ donor cells to mount a sustained effector response to allogeneic stimulation may be due to altered $CD4^+$ T cell polarization.

We also found that IL-7Rα failed to become highly expressed on $BTLA^{-/-}$ cells to the same extent as $BTLA^{+/+}$ donor $CD4^+$ cells. IL-7 is critical for homeostatic survival of naive T cells (59) and regulates the transition of $CD4^+$ effector T cells to long-lived and memory T cells (36–38). It was also recently reported that persistence of GVHD in an irradiated model system involved the development of alloreactive $CD4^+$ or $CD8^+$ memory T cells whose survival required the cytokines IL-2, IL-7, and IL-15 despite chronic allostimulation (60, 61). Conceivably, failure of $BTLA^{-/-}$ $CD4^+$ cells to re-express IL-7Rα in the nonirradiated GVHD model could prevent necessary survival signaling such as BCL-2 (62) or PI3K (63), causing the contraction observed after day 10 in vivo.

HVEM activity was shown recently to be required for manifestation of disease in a similar parental-into-F_1 nonirradiated model of GVHD (64). $HVEM^{-/-}$ and $LIGHT^{-/-}$ donor T cells showed decreased survival and reduced antihost CTL activity compared with wild type donor cells 7–10 days following transfer (64). Previously, blockade of LIGHT using soluble LTβR-Ig or anti-LIGHT Ab was found to reduced severity of GVHD in this system (12). Notably, cotransfer of WT and $LIGHT^{-/-}$ T cells showed that wild-type donor cells had a significant survival advantage after 11 days (64).

That study (64), taken together with the results reported here, indicate that HVEM, LIGHT, and BTLA all have similar actions on promoting donor cell survival in the parental-into-F_1 model of GVHD. We have independently confirmed that $HVEM^{-/-}$ donor cells show reduced survival in this model (data not shown), as reported previously (64). If HVEM signaling, activated by LIGHT or LTα, delivers a prosurvival signal required for donor cell maintenance, then our results suggest that BTLA may be playing some role in augmenting this signaling pathway. Thus, sustaining a chronic alloresponse may require a complex involving BTLA, LIGHT, and HVEM. In the absence of BTLA, the LIGHT-HVEM complex may either induce an apoptotic signal or be insufficient to maintain cell expansion and survival. In summary, our data identify a condition in which BTLA unexpectedly promotes, rather than inhibits, an immune response. We do not know whether this

action is mediated by BTLA signaling or by BTLA acting as a ligand for HVEM, with HVEM mediating the prosurvival signals. Distinguishing between these and other possibilities will likely require extensive additional analysis and involve mutations of both BTLA and HVEM.

Disclosures

The authors have no financial conflict of interest.

References

1. Watanabe, N., M. Gavrieli, J. R. Sedy, J. Yang, F. Fallarino, S. K. Loftin, M. A. Hurchla, N. Zimmerman, J. Sim, X. Zang, et al. 2003. BTLA is a lymphocyte inhibitory receptor with similarities to CTLA-4 and PD-1. *Nat. Immunol.* 4: 670–679.
2. Hurchla, M. A., J. R. Sedy, M. Gavrieli, C. G. Drake, T. L. Murphy, and K. M. Murphy. 2005. B and T lymphocyte attenuator exhibits structural and expression polymorphisms and is highly induced in anergic $CD4^+$ T cells. *J. Immunol.* 174: 3377–3385.
3. Gavrieli, M., N. Watanabe, S. K. Loftin, T. L. Murphy, and K. M. Murphy. 2003. Characterization of phosphotyrosine binding motifs in the cytoplasmic domain of B and T lymphocyte attenuator required for association with protein tyrosine phosphatases SHP-1 and SHP-2. *Biochem. Biophys. Res. Commun.* 312: 1236–1243.
4. Krieg, C., P. Han, R. Stone, O. D. Goularte, and J. Kaye. 2005. Functional analysis of B and T lymphocyte attenuator engagement on $CD4^+$ and $CD8^+$ T cells. *J. Immunol.* 175: 6420–6427.
5. Sedy, J. R., M. Gavrieli, K. G. Potter, M. A. Hurchla, R. C. Lindsley, K. Hildner, S. Scheu, K. Pfeffer, C. F. Ware, T. L. Murphy, and K. M. Murphy. 2005. B and T lymphocyte attenuator regulates T cell activation through interaction with herpesvirus entry mediator. *Nat. Immunol.* 6: 90–98.
6. Croft, M. 2005. The evolving crosstalk between co-stimulatory and co-inhibitory receptors: HVEM-BTLA. *Trends Immunol.* 26: 292–294.
7. Chemnitz, J. M., A. R. Lanfranco, I. Braunstein, and J. L. Riley. 2006. B and T lymphocyte attenuator-mediated signal transduction provides a potent inhibitory signal to primary human CD4 T cells that can be initiated by multiple phosphotyrosine motifs. *J. Immunol.* 176: 6603–6614.
8. Gavrieli, M., and K. M. Murphy. 2006. Association of Grb-2 and PI3K p85 with phosphotyrosile peptides derived from BTLA. *Biochem. Biophys. Res. Commun.* 345: 1440–1445.
9. Mauri, D. N., R. Ebner, R. I. Montgomery, K. D. Kochel, T. C. Cheung, G. L. Yu, S. Ruben, M. Murphy, R. J. Eisenberg, G. H. Cohen, et al. 1998. LIGHT, a new member of the TNF superfamily, and lymphotoxin α are ligands for herpesvirus entry mediator. *Immunity* 8: 21–30.
10. Scheu, S., J. Alferink, T. Potzel, W. Barchet, U. Kalinke, and K. Pfeffer. 2002. Targeted disruption of LIGHT causes defects in costimulatory T cell activation and reveals cooperation with lymphotoxin β in mesenteric lymph node genesis. *J. Exp. Med.* 195: 1613–1624.
11. Tamada, K., K. Shimozaki, A. I. Chapoval, Y. Zhai, J. Su, S. F. Chen, S. L. Hsieh, S. Nagata, J. Ni, and L. Chen. 2000. LIGHT, a TNF-like molecule, costimulates T cell proliferation and is required for dendritic cell-mediated allogeneic T cell response. *J. Immunol.* 164: 4105–4110.
12. Tamada, K., K. Shimozaki, A. I. Chapoval, G. Zhu, G. Sica, D. Flies, T. Boone, H. Hsu, Y. X. Fu, S. Nagata, et al. 2000. Modulation of T cell-mediated immunity in tumor and graft-versus-host disease models through the LIGHT co-stimulatory pathway. *Nat. Med.* 6: 283–289.
13. Gonzalez, L. C., K. M. Loyet, J. Calemine-Fenaux, V. Chauhan, B. Wranik, W. Ouyang, and D. L. Eaton. 2005. A coreceptor interaction between the CD28 and TNF receptor family members B and T lymphocyte attenuator and herpesvirus entry mediator. *Proc. Natl. Acad. Sci. USA* 102: 1116–1121.
14. Compaan, D. M., L. C. Gonzalez, I. Tom, K. M. Loyet, D. Eaton, and S. G. Hymowitz. 2005. Attenuating lymphocyte activity: the crystal structure of the BTLA-HVEM complex. *J. Biol. Chem.* 280: 39553–39561.
15. Cheung, T. C., I. R. Humphreys, K. G. Potter, P. S. Norris, H. M. Shumway, B. R. Tran, G. Patterson, R. Jean-Jacques, M. Yoon, P. G. Spear, et al. 2005. Evolutionarily divergent herpesviruses modulate T cell activation by targeting the herpesvirus entry mediator cosignaling pathway. *Proc. Natl. Acad. Sci. USA* 102: 13218–13223.
16. Reddy, P., and J. L. Ferrara. 2003. Immunobiology of acute graft-versus-host disease. *Blood Rev.* 17: 187–194.
17. Welniak, L. A., B. R. Blazar, and W. J. Murphy. Immunobiology of allogeneic hematopoietic stem cell transplantation. *Annu. Rev. Immunol.* In press.
18. Shearer, G. M., and R. P. Polisson. 1980. Mutual recognition of parental and F_1 lymphocytes: selective abrogation of cytotoxic potential of F_1 lymphocytes by parental lymphocytes. *J. Exp. Med.* 151: 20–31.
19. Hakim, F. T., S. O. Sharrow, S. Payne, and G. M. Shearer. 1991. Repopulation of host lymphohematopoietic systems by donor cells during graft-versus-host reaction in unirradiated adult F_1 mice injected with parental lymphocytes. *J. Immunol.* 146: 2108–2115.
20. Via, C. S. 1991. Kinetics of T cell activation in acute and chronic forms of murine graft-versus-host disease. *J. Immunol.* 146: 2603–2609.
21. Via, C. S., S. O. Sharrow, and G. M. Shearer. 1987. Role of cytotoxic T lymphocytes in the prevention of lupus-like disease occurring in a murine model of graft-vs-host disease. *J. Immunol.* 139: 1840–1849.
22. Ferrara, J. L. 1993. Cytokine dysregulation as a mechanism of graft versus host disease. *Curr. Opin. Immunol.* 5: 794–799.
23. Iwasaki, T., T. Hamano, K. Saheki, T. Kuroiwa, Y. Kataoka, Y. Takemoto, A. Ogata, J. Fujimoto, and E. Kakishita. 2000. Graft-versus-host-disease-associated donor cell engraftment in an F-1 hybrid model is dependent upon the Fas pathway. *Immunology* 99: 94–100.
24. Gleichmann, E., E. H. Van Elven, and J. P. Van der Veen. 1982. A systemic lupus erythematosus (SLE)-like disease in mice induced by abnormal T-B cell cooperation: preferential formation of autoantibodies characteristic of SLE. *Eur. J. Immunol.* 12: 152–159.
25. Dewit, D., M. Vanmechelen, C. Zanin, J. M. Doutrelepont, T. Velu, C. Gerard, D. Abramowicz, J. P. Scheerlinck, P. Debaetselier, J. Urbain, et al. 1993. Preferential activation of Th2 cells in chronic graft-versus-host reaction. *J. Immunol.* 150: 361–366.
26. Tschetter, J. R., E. Mozes, and G. M. Shearer. 2000. Progression from acute to chronic disease in a murine parent-into-F_1 model of graft-versus-host disease. *J. Immunol.* 165: 5987–5994.
27. Blazar, B. R., A. H. Sharpe, P. A. Taylor, A. PanoskaltsisMortari, G. S. Gray, R. Korngold, and D. A. Vallera. 1996. Infusion of anti-B7.1 (CD80) and anti-B7.2 (CD86) monoclonal antibodies inhibits murine graft-versus-host disease lethality in part via direct effects on $CD4^+$ and $CD8^+$ T cells. *J. Immunol.* 157: 3250–3259.
28. Lang, T. J., P. Nguyen, R. Peach, W. C. Gause, and C. S. Via. 2002. In vivo CD86 blockade inhibits $CD4^+$ T cell activation, whereas CD80 blockade potentiates $CD8^+$ T cell activation and CTL effector function. *J. Immunol.* 168: 3786–3792.
29. Blazar, B. R., P. A. Taylor, P. S. Linsley, and D. A. Vallera. 1994. In vivo blockade of CD28/CTLA4: B7/BB1 interaction with CTLA4-Ig reduces lethal murine graft-versus-host disease across the major histocompatibility complex barrier in mice. *Blood* 83: 3815–3825.
30. Hakim, F. T., R. Cepeda, G. S. Gray, C. H. June, and R. Abe. 1995. Acute graft-versus-host reaction can be aborted by blockade of costimulatory molecules. *J. Immunol.* 155: 1757–1766.
31. Via, C. S., V. Rus, P. Nguyen, P. Linsley, and W. C. Gause. 1996. Differential effect of CTLA4Ig on murine graft-versus-host disease (GVHD) development—CTLA4Ig prevents both acute and chronic GVHD development but reverses only chronic GVHD. *J. Immunol.* 157: 4258–4267.
32. Yu, X. Z., P. J. Martin, and C. Anasetti. 1998. Role of CD28 in acute graft-versus-host disease. *Blood* 92: 2963–2970.
33. Ogawa, S., G. Nagamatsu, M. Watanabe, S. Watanabe, T. Hayashi, S. Horita, K. Nitta, H. Nihei, K. Tezuka, and R. Abe. 2001. Opposing effects of anti-activation-inducible lymphocyte-immunomodulatory molecule/inducible costimulator antibody on the development of acute versus chronic graft-versus-host disease. *J. Immunol.* 167: 5741–5748.
34. Blazar, B. R., P. A. Taylor, A. Panoskaltsis-Mortari, A. H. Sharpe, and D. A. Vallera. 1999. Opposing roles of CD28:B7 and CTLA-4:B7 pathways in regulating in vivo alloresponses in murine recipients of MHC disparate T cells. *J. Immunol.* 162: 6368–6377.
35. Blazar, B. R., B. M. Carreno, A. Panoskaltsis-Mortari, L. Carter, Y. Iwai, H. Yagita, H. Nishimura, and P. A. Taylor. 2003. Blockade of programmed death-1 engagement accelerates graft-versus-host disease lethality by an IFN-γ-dependent mechanism. *J. Immunol.* 171: 1272–1277.
36. Li, J., G. Huston, and S. L. Swain. 2003. IL-7 promotes the transition of CD4 effectors to persistent memory cells. *J. Exp. Med.* 198: 1807–1815.
37. Kondrack, R. M., J. Harbertson, J. T. Tan, M. E. McBreen, C. D. Surh, and L. M. Bradley. 2003. Interleukin-7 regulates the survival and generation of memory CD4 cells. *J. Exp. Med.* 198: 1797–1806.
38. Seddon, B., P. Tomlinson, and R. Zamoyska. 2003. Interleukin-7 and T cell receptor signals regulate homeostasis of CD4 memory cells. *Nat.* 4: 680–686.
39. Hoshino, K., H. Tsutsui, T. Kawai, K. Takeda, K. Nakanishi, Y. Takeda, and S. Akira. 1999. Cutting edge: generation of IL-18 receptor-deficient mice—evidence for IL-1 receptor-related protein as an essential IL-18 binding receptor. *J. Immunol.* 162: 5041–5044.
40. Murphy, K. M., and S. L. Reiner. 2002. The lineage decisions of helper T cells. *Nat. Rev. Immunol.* 2: 933–944.
41. Jedema, I., N. M. van der Werff, R. M. Barge, R. Willemze, and J. H. Falkenburg. 2004. New CFSE-based assay to determine susceptibility to lysis by cytotoxic T cells of leukemic precursor cells within a heterogeneous target cell population. *Blood* 103: 2677–2682.
42. Morris, S. C., R. L. Cheek, P. L. Cohen, and R. A. Eisenberg. 1990. Autoantibodies in chronic graft versus host result from cognate T-B interactions. *J. Exp. Med.* 171: 503–517.
43. Mitcham, J. L., P. Parnet, T. P. Bonnert, K. E. Garka, M. J. Gerhart, J. L. Slack, M. A. Gayle, S. K. Dower, and J. E. Sims. 1996. T1/ST2 signaling establishes it as a member of an expanding interleukin-1 receptor family. *J. Biol. Chem.* 271: 5777–5783.
44. Han, P., O. D. Goularte, K. Rufner, B. Wilkinson, and J. Kaye. 2004. An inhibitory Ig superfamily protein expressed by lymphocytes and APCs is also an early marker of thymocyte positive selection. *J. Immunol.* 172: 5931–5939.
45. Deppong, C., T. I. Juehne, M. Hurchla, L. D. Friend, D. D. Shah, C. M. Rose, T. L. Bricker, L. P. Shornick, E. C. Crouch, T. L. Murphy, et al. 2006. Cutting edge: B and T lymphocyte attenuator and programmed death receptor-1 inhibitory receptors are required for termination of acute allergic airway inflammation. *J. Immunol.* 176: 3909–3913.
46. Krieg, C., O. Boyman, Y. X. Fu, and J. Kaye. 2007. B and T lymphocyte attenuator regulates $CD8^+$ T cell-intrinsic homeostasis and memory cell generation. *Nat. Immunol.* 8: 162–171.

47. Corry, R. J., H. J. Winn, and P. S. Russell. 1973. Primarily vascularized allografts of hearts in mice. The role of H-2D, H-2K, and non-H-2 antigens in rejection. *Transplantation* 16: 343–350.
48. Tao, R., L. Wang, R. Han, T. Wang, Q. Ye, T. Honjo, T. L. Murphy, K. M. Murphy, and W. W. Hancock. 2005. Differential effects of B and T lymphocyte attenuator and programmed death-1 on acceptance of partially versus fully MHC-mismatched cardiac allografts. *J. Immunol.* 175: 5774–5782.
49. Gleichmann, E., and H. Gleichmann. 1985. Pathogenesis of graft-versus-host reactions (GVHR) and GVH-like diseases. *J. Invest. Dermatol.* 85: 115s–120s.
50. Shustov, A., I. Luzina, P. Nguyen, J. C. Papadimitriou, B. Handwerger, K. B. Elkon, and C. S. Via. 2000. Role of perforin in controlling B cell hyperactivity and humoral autoimmunity. *J. Clin. Invest.* 106: R39–R47.
51. Baker, M. B., R. L. Riley, E. R. Podack, and R. B. Levy. 1997. Graft-versus-host-disease-associated lymphoid hypoplasia and B cell dysfunction is dependent upon donor T cell-mediated Fas-ligand function, but not perforin function. *Proc. Natl. Acad. Sci. USA* 94: 1366–1371.
52. Ellison, C. A., J. M. Fischer, K. T. HayGlass, and J. G. Gartner. 1998. Murine graft-versus-host disease in an F_1-hybrid model using IFN-γ gene knockout donors. *J. Immunol.* 161: 631–640.
53. Murphy, W. J., L. A. Welniak, D. D. Taub, R. H. Wiltrout, P. A. Taylor, D. A. Vallera, M. Kopf, H. Young, D. L. Longo, and B. R. Blazar. 1998. Differential effects of the absence of interferon-γ and IL-4 in acute graft-versus-host disease after allogeneic bone marrow transplantation in mice. *J. Clin. Invest.* 102: 1742–1748.
54. Krenger, W., K. M. Snyder, J. C. H. Byon, G. Falzarano, and J. L. M. Ferrara. 1995. Polarized type-2 alloreactive $Cd4^+$ and $Cd8^+$ donor T cells fail to induce experimental acute graft-versus-host disease. *J. Immunol.* 155: 585–593.
55. Fowler, D. H., K. Kurasawa, A. Husebekk, P. A. Cohen, and R. E. Gress. 1994. Cells of Th2 cytokine phenotype prevent LPS-induced lethality during murine graft-versus-host reaction: regulation of cytokines and $CD8^+$ lymphoid engraftment. *J. Immunol.* 152: 1004–1013.
56. Rus, V., A. Svetic, P. Nguyen, W. C. Gause, and C. S. Via. 1995. Kinetics of Th1 and Th2 cytokine production during the early course of acute and chronic murine graft-versus-host disease: regulatory role of donor $CD8^+$ T cells. *J. Immunol.* 155: 2396–2406.
57. Smeltz, R. B., J. Chen, J. Hu-Li, and E. M. Shevach. 2001. Regulation of interleukin (IL)-18 receptor α chain expression on $CD4^+$ T cells during T helper (Th)1/Th2 differentiation: critical downregulatory role of IL-4. *J. Exp. Med.* 194: 143–153.
58. Kim, C. H., E. J. Kunkel, J. Boisvert, B. Johnston, J. J. Campbell, M. C. Genovese, H. B. Greenberg, and E. C. Butcher. 2001. Bonzo/CXCR6 expression defines type 1-polarized T cell subsets with extralymphoid tissue homing potential. *J. Clin. Invest.* 107: 595–601.
59. Tan, J. T., E. Dudl, E. LeRoy, R. Murray, J. Sprent, K. I. Weinberg, and C. D. Surh. 2001. IL-7 is critical for homeostatic proliferation and survival of naive T cells. *Proc. Natl. Acad. Sci. USA* 98: 8732–8737.
60. Zhang, Y., G. Joe, E. Hexner, J. Zhu, and S. G. Emerson. 2005. Alloreactive memory T cells are responsible for the persistence of graft-versus-host disease. *J. Immunol.* 174: 3051–3058.
61. Zhang, Y., G. Joe, E. Hexner, J. Zhu, and S. G. Emerson. 2005. Host-reactive $CD8^+$ memory stem cells in graft-versus-host disease. *Nat. Med.* 11: 1299–1305.
62. Freeden-Jeffry, U., N. Solvason, M. Howard, and R. Murray. 1997. The earliest T lineage-committed cells depend on IL-7 for Bcl-2 expression and normal cell cycle progression. *Immunity* 7: 147–154.
63. Sharfe, N., H. K. Dadi, and C. M. Roifman. 1995. JAK3 protein tyrosine kinase mediates interleukin-7-induced activation of phosphatidylinositol-3′ kinase. *Blood* 86: 2077–2085.
64. Xu, Y., A. S. Flies, D. B. Flies, G. Zhu, S. Anand, S. J. Flies, H. Xu, R. A. Anders, W. W. Hancock, L. Chen, and K. Tamada. Selective targeting of the LIGHT-HVEM co-stimulatory system for the treatment of graft-versus-host disease. *Blood.* In press.

nature immunology

B and T lymphocyte attenuator regulates T cell activation through interaction with herpesvirus entry mediator

John R Sedy[1], Maya Gavrieli[1], Karen G Potter[2], Michelle A Hurchla[1], R Coleman Lindsley[1], Kai Hildner[1], Stefanie Scheu[3], Klaus Pfeffer[3], Carl F Ware[2], Theresa L Murphy[1] & Kenneth M Murphy[1,4]

B and T lymphocyte attenuator (BTLA) provides an inhibitory signal to B and T cells. Previously, indirect observations suggested that B7x was a ligand for BTLA. Here we show that BTLA does not bind B7x; instead, we identify herpesvirus entry mediator (HVEM) as the unique BTLA ligand. BTLA bound the most membrane-distal cysteine-rich domain of HVEM, distinct from regions where the ligands LIGHT and lymphotoxin-α bound HVEM. HVEM induced BTLA tyrosine phosphorylation and association of the tyrosine phosphatase SHP-2 and repressed antigen-driven T cell proliferation, providing an example of reverse signaling to a non–tumor necrosis factor family ligand. The conservation of the BTLA-HVEM interaction between mouse and human suggests that this system is an important pathway regulating lymphocyte activation and/or homeostasis in the immune response.

The lymphoid-specific cell surface receptor B and T lymphocyte attenuator (BTLA) inhibits lymphocytes during immune responses[1]. Although identified in a screen for T helper type 1–specific genes, BTLA shows high expression by resting B cells[1], is induced on anergic $CD4^+$ T cells (M.A.H., J.R.S., M.G., C.G. Drake, T.L.M. and K.M.M., data not shown) and has lower expression on macrophages, dendritic cells (DCs) and natural killer cells[2]. The cytoplasmic domain of BTLA contains one potential recruitment site for growth factor receptor–bound protein 2 and an immunoreceptor tyrosine-based inhibitory motif and switch motif[1], which after tyrosine phosphorylation associate with Src homology domain 2–containing protein tyrosine phosphatases SHP-1 and SHP-2 (refs. 1,3).

BTLA is polymorphic between C57BL/6 and BALB/c mice[4], with the C57BL/6 allele containing six cysteine residues in its extracellular domain and the BALB/c allele containing five. We examined 23 mouse strains and found one additional allele in the MRL/lpr and four other strains differing from the BALB/c allele at a single residue. We also identified evidence of expression polymorphisms within lymphoid subsets, with C57BL/6 but not BALB/c mice expressing BTLA on macrophages and natural killer cells (data not shown).

There has been an indirect indication that the B7 family member B7x (also identified as B7S1 and B7-H4)[1,5,6] might interact with BTLA; a B7x-Fc fusion protein showed lower binding to $Btla^{-/-}$ lymphocytes than to wild-type lymphocytes. However, this might have reflected indirect effects of BTLA deficiency and not a direct BTLA-B7x binding interaction. Also, the B7x-Fc fusion protein showed a much weaker interaction with lymphocytes than did B7-1–Fc (CD80), B7-2–Fc (CD86) and B7h-Fc fusion proteins. We therefore sought to obtain direct evidence regarding the potential ligand interactions of BTLA.

Here, we first tested for direct interactions between BTLA and B7x. We obtained no evidence for a direct interaction using tetramers and Fc fusion proteins of BTLA and B7x with transfected cells expressing each of these proteins. In addition, we found specific interactions of BTLA-Fc fusion proteins with naive T cells, which do not express B7x[5–7], also challenging the idea of a direct interaction between BTLA and B7x. These results motivated an effort to clone BTLA-interacting ligands.

We identify herpesvirus entry mediator (HVEM) as the unique ligand for BTLA in mice. Mouse BTLA-Fc fusion proteins and BTLA tetramers selectively interacted with mouse HVEM and, furthermore, human BTLA-Fc fusion proteins interacted with human HVEM, suggesting some conservation between species of the BTLA-HVEM interaction. We did not identify positive evidence of additional BTLA ligands remaining in HVEM-deficient mouse lymphocytes. The BTLA extracellular immunoglobulin domain interacted with the most membrane-distal cysteine-rich domain (CRD1) of HVEM, indicating a difference in binding of BTLA to HVEM compared with that of the ligands LIGHT and lymphotoxin-α (LTα). Finally, HVEM induced BTLA tyrosine phosphorylation and inhibited T cell proliferation in a BTLA-dependent way. The binding between BTLA and HVEM is a previously unknown structural interaction allowing reverse signaling

[1]Department of Pathology and Center for Immunology, Washington University School of Medicine, St. Louis, Missouri 63110, USA. [2]Division of Molecular Immunology, La Jolla Institute for Allergy and Immunology, San Diego, California 92121, USA. [3]Institute of Medical Microbiology, University of Düsseldorf, Düsseldorf, Germany. [4]Howard Hughes Medical Institute, Washington University School of Medicine, St. Louis, Missouri 63110, USA. Correspondence should be addressed to K.M.M. (murphy@pathology.wustl.edu).

Published online 28 November 2004; doi:10.1038/ni1144

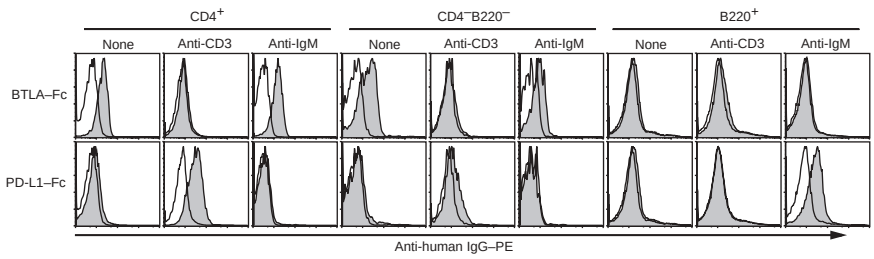

Figure 1 BTLA recognizes a ligand on naive T cells. Splenocytes from BALB/c and C57BL/6 mice were collected and either were directly stained (None) or were activated with plate-bound 500A2 (Anti-CD3; 1:200 dilution of ascites fluid) or soluble anti-IgM (10 μg/ml) for 48 h, and then were stained with BTLA-Fc or PD-L1–Fc fusion protein (shaded histograms) followed by anti-human IgG–phycoerythrin (Anti-human IgG–PE), anti-CD4–tricolor and anti-B220–FITC. Open histograms, staining with human IgG1 isotype control in place of Fc fusion protein.

from a tumor necrosis factor receptor (TNFR) family member toward lymphocytes that may be a barrier to T cell activation.

RESULTS

BTLA binds naive T cells but does not bind B7x

To test for direct interactions between BTLA and B7x, we made NIH 3T3 cell lines stably expressing the extracellular domains of B7x, BTLA, and programmed death 1 (PD-1) and its ligand (PD-L1), and stained the cells with PD-1 and BTLA tetramers and with PD-L1 and B7x Fc fusion proteins (**Supplementary Fig. 1** online). Whereas PD-1 tetramer bound to cells expressing PD-L1, as expected, the BTLA tetramer did not bind to cells expressing PD-L1 or B7x. Furthermore, our B7x-Fc fusion protein did not bind cells expressing BTLA.

To identify potential ligands on normal lymphocytes, we next used a BTLA-Fc fusion protein and BTLA tetramer to stain splenocytes (**Figs. 1** and **2**). As a control, the PD-L1–Fc fusion protein showed selective binding to activated but not resting $CD4^+$ T cells and $B220^+$ B cells (**Fig. 1**), as expected and consistent with the reported inducibility of PD-1 expression[8]. Notably, our BTLA-Fc fusion protein showed specific binding to resting $CD4^+$ and $CD8^+$ T cells but not to $B220^+$ B cells (**Fig. 1**). In addition, this binding was greatly reduced after T cell activation by treatment with antibody to CD3 (anti-CD3) but was not affected by B cell activation. As B7x is not reported to be expressed by naive T cells[5–7], the binding of the BTLA-Fc fusion protein to T cells is not consistent with an interaction with B7x. However, we independently confirmed that B7x was not expressed by T cells by examining the expression of B7x and several other CD28-B7 family members (data not shown). B7x mRNA was most highly expressed in heart and lung but was absent from spleen, lymph node and naive $CD4^+$ T cells. In contrast, we confirmed the expected lymphoid-specific expression pattern for several CD28-B7 family members, including ICOS, PD-1 and BTLA (data not shown).

To confirm and characterize the potential ligand on T cells identified by the BTLA-Fc fusion protein, we next analyzed the properties of BTLA tetramers binding to lymphocytes (**Fig. 2**). The BTLA tetramer showed strong binding to both $CD4^+$ and $CD8^+$ T cells obtained from both spleen and lymph nodes and bound weakly to non–T lymphocytes (**Fig. 2a**). Furthermore, binding to T cells was reduced after anti-CD3 stimulation (**Fig. 2b**), similar to our results obtained with BTLA-Fc fusion proteins (**Fig. 1**). In contrast, treatment of splenocytes with anti–immunoglobulin M (anti-IgM) or lipopolysaccharide did not reduce BTLA tetramer staining of $CD4^+$ T cells. BTLA tetramers showed very slight binding to resting and activated B cells (**Fig. 2b**). We also examined BTLA tetramer staining in thymic subsets (**Fig. 2c**). BTLA tetramer staining was lowest in $CD4^+CD8^+$ (double-positive) thymocytes and showed more staining in mature $CD4^+$ or $CD8^+$ thymocytes and double-negative ($CD4^-CD8^-$) thymocytes, again indicating some physiological regulation of the BTLA ligand. As BTLA tetramer binding was modulated 48 h after anti-CD3 stimulation of T cells, we did a more detailed kinetic analysis using DO11.10 T cells activated *in vitro* with ovalbumin (OVA) peptide (**Fig. 3**). Again, BTLA tetramer binding was regulated during activation, initially increasing by twofold at 24 and 48 h after antigen-specific stimulation, decreasing on day 3 and day 4, and increasing again by day 7. Expression of this BTLA ligand was similar in both

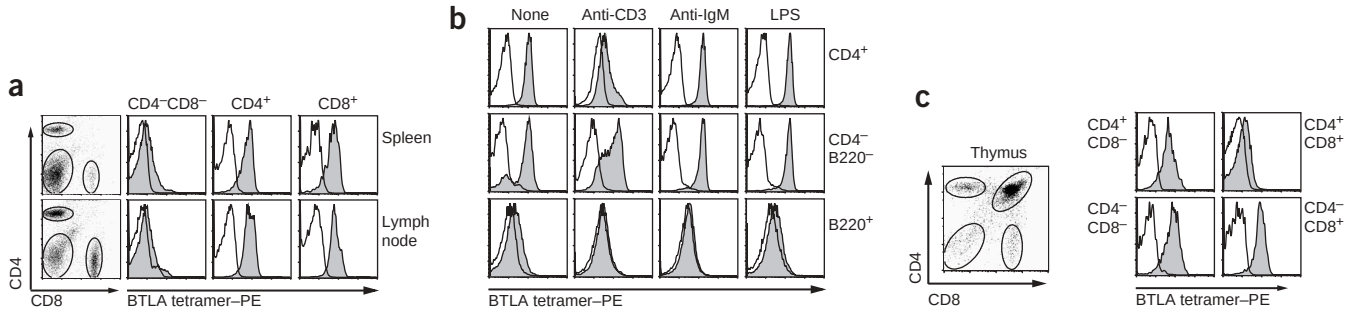

Figure 2 BTLA tetramer staining identifies a ligand on $CD4^+$ and $CD8^+$ cells. (**a**) Splenocytes and lymph node cells from pooled C57BL/6 and BALB/c mice were stained with anti-CD8–FITC, anti-CD4–CyChrome, and either streptavidin-phycoerythrin (open histograms) or BTLA tetramer–phycoerythrin (shaded histograms). Dot plots (left) show the CD4-CD8 gates used for single-color histograms of BTLA tetramer–phycoerythrin staining (right). (**b**) Splenocytes from pooled C57BL/6 and BALB/c mice were left untreated or were activated 48 h with anti-CD3 or anti-IgM as described in **Figure 1** or with lipopolysaccharide (1 μg/ml) for 24 h and were stained with anti-B220–FITC, anti-CD4–CyChrome, and either streptavidin-phycoerythrin (open histograms) or BTLA tetramer–phycoerythrin (shaded histograms). (**c**) Thymocytes from pooled C57BL/6 and BALB/c mice were stained with anti-CD8–FITC, anti-CD4–CyChrome, and either streptavidin-phycoerythrin (open histograms) or BTLA tetramer–phycoerythrin (shaded histograms). The dot plot (left) shows the CD4/CD8 gates used for the single-color histograms of BTLA-tetramer staining.

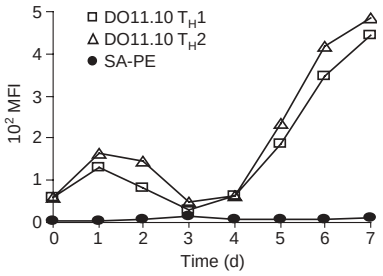

Figure 3 BTLA ligand expression is modulated during T cell activation. DO11.10 splenocytes were stimulated with 0.3 μM OVA peptide in T helper type 1 conditions (T_H1; 10 U/ml of IL-12 and 10 μg/ml of anti-IL-4) or T helper type 2 conditions (T_H2; 100 U/ml of IL-4 and 3 μg/ml of anti-IL-12). Cultures were collected after activation (time, horizontal axis) and were stained with anti-CD4–FITC and BTLA tetramer–phycoerythrin. Filled circles, streptavidin-phycoerythrin (SA-PE) staining of T helper type 1 cultures without BTLA tetramer. MFI, mean fluorescence intensity.

T helper type 1– and T helper type 2–inducing conditions. Thus, BTLA tetramers and BTLA-Fc fusion proteins have very similar binding properties to lymphocytes, and a BTLA ligand is expressed by resting T cells and undergoes regulation during thymocyte development and T cell activation.

Cloning a BTLA-interacting protein

We constructed a retroviral cDNA library from lymphocytes and transduced two host cell lines, BJAB and NIH 3T3, that were negative for BTLA tetramer binding (**Fig. 4a**). After four successive rounds of sorting, we obtained lines uniformly positive for BTLA tetramer staining, which we used to amplify retrovirus-specific inserts. From BJAB cells, we obtained a predominant RT-PCR product that we identified as mouse HVEM (**Supplementary Fig. 2** online). From NIH 3T3 cells we also obtained mouse HVEM as the main component of RT-PCR isolates. Among the minor retroviral inserts identified from NIH 3T3 cells, 4-1BB was the only transmembrane receptor; it also belongs to the TNFR superfamily[9].

We next tested these isolates as candidates for direct interactions with BTLA tetramers. We expressed full-length cDNA clones of mouse HVEM, human HVEM, mouse 4-1BB and mouse LTβR, which binds the same ligands (LIGHT and LTα) as HVEM, in BJAB cells and analyzed these cells for binding to BTLA tetramers. We specifically constructed BTLA tetramers from both the C57BL/6 and BALB/c alleles to identify any potential allelic differences in binding (**Fig. 4b**). We found specific binding of both forms of BTLA tetramers to green fluorescent protein (GFP)–positive BJAB cells expressing mouse HVEM but not to BJAB cells expressing human HVEM, mouse 4-1BB or mouse LTβR or to GFP-negative uninfected BJAB cells.

HVEM induces BTLA phosphorylation

We next sought to determine if HVEM could induce BTLA phosphorylation (**Fig. 4c,d**). We analyzed BTLA phosphorylation in EL4 cells using immunoprecipitation immunoblot analysis as described above[1,3]. EL4 cells had low expression of BTLA but no detectable HVEM, as assessed by BTLA tetramer binding (**Supplementary Fig. 3** online). We therefore examined EL4 cells for BTLA phosphorylation and SHP-2 coimmunoprecipitation after contact with mouse HVEM expressed by BJAB cells. EL4 cells alone showed neither coimmunoprecipitation of SHP-2 with BTLA (**Fig. 4c**) nor direct tyrosine phosphorylation of BTLA (**Fig. 4d**). Mixing of EL4 cells with HVEM-expressing BJAB cells induced both coimmunoprecipitation of SHP-2 with BTLA and tyrosine phosphorylation of BTLA. In contrast, mixing EL4 cells with HVEM-negative BJAB cells induced neither coimmunoprecipitation of SHP-2 with BTLA nor BTLA phosphorylation. As controls, pervanadate treatment of EL-4 cells induced coimmunoprecipitation of SHP-2 and tyrosine phosphorylation of BTLA, but BJAB cells alone, either HVEM-negative or expressing HVEM, showed neither SHP-2 coimmunoprecipitation nor BTLA phosphorylation. Thus, these results show that HVEM can induce BTLA tyrosine phosphorylation and association with SHP-2.

HVEM-BTLA interactions are conserved in human

Because tetramers of mouse BTLA bound mouse HVEM but not human HVEM, we sought to determine if the BTLA-HVEM interaction was conserved in humans. Therefore, we generated a human BTLA-Fc fusion protein and characterized its interactions with mouse and human HVEM (**Fig. 4e**). The mouse BTLA-Fc fusion protein bound to BJAB cells expressing mouse HVEM but not cells expressing human HVEM, confirming the data obtained with mouse BTLA tetramers (**Fig. 4b**). In addition, the human BTLA-Fc fusion protein bound to BJAB cells expressing human HVEM (**Fig. 4e**). The human BTLA-Fc fusion protein also bound, although more weakly, to BJAB cells expressing mouse HVEM. These interactions were specific, as the isotype control antibody and the B7x-Fc fusion protein did not bind to BJAB cells expressing either mouse or human HVEM. Thus, the interaction between BTLA and HVEM occurs in human lymphocytes, as it does in mouse lymphocytes. Also, although cross-species interactions are noted for human BTLA and mouse HVEM (**Fig. 4e**), it seems that this cross-species interaction is weaker than the intraspecies interaction.

BTLA interacts with the CRD1 region of HVEM

HVEM is a member of the TNFR superfamily and interacts with the two known TNF family members LIGHT and LTα[9,10]. Because HVEM has multiple ligands, we sought to determine whether we could detect additional ligands for BTLA. Thus, we compared binding of BTLA tetramers to wild-type and HVEM-deficient lymphocytes (**Fig. 5a**). BTLA tetramers showed no detectable specific binding to HVEM-deficient $CD4^+$ or $CD8^+$ T cells but showed the expected binding to wild-type T cells. Even the low binding of BTLA tetramer to B cells was reduced to undetectable amounts in HVEM-deficient B cells (**Fig. 5a**). Thus, we found no evidence of additional ligands for BTLA in mice.

The interaction between HVEM and LIGHT can be detected with an HVEM-Fc fusion protein containing the four extracellular CRD regions of HVEM fused to the Fc region of human IgG1 (ref. 10). We therefore sought to determine whether this HVEM-Fc fusion protein can also bind BTLA (**Fig. 5b**). Because LIGHT is expressed by $CD11c^+$ DCs but not by $B220^+$ B cells[11,12], we compared the binding of HVEM-Fc fusion protein to B cells and DCs from wild-type and BTLA-deficient mice (**Fig. 5b**). The HVEM-Fc fusion protein bound to wild-type B cells but not to $Btla^{-/-}$ B cells. In contrast, the HVEM-Fc fusion protein bound to wild-type DCs with only slightly reduced binding to $Btla^{-/-}$ DCs. We next compared the binding of HVEM-Fc fusion protein to wild-type and LIGHT-deficient ($Tnfsf14^{-/-}$) B cells and DCs (**Fig. 5c**). The HVEM-Fc fusion protein bound to wild-type and $Tnfsf14^{-/-}$ B cells and DCs with nearly equal intensity. In addition, HVEM expression was actually increased in $Btla^{-/-}$ mice compared with that in wild-type mice (**Supplementary Fig. 4** online). This result might indicate that endogenous HVEM expression is regulated by interaction with BTLA, similar to the reported regulation of HVEM expression by LIGHT[13]. Furthermore, this result formally

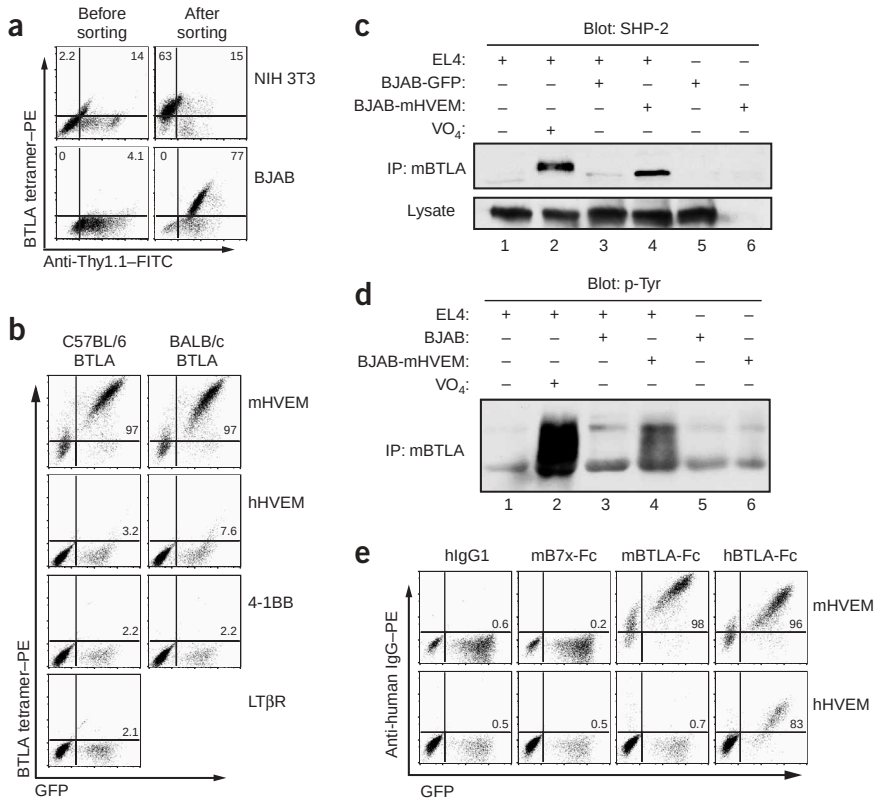

Figure 4 HVEM is a ligand for BTLA. (**a**) NIH 3T3 cells and BJAB cells were transduced with splenocyte cDNA libraries and were directly stained with anti-Thy1.1–FITC and the C57BL/6 BTLA tetramer–phycoerythrin (Before sorting). These cells were sorted for the highest 0.5% population of BTLA tetramer staining with BTLA-phycoerythrin tetramer and Thy1.1-FITC and were subjected to an additional three rounds of similar sequential purification. After the fourth round of sorting, cell populations were expanded and cells were stained (After sorting). Numbers in each quadrant indicate the percentage of live cells in the indicated gate. (**b**) BJAB cells were transduced with the retroviruses mHVEM-IRES-GFP (mHVEM; mouse), hHVEM-IRES-GFP (hHVEM; human), 4-1BB-IRES-GFP (4-1BB; mouse) and LTβR-IRES-GFP (LTβR; mouse) and were stained with C57BL/6 BTLA tetramer–phycoerythrin or BALB/c BTLA tetramer–phycoerythrin. Numbers in dot plots indicate the percentage of BTLA tetramer staining in the GFP-positive population. (**c**,**d**) HVEM activates BTLA phosphorylation and SHP-2 association. EL-4 cells (EL4), BJAB cells expressing GFP (BJAB-GFP) or BJAB cells expressing mouse HVEM (BJAB-mHVEM) were added (+) or not added (–) for 4 min at 37 °C at a density of 25 × 10^6 cells/ml. Cells were left untreated (–) or were treated (+) with pervanadate (VO_4) for 4 min. Total cell lysates were prepared and were immunoprecipitated with 6A6 (anti–mouse BTLA), and immunoblots were probed for SHP-2 (**c**) or for phosphotyrosine (**d**) in immunoprecipitates (IP) or in lysates without immunoprecipitation. Immunoblots using the isotype control for immunoprecipitation were negative for SHP-2 association (data not shown). Data in **c** and **d** are representative of four independent experiments. (**e**) BJAB cells were transduced with retrovirus mHVEM-ires-GFP or hHVEM-ires-GFP and were stained with human IgG1 isotype control (hIgG1), mB7x-Fc, mBTLA-Fc or hBTLA-Fc followed by anti-human IgG–phycoerythrin. Numbers in dot plots show the percentage of fusion protein staining in the GFP-positive population.

shows that HVEM expression does not require BTLA as a 'chaperone'. These results might suggest that BTLA is the only ligand for HVEM on B cells, but such conclusions based solely on soluble staining reagents may be misleading, and it is possible that HVEM could also interact with other unknown molecules on B cells. For DCs, it seems that both BTLA and LIGHT are ligands for HVEM.

We sought to identify which domains of HVEM are involved in BTLA interactions. HVEM has four extracellular CRDs; it binds LIGHT and LTα through CRD2 and CRD3 (ref. 14) and binds herpes glycoprotein D through CRD1 (refs. 14,15). We constructed a series of HVEM mutants, including a mouse HVEM GFP fusion protein, an HVEM deletion mutant lacking the N-terminal CRD1 as a GFP fusion protein, an intact human HVEM, and a chimeric HVEM containing mouse CRD1 linked to human CRD2. We expressed this panel of HVEM mutants in BJAB cells and examined binding of the mouse BTLA tetramer (**Fig. 5d**). As expected, the BTLA tetramer did not bind uninfected BJAB cells but bound to wild-type mouse HVEM. However, the mouse BTLA tetramer did not bind to the HVEM mutant lacking CRD1. In addition, BTLA tetramer did not bind to human HVEM but did bind to the mouse-human chimeric HVEM (**Fig. 5d**). As a control, we assessed the amounts of human HVEM expressed by these cell lines (**Fig. 5d**), confirming expression of the human and chimeric HVEM molecules. These results indicate an important function for the CRD1 domain of mouse HVEM for BLTA interactions but do not exclude the possibility of a contribution by other domains.

HVEM inhibits antigen-driven T cell proliferation

HVEM is expressed by several types of cells, including T cells, B cells and DCs[12,13,16,17], complicating the analysis of potential interactions between cells expressing LIGHT, BTLA and HVEM. Thus, we first sought to confirm the reported costimulatory effects of LIGHT on $CD4^+$ T cells in our system[11]. We stimulated highly purified $CD4^+$ T cells with increasing amounts of anti-CD3 in the presence of various concentrations of plate-bound LIGHT (**Fig. 6a**). At suboptimal concentrations of anti-CD3 stimulation, LIGHT strongly augmented T cell proliferation in a dose-dependent way. At the highest dose of anti-CD3, the costimulatory effect of LIGHT was reduced slightly because of an increase in the LIGHT-independent proliferation. These data confirm reports that LIGHT engagement of HVEM provides positive costimulation.

We next tested whether BTLA or HVEM expression by antigen-presenting cells (APCs) inhibited or activated T cells. For this, we produced a panel of Chinese hamster ovary (CHO) cells expressing various combinations of $I\text{-}A^d$ and B7-1 (ref. 18) plus either BTLA or HVEM using retrovirus transduction and cell sorting. We confirmed expression of $I\text{-}A^d$, B7-1, BTLA and HVEM by these cell lines using flow cytometry (**Supplementary Fig. 5** online). We sought to determine if BTLA expression by APCs costimulated DO11.10 T cells (**Fig. 6b**). CHO cells expressing $I\text{-}A^d$ alone supported minimal T cell proliferation, similar to that seen with T cells and peptide alone. As a positive control, CHO cells expressing $I\text{-}A^d$ and B7-1 supported higher proliferation in response to OVA peptide. In contrast, BTLA

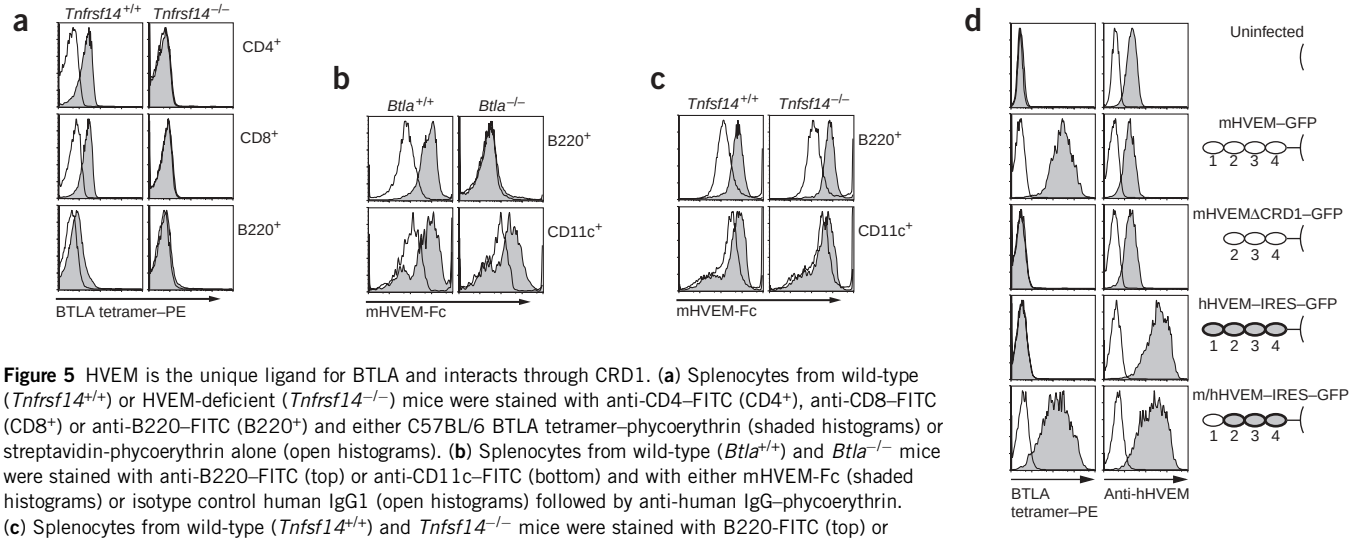

Figure 5 HVEM is the unique ligand for BTLA and interacts through CRD1. (**a**) Splenocytes from wild-type (*Tnfrsf14*$^{+/+}$) or HVEM-deficient (*Tnfrsf14*$^{-/-}$) mice were stained with anti-CD4–FITC (CD4$^+$), anti-CD8–FITC (CD8$^+$) or anti-B220–FITC (B220$^+$) and either C57BL/6 BTLA tetramer–phycoerythrin (shaded histograms) or streptavidin-phycoerythrin alone (open histograms). (**b**) Splenocytes from wild-type (*Btla*$^{+/+}$) and *Btla*$^{-/-}$ mice were stained with anti-B220–FITC (top) or anti-CD11c–FITC (bottom) and with either mHVEM-Fc (shaded histograms) or isotype control human IgG1 (open histograms) followed by anti-human IgG–phycoerythrin. (**c**) Splenocytes from wild-type (*Tnfsf14*$^{+/+}$) and *Tnfsf14*$^{-/-}$ mice were stained with B220-FITC (top) or CD11c-FITC (bottom) and mHVEM-Fc or isotype control human IgG1 (open histograms), followed by anti-human IgG-phycoerythrin. (**d**) BJAB cells were left uninfected or were transduced with retroviruses expressing mouse HVEM-GFP fusion protein (mHVEM–GFP), the HVEM deletion mutant lacking N-terminal CRD1 as a GFP fusion protein (mHVEMΔCRD1–GFP), intact human HVEM (hHVEM–IRES–GFP) or chimeric HVEM containing mouse CRD1 linked to human CRD2 (m/hHVEM–IRES–GFP). Left, cells stained with BTLA tetramer–phycoerythrin (shaded histograms) or streptavidin-phycoerythrin alone (open histograms); right, cells stained with either anti-hHVEM (shaded histograms) or a mouse IgG1 isotype control (9E10) followed by goat anti-mouse IgG1–phycoerythrin. Single-color histograms were gated on GFP-positive live cells. Right margin, composition of the HVEM constructs, with mouse CRDs (open ovals) and human CRDs (shaded ovals).

expression by APCs did not augment T cell proliferation induced by CHO cells expressing I-A^d alone (**Fig. 6b**), as did expression of B7-1, suggesting that BTLA does not provide costimulation to T cells through HVEM engagement.

Whereas BTLA, unlike LIGHT, may not activate HVEM, HVEM seems to activate BTLA, as evidenced by BTLA phosphorylation and SHP-2 association (**Fig. 4c,d**). Thus, we sought to determine whether HVEM expression by APCs influenced T cell proliferation (**Fig. 6c**). The peptide dose–dependent proliferation supported by CHO cells expressing I-A^d alone was reduced when HVEM was coexpressed on these CHO cells (**Fig. 6c**). Furthermore, as expected, B7-1 increased T cell proliferation induced by peptide and I-A^d (**Fig. 6d**), shifting the dose-response to lower concentrations of peptide. Again, coexpression of HVEM on these CHO cells reduced peptide-dependent T cell

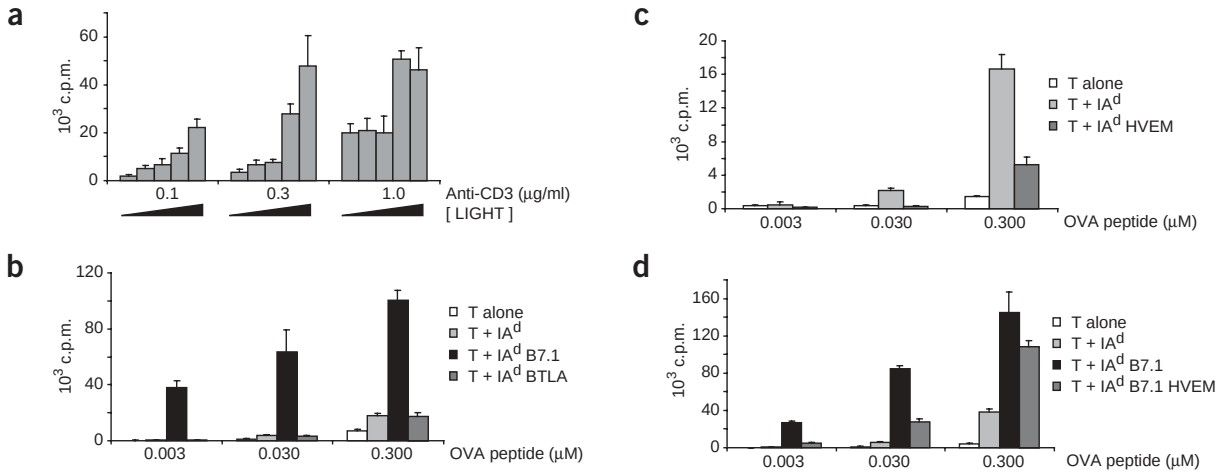

Figure 6 HVEM expression on APCs inhibits T cell proliferation. (**a**) CD4$^+$ cells were purified from BALB/c mice by magnetic separation and were stimulated (1×10^6 cells/ml) with plate-bound anti-CD3 (2C11; dose, horizontal axis) and increasing concentrations (wedges; 0, 0.3, 1.0, 3.0 and 10.0 μg/ml) of plate-bound LIGHT. Cultures were pulsed with [^{3}H]thymidine at 48 h and were collected at 60 h. Data represent c.p.m. ± s.d. from one of three similar experiments. (**b**) CD4$^+$ T cells from DO11.10 mice were purified by magnetic separation, followed by cell sorting for CD4$^+$B220$^-$CD11c$^-$ cells to more than 98% purity, and were added to cultures alone (T alone) or with (T +) CHO cells expressing I-A^d, I-A^d and B7.1, or I-A^d and BTLA, plus various concentration of OVA peptide (horizontal axis), and proliferation was measured as described in **a**. (**c**) T cells prepared as described in **b** were cultured alone or with CHO cells expressing I-A^d, or I-A^d and HVEM, plus various concentrations of OVA peptide, and proliferation was measured as described in **a**. (**d**) T cells prepared as described in **b** were cultured alone or with CHO cells expressing I-A^d, or I-A^d and B7.1, or I-A^d, B7.1 and HVEM, and were activated with various concentration of OVA peptide. Proliferation was measured as described in **a**.

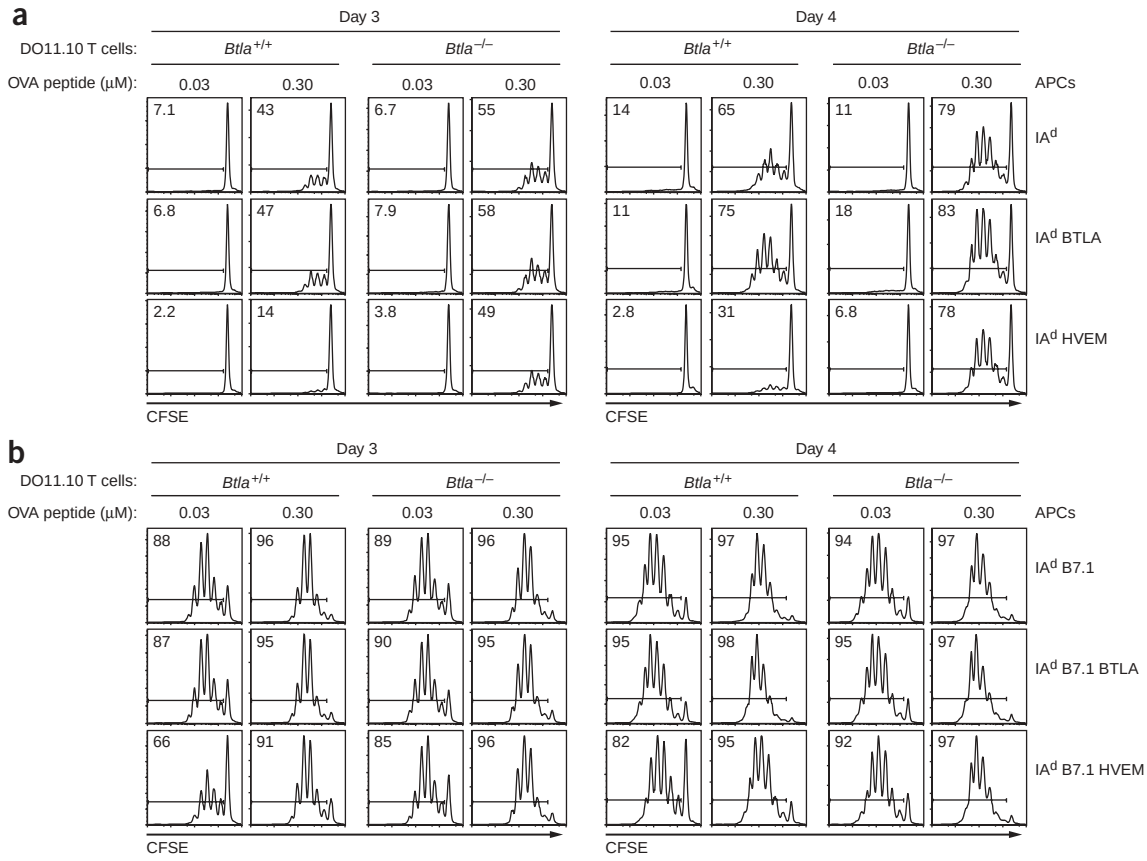

Figure 7 HVEM inhibits T cell proliferation in a BTLA-dependent way. (**a**) Highly purified DO11.10 CD4+ T cells from wild-type (*Btla*$^{+/+}$) or *Btla*$^{-/-}$ mice were prepared as described in **Figure 6**, were labeled with CFSE and were cultured for 3 or 4 d with CHO cells expressing I-A^d, or I-A^d and BTLA, or I-A^d and HVEM, plus 0.03 or 0.3 μM OVA peptide. Cells were analyzed by flow cytometry. Data are single-color histograms of CFSE gated on CD4+ T cells. Numbers indicate percentage of live cells that have divided at least once, as indicated by the gate drawn. (**b**) T cells prepared as described in **a** were cultured for 3 or 4 d with CHO cells expressing I-A^d and B7.1, I-A^d, B7.1 and BTLA, or I-A^d, B7.1 and HVEM, plus 0.03 or 0.3 μM OVA peptide, and were analyzed as described in **a**. Numbers indicate percentage of live cells that have divided at least once.

proliferation. The inhibition produced by HVEM at the highest peptide concentrations was smaller than the inhibition seen with intermediate stimulation.

We extended this analysis using T cells labeled with carboxyfluorescein diacetate succinimidyl diester (CFSE; **Fig. 7**). In addition, we tested whether the inhibitory effect of HVEM on T cell proliferation required BTLA by using *Btla*$^{-/-}$ DO11.10 T cells. Using CHO cells lacking B7-1 expression, we did not note T cell proliferation at the lowest dose of OVA peptide (0.03 μM) on days 3 and 4 (**Fig. 7a**). However, higher peptide concentrations (0.3 μM) induced T cell proliferation on days 3 and 4. In these conditions, expression of BTLA on CHO cells had no effect on T cell proliferation at any time. However, expression of HVEM on CHO cells greatly reduced T cell proliferation, which occurred only in wild-type DO11.10 T cells, not *Btla*$^{-/-}$ T cells, and was evident on days 3 and 4 after activation.

We next examined the effects of HVEM on T cell proliferation in response to antigen presentation by CHO cells expressing B7-1 (**Fig. 7b**). Again, B7-1 increased T cell proliferation induced by peptide and I-A^d, shifting the dose-response to lower concentrations of peptide, as demonstrated by larger numbers of cellular divisions at lower doses of peptide; this was clearly evident on day 3 as well as day 4. In these conditions, coexpression of BTLA on CHO cells had no effect on T cell proliferation. In contrast, coexpression of HVEM on CHO cells caused a reduction in proliferation of wild-type DO11.10 T cells, but this was evident only at the lowest peptide dose and was evident only on day 3, not day 4, after T cell activation. This inhibition of T cell proliferation was specific to BTLA, as we found it only in wild-type but not *Btla*$^{-/-}$ T cells. In summary, HVEM inhibits both costimulation-independent and costimulation-dependent proliferation, but is more effective in blocking activation of antigen stimulated T cells at low B7-1 expression. Furthermore, HVEM-mediated inhibition of T cell proliferation requires BTLA expression by T cells.

DISCUSSION

Here we have made the unexpected observation that BTLA, a member of the immunoglobulin superfamily, functionally interacts with HVEM, a member of the TNFR superfamily. The initial suggestion that BTLA and B7x might interact was based on indirect observations of decreased binding of a B7x-Fc fusion protein to *Btla*$^{-/-}$ lymphocytes[1]. However, in this study we were not able to provide any evidence for a direct BTLA-B7x interaction using tetramers and Fc fusion proteins of BTLA and B7x for binding to transfected cells expressing each of these proteins. Instead, we found evidence of a BTLA ligand expressed on resting T cells, which do not express B7x[5–7]. Using expression cloning, we have identified HVEM as the unique BTLA ligand in mice and have shown that this BTLA-HVEM

interaction is also conserved in human. BTLA binds the CRD1 of HVEM, in contrast to LIGHT and LTα, which bind CRD2 and CRD3 (ref. 14). Finally, we have demonstrated that HVEM expressed on APCs induces BTLA phosphorylation and inhibits T cell proliferation in a BTLA-dependent way, particularly with low costimulation.

The interaction between BTLA and HVEM has structural and functional importance. We are not aware of any other examples of a known TNFR family member's being the ligand for an immunoglobulin superfamily receptor[19]. TNFR family members normally interact with TNF family cytokines, with the exception of NGFR, a receptor that binds neurotrophins of the growth factor cysteine knot superfamily[20]. Herpes simplex virus glycoprotein D, which binds HVEM using an N-terminal hairpin loop extension rather than its immunoglobulin domain, is expressed only by herpesviruses and has no apparent mammalian homolog. Thus, the conserved binding of HVEM to an immunoglobulin superfamily receptor is structurally unique.

It is relevant that the interaction between BTLA and HVEM may be a unique example of reverse signaling mediated by a TNFR family member through a non–TNF family member. Several TNFR family members reportedly transmit reverse signals to cells through their TNF family ligand, including TNFR1 through membrane TNF[21], CD30 through CD30L[22], HVEM through LIGHT[23] and Fas through FasL[24], although the way in which such signaling occurs is still unclear. Here we have shown that HVEM induces the tyrosine phosphorylation of BTLA and association with SHP-2, suggesting a similarity in the inhibitory mechanism to that of the inhibitory receptors CTLA-4 and PD-1 (refs. 18,25). In previous reports it was difficult to induce BTLA phosphorylation, which required pervanadate treatment or artificial crosslinking with antigen receptors[1]. Here we have shown that HVEM expressed by tumor cell lines is sufficient for the biochemical activation of BTLA on other cells. We found BTLA phosphorylation occurred during the collection of splenocytes (data not shown), which could result from contact between B cells expressing BTLA with T cells expressing HVEM, although we have not fully characterized that phenomenon. Thus, these results clearly document the ability of this TNFR family member to 'reverse' signal through BTLA.

Previous *in vitro* examination of *Btla*$^{-/-}$ T cells showed relatively modest changes in proliferation[1,2]. However, the conditions used in those studies may not have been ideal for emphasizing the involvement of BTLA by inducing its activation or for demonstrating the involvement of HVEM-mediated T cell inhibition. For example, relatively dilute T cell cultures activated with anti-CD3 may not provide the density to allow potential T cell–T cell interaction to engage BTLA by HVEM. Here we found conditions in which HVEM inhibited T cell proliferation in a strictly BTLA-dependent way. HVEM is expressed by several types of lymphoid cells, and we have not yet identified the relevant source of HVEM *in vivo*. HVEM is expressed not only by T cells but also by immature DCs, a property unique among the TNFR family[12,26]. Conceivably, immature DCs with low expression of B7 molecules might express HVEM as a mechanism to generate a 'safety threshold' to control nonspecific T cell activation. However, T cells also express abundant HVEM and modulate its level during activation. Thus, there could be a function for T cell–T cell interactions that might autoregulate T cell population expansion depending on density and location. Indeed, there have been suggestions of T cell–T cell interactions involving interactions between B7 and CTLA-4 (refs. 27,28).

Here we sought to document the unexpected interaction between BTLA and HVEM, and thus we have focused on showing functional responses of T cells in response to BTLA ligation by HVEM. However, B cells also express BTLA, and we suspect a function for HVEM in regulating antibody responses through BTLA as well (data not shown). So far, *Btla*$^{-/-}$ mice have shown only relatively minor changes in antibody responses. However, we have not yet examined autoantibody production over time or in response to experimental models of autoimmunity or to pathogens. Alternatively, BTLA expression by B cells may have some function other than B cell–intrinsic inhibition, such as by exerting an effect on LIGHT-HVEM signaling in other cells.

We have demonstrated reverse signaling by HVEM through BTLA but have not shown whether BTLA activates HVEM or what effects BTLA might exert on LIGHT or LTα interactions with HVEM. LIGHT can costimulate T cells through HVEM activation[11,23]. Our finding that BTLA expression by CHO cells did not increase T cell proliferation could be interpreted as evidence against HVEM activation by BTLA. Structural considerations favor the suggestion that BTLA should not activate HVEM signaling, as trimerization of TNFR members by ligands seems to be involved, but clearly this issue requires further examination[19]. Conceivably, binding of BTLA to HVEM might also structurally preclude the binding of LIGHT or LTα to HVEM. In this way, BTLA expression by one cell could potentially attenuate LIGHT or LTα activation of HVEM. It will therefore be important to determine biochemically whether binding of BTLA to HVEM is inhibitory for interactions of LIGHT and LTα with HVEM. So far, structural studies of HVEM have analyzed only its interaction with herpesvirus glycoprotein D[15] but not with LIGHT or LTα. Thus, functional, biochemical and structural studies may be required to determine whether BTLA influences LIGHT-dependent or LTα-dependent responses through HVEM.

METHODS

Mice. C57BL/6 and BALB/c mice (Jackson Labs) were bred in our facility. *Btla*$^{-/-}$ mice[1] were backcrossed to BALB/c for nine generations and were subsequently crossed onto the DO11.10 T cell receptor–transgenic background[29]. LIGHT-deficient mice were as described[30] and HVEM-deficient (*Tnfrsf14*$^{-/-}$) mice will be described elsewhere (data not shown).

Plasmids and retroviral constructs. The sequences of all oligonucleotides are provided in **Supplementary Table 1** online. For preparation of B7x-B7h-GFP-RV, a PCR product made with primers 5′Bgl2 mB7x and B7xB7h bottom using IMAGE cDNA clone 3709434 as the template, plus a PCR product made with primers B7xB7h top and 3′R1 GFP using the B7h-GFP plasmid (a gift from W. Sha, University of California, Berkeley, California) as the template, were annealed and amplified with *Pfu* polymerase with primers 5′Bgl2 mB7x and 3′R1 GFP. This product, encoding the B7x extracellular domain, B7h transmembrane and cytoplasmic domains fused to GFP, was digested with *Bgl*II and *Eco*RI and was cloned into IRES-GFP-RV that had been digested with *Bgl*II and *Eco*RI.

The plasmid huHVEM-IRES-GFP-RV was produced by amplification of huHVEM with primers 5′Bgl2 huHVEM and 3′Xho1 huHVEM using IMAGE cDNA clone 5798167 (Invitrogen) as the template, followed by digestion with *Bgl*II and *Xho*I and ligation into Tb-lym-IRES-GFP-RV that had been digested with *Bgl*II and *Xho*I, replacing the Tb-lym cDNA with that of huHVEM. Similarly, m4-1BB-IRES-GFP-RV was prepared with primers 5′Bgl2 m4-1BB and 3′Xho1 m4-1BB using library plasmid as the template, followed by digestion with *Bgl*II and *Xho*I and ligation into Tb-lym-IRES-GFP-RV. The plasmid mLTβR-IRES-GFP-RV was prepared with primers 5′Bgl2 mLTβR and 3′Sal1 mLTβR using IMAGE cDNA clone 5293090 (Invitrogen) as the template, followed by digestion with *Bgl*II and *Sal*I and ligation into Tb-lym-IRES-GFP-RV. The plasmid mHVEM-FL-IRES-GFP-RV was similarly prepared with primers 5′Bgl2 mHVEM and 3′Xho1 mHVEM using, as the template, cDNA from library infected BJAB cells sorted for BTLA tetramer binding, followed by digestion with *Bgl*II and *Xho*I and ligation into Tb-lym-IRES-GFP-RV. Three amino acid changes (N58S, K92R and E128G) in mouse HVEM cDNA cloned from the retrovirus library, compared with that of mouse HVEM cDNA from the 129 SvEv mouse strain, were implemented by Quick Change mutagenesis

(Stratagene) to generate mHVEM(129)-IRES-GFP-RV with serial application of the primers S-N top plus S-N bot; R-K top plus R-K bot; and G-E top plus G-E bot.

The plasmid mHVEM-FL-GFP-RV was made from two PCR products, with primers 5′Bgl2 mHVEM and mHVEM/GFP bot using mHVEM-FL-IRES-GFP-RV as the template, and primers mHVEM/GFP top and 3′GFP + Sal using mHVEM-FL-IRES-GFP-RV as the template; the PCR products were annealed, amplified with primers 5′Bgl2 mHVEM and 3′GFP + Sal, digested with *Bgl*II and *Sal*I and ligated into IRES-GFP-RV that had been digested with *Bgl*II and *Sal*I. The plasmid mHVEM-FL-GFP-RVΔCRD1 was made by Quick Change mutagenesis from mHVEM-FL-GFP-RV with primers mHVEM d1 top and mHVEM d1 bot. The plasmid m/hHVEM-IRES-GFP-RV (mouse CRD1 fused to human CRD2) was made from two PCR products, with primers 5′Bgl2 mHVEM and m/hHVEM bot using mHVEM-FL-IRES-GFP-RV as the template, and primers m/hHVEM top and 3′Xho hHVEM using hHVEM-IRES-GFP-RV as the template; the PCR products were annealed, amplified with primers 5′Bgl2 mHVEM and 3′Xho huHVEM, digested with *Bgl*II and *Xho*I and ligated into Tb-lym-IRES-GFP-RV that had been digested with *Bgl*II and *Xho*I. C57BL/6-BTLA-GFP-RV, a BTLA-GFP chimera, was prepared from two PCR products, with primers J10RV1 (Bgl 2) and 3′J10+10 using C57BL/6 BTLA cDNA as the template, and primers 5′GFP+10 and 3′GFP+Sal using GFP cDNA as the template; the PCR products were annealed, amplified with J10RV1 (Bgl 2) and 3′GFP+Sal, digested with *Bgl*II and *Sal*I and ligated into Tb-lym-IRES-GFP-RV that had been digested with *Bgl*II and *Xho*I. A cytoplasmic deletion of this construct, BTLA-trunc-GFP-RV, was made by site-directed mutagenesis (Stratagene) with primers mj11trunc top and mj11trunc bottom.

PD-1-GFP-RV was made by amplification of the PD-1 coding region with primers PD15′ and PD13′ using PD-1 cDNA as the template (a gift from T. Honjo, Kyoto University, Kyoto, Japan); the PCR product was digested with *Bgl*II and *Bam*HI and was cloned into AIB3-GFP MSCV that had been digested with *Bgl*II and *Bam*HI (a gift from W. Sha). Similarly, PD-L1-GFP-RV was made by amplification of the region encoding PD-L1 with primers PD-L1G5′ and PD-L1G3′ using PD-L1 cDNA (a gift from T. Honjo) as the template; the PCR product was digested with *Bgl*II and *Bam*HI and was ligated into AIB3-GFP MSCV.

PD-1 pET28 was made by amplification of the immunoglobulin domain of PD-1 with primers PD1Tet5′ and PD1Tet3′ using PD-1-GFP-RV plasmid as the template, followed by digestion with *Nco*I and *Bam*HI and ligation intoMLL1-pET28 (a gift from D. Fremont, Washington University, St. Louis, Missouri) that had been digested with *Nco*I and *Bam*HI. Similarly, B6-BTLA pET28 was made by amplification of the extracellular immunoglobulin domain of BTLA with primers J11TetMus5′ and J11TetB63′ using C57BL/6 BTLA-GFP-RV plasmid as the template, followed by digestion with *Nco*I and *Bam*HI and ligation into MLL1-pET28. Similarly, BALB-BTLA pET28 was made with primers J11TetMus5′ and J11TetWEHI3′ using mJ11W1 as the template[1], and digestion with *Nco*I and *Bam*HI and ligation into MML1-pET28. The immunoglobulin domain was 'corrected' to authentic BALB/c allelic sequence (data not shown) by serial mutagenesis with primers W1e23k5′ and W1e23k3′ followed by primers W1h38n3B and W1h38n5C.

Fc fusion proteins. For the creation of CD47-Fc-αTP-ires-GFP-RV, a bicistronic retroviral vector for Fc fusion proteins, CP318 (a gift from Lewis Lanier, University of California, San Francisco, California)[31,32] was digested with *Pfl*F I and *Not*I, treated with Vent polymerase and ligated into mIL-12R-ires-GFP-RV that had been digested with *Bgl*II and *Xho*I and treated with mung bean nuclease. The plasmids mBTLA-Fc-αTP-ires-GFP-RV, mB7x-Fc-αTP-ires-GFP-RV, mPD-L1–Fc-αTP-ires-GFP-RV and hBTLA-Fc–αTP-ires-GFP-RV were made by ligation of the following *Xho*I-digested PCR products containing the immunoglobulin domains regions of these genes into the *Xho*I site of CD47-Fc-αTP-ires-GFP-RV. The product mBTLA was made with primers 5′xho mJ11 dodecamer and 3′xho mJ11 dodecamer using as a template the C57BL/6 splenocyte phage library (Stratagene). The product mB7x was made with primers 5′xho mB7x dodecamer and 3′xho mB7x dodecamer using IMAGE cDNA clone 3709434 (Invitrogen) as the template. PD-L1 was made with primers 5′xho mPDL2 dodecamer and 3′Xho PDL1 dodecamer using pBacPAK8-PDL1 (a gift from T. Honjo) as the template. Human BTLA was made with primers 5′Xho hJ11 Ig and 3′Xho hJ11 Ig using hJ11(corr)ires-GFP-RV as the template.

Fc fusion proteins were produced by transfection of Phoenix E cells, were purified with Affi-prep protein A columns (Biorad) and were dialyzed against PBS and stored at −70 °C. For flow cytometry, cells were stained with 200 ng of purified Fc-fusion protein or, for hBTLA-Fc fusion protein, 1 ml of supernatant, followed by phycoerythrin-conjugated anti-human IgG (heavy plus light) that had been adsorbed against proteins from mouse, rat, cow and other species (Jackson Immunoresearch), and anti-mCD4–tricolor (Caltag) and anti-mB220–fluorescein isothiocyanate (FITC; BD-Pharmingen).

Production of tetramers. Tetramers produced with plasmid PD-1 pET28, B6-BTLA pET28 or BALB-BTLA pET28 were transformed into BL21-CodonPlus (DE3) RIPL Competent Cells (Stratagene) essentially as described[33]. Purified proteins were biotinylated *in vitro* with BirA ligase (Avidity), purified by gel filtration and concentrated. Tetramers were formed by the addition of biotinylated protein to streptavidin-phycoerythrin at a molar ratio of 1:4.

Cell lines. BJAB and NIH 3T3 cells were from A. Chan (Washington University, St. Louis, Missouri); EL-4 cells were from T. Ley (Washington University, St. Louis, Missouri); 293T cells were from R. Schreiber (Washington University, St. Louis, Missouri); CHO cells were from A. Sharpe (Harvard University, Boston, Massachusetts)[18]; and Phoenix A and E packaging cells were from American Type Culture Collection. Retrovirus constructs were packaged either in Phoenix A or E cells by calcium phosphate transfection as described[34]. CHO cells were transduced by retrovirus packaged by transfection of 293T cells with pYITG plus pCGP (a gift from W. Sha) and were sorted for GFP to more than 95% purity, followed by staining with 6A6 (anti-BTLA) or BTLA-phycoerythrin tetramers.

Retrovirus library. Purified BALB/c and C57BL/6 splenocytes were left unstimulated or were activated for 48 h with plate-bound anti-CD3 (500A.2 ascites) or soluble anti-IgM (Jackson Immunoresearch), then RNA was purified (RNeasy mini kit; Qiagen) and mRNA was made with the Nucleotrap mRNA purification kit (Clontech), full-length cDNA was made with the SMART cDNA Library Construction Kit (Clontech) and double-stranded cDNA was made by long-distance PCR with 5′PCR primer and CDS III/3′PCR primer; the PCR products were digested with *Sfi*I, size fractionated, amplified cDNA ligated into *Sfi*1-digested MSCV-ires-Thy1.1 retrovirus vector (a gift from W. Sha) and were transduced into XL-10 gold (Stratagene) for a library transcript complexity of 2×10^6. The library plasmid was purified without further amplification by CsCl gradient ultracentrifugation. Infected NIH-3T3 cells (8×10^6) and infected BJAB cells (6×10^6) were generated from retrovirus made by calcium phosphate transfection of Phoenix E cells; the total number of infected cells was assessed by anti-Thy1.1–FITC (eBioscience) staining. Serial rounds of cell sorting used anti-Thy1.1–FITC and BALB/c and C57BL/6 BTLA tetramers. When the sorted cells were more than 80% positive for Thy1.1 and BTLA tetramer, RNA was prepared and reverse-transcribed, cDNA was amplified with Taq polymerase and primers Sfi 5′ and Sfi 3′, and PCR products were cloned into pGEM-T Easy (Promega).

T cell purification and stimulation. T cell were purified (>90%) with anti-CD4 magnetic beads (Miltenyi) and, where indicated (**Figs. 6b–d,7**) by subsequent sorting for populations that were negative for B220-FITC and CD11c-phycoerythrin and positive for CD4-CyChrome (>98%). For T cell stimulation with anti-CD3 and LIGHT, 2C11 (BD Pharmingen) was coated onto 96-well plates, followed by LIGHT (PeproTech) at the indicated doses (**Fig. 6a**). Purified T cells were plated at a density of 1×10^6 cells/ml in 100 μl media per well. CHO cells were treated in media for 16 h at 37 °C with 50 μg/ml of mitomycin C (Sigma), were washed twice in PBS and were plated at a density of 1×10^6 cells/ml in 100 μl media in 96-well plates for proliferation assays or in 1 ml media in 24-well plates for CFSE analysis. For proliferation assays, purified T cells were plated directly onto CHO cells at a density of 1×10^6 cells/ml in 100 μl media and OVA peptide. After 48 h, cells were pulsed for 12 h with 1 μCi/well of [^{3}H]thymidine. For CFSE analysis, purified T cells were washed three times with PBS, were incubated for 8 min at 20 °C with 1 μM CFSE (Molecular Probes), were 'quenched' with fetal calf serum, were washed twice with media and were plated directly onto CHO cells

at a density of 1×10^6 cells/ml in 1 ml media plus OVA peptide. After 3 and 4 d, cells were stained with CD4-FITC and were analyzed by flow cytometry.

Immunoblot analysis. Pervanadate stimulation was done as described[3]. For cell-mixing experiments, 25×10^6 EL4 cells were mixed with 25×10^6 BJAB cells expressing GFP or 25×10^6 BJAB cells expressing mouse HVEM in 1 ml for 4 min at 37 °C and were lysed as described[3]. Extracts were precleared with protein G–Sepharose (Pharmacia), followed by immunoprecipitation with 9 μg of 6A6 (anti-mBTLA) or isotype control Armenian hamster IgG (Santa Cruz) and 40 μl protein G–Sepharose (Pharmacia), then were washed and analyzed by SDS-PAGE. Immunoblot analyses for SHP-2 and phosphotyrosine were done as described[1,3].

Note: Supplementary information is available on the Nature Immunology website.

ACKNOWLEDGMENTS

We thank D. Fremont, C. Nelson and O. Naidenko for help with tetramer production and for discussions, and V. Grigura and J.C. Walsh for technical assistance. Supported by the Howard Hughes Medical Institute (K.M.M.) and the National Institutes of Health (PO1 AI31238 and P50 HL54619 to K.M.M.; AI33068, CA69381 and AI48073 to C.F.W.; and AG00252 to K.P.).

COMPETING INTERESTS STATEMENT

The authors declare competing financial interests (see the *Nature Immunology* website for details).

Received 1 October; accepted 5 November 2004
Published online at http://www.nature.com/natureimmunology/

1. Watanabe, N. *et al.* BTLA is a lymphocyte inhibitory receptor with similarities to CTLA-4 and PD-1. *Nat. Immunol.* **4**, 670–679 (2003).
2. Han, P. *et al.* An inhibitory Ig superfamily protein expressed by lymphocytes and APCs is also an early marker of thymocyte positive selection. *J. Immunol.* **172**, 5931–5939 (2004).
3. Gavrieli, M. *et al.* Characterization of phosphotyrosine binding motifs in the cytoplasmic domain of B and T lymphocyte attenuator required for association with protein tyrosine phosphatases SHP-1 and SHP-2. *Biochem. Biophys. Res. Commun.* **312**, 1236–1243 (2003).
4. Suzuki, Y. *et al.* HAX-1, a novel intracellular protein, localized on mitochondria, directly associates with HS1, a substrate of Src family tyrosine kinases. *J. Immunol.* **158**, 2736–2744 (1997).
5. Prasad, D.V. *et al.* B7S1, a novel B7 family member that negatively regulates T cell activation. *Immunity* **18**, 863–873 (2003).
6. Sica, G.L. *et al.* B7-H4, a molecule of the B7 family, negatively regulates T cell immunity. *Immunity* **18**, 849–861 (2003).
7. Zang, X. *et al.* B7x: a widely expressed B7 family member that inhibits T cell activation. *Proc. Natl. Acad. Sci. USA* **100**, 10388–10392 (2003).
8. Agata, Y. *et al.* Expression of the PD-1 antigen on the surface of stimulated mouse T and B lymphocytes. *Int. Immunol.* **8**, 765–772 (1996).
9. Croft, M. Co-stimulatory members of the TNFR family: keys to effective T-cell immunity? *Nat. Rev. Immunol.* **3**, 609–620 (2003).
10. Mauri, D.N. *et al.* LIGHT, a new member of the TNF superfamily, and lymphotoxin alpha are ligands for herpesvirus entry mediator. *Immunity* **8**, 21–30 (1998).
11. Tamada, K. *et al.* LIGHT, a TNF-like molecule, costimulates T cell proliferation and is required for dendritic cell-mediated allogeneic T cell response. *J. Immunol.* **164**, 4105–4110 (2000).
12. Morel, Y. *et al.* The TNF superfamily members LIGHT and CD154 (CD40 ligand) costimulate induction of dendritic cell maturation and elicit specific CTL activity. *J. Immunol.* **167**, 2479–2486 (2001).
13. Morel, Y. *et al.* Reciprocal expression of the TNF family receptor herpes virus entry mediator and its ligand LIGHT on activated T cells: LIGHT down-regulates its own receptor. *J. Immunol.* **165**, 4397–4404 (2000).
14. Sarrias, M.R. *et al.* The three HveA receptor ligands, gD, LT-α and LIGHT bind to distinct sites on HveA. *Mol. Immunol.* **37**, 665–673 (2000).
15. Carfi, A. *et al.* Herpes simplex virus glycoprotein D bound to the human receptor HveA. *Mol. Cell* **8**, 169–179 (2001).
16. Kwon, B.S. *et al.* A newly identified member of the tumor necrosis factor receptor superfamily with a wide tissue distribution and involvement in lymphocyte activation. *J. Biol. Chem.* **272**, 14272–14276 (1997).
17. Jung, H.W. *et al.* High levels of soluble herpes virus entry mediator in sera of patients with allergic and autoimmune diseases. *Exp. Mol. Med.* **35**, 501–508 (2003).
18. Latchman, Y. *et al.* PD-L2 is a second ligand for PD-I and inhibits T cell activation. *Nat. Immunol.* **2**, 261–268 (2001).
19. Bodmer, J.L., Schneider, P. & Tschopp, J. The molecular architecture of the TNF superfamily. *Trends Biochem. Sci.* **27**, 19–26 (2002).
20. McDonald, N.Q. & Hendrickson, W.A. A structural superfamily of growth factors containing a cystine knot motif. *Cell* **73**, 421–424 (1993).
21. Kirchner, S. *et al.* LPS resistance in monocytic cells caused by reverse signaling through transmembrane TNF (mTNF) is mediated by the MAPK/ERK pathway. *J. Leukoc. Biol.* **75**, 324–331 (2004).
22. Wiley, S.R., Goodwin, R.G. & Smith, C.A. Reverse signaling via CD30 ligand. *J. Immunol.* **157**, 3635–3639 (1996).
23. Shi, G. *et al.* Mouse T cells receive costimulatory signals from LIGHT, a TNF family member. *Blood* **100**, 3279–3286 (2002).
24. Suzuki, I. & Fink, P.J. Maximal proliferation of cytotoxic T lymphocytes requires reverse signaling through Fas ligand. *J. Exp. Med.* **187**, 123–128 (1998).
25. Lee, K.M. *et al.* Molecular basis of T cell inactivation by CTLA-4. *Science* **282**, 2263–2266 (1998).
26. Granger, S.W. & Rickert, S. LIGHT-HVEM signaling and the regulation of T cell-mediated immunity. *Cytokine Growth Factor Rev.* **14**, 289–296 (2003).
27. Paust, S. *et al.* Engagement of B7 on effector T cells by regulatory T cells prevents autoimmune disease. *Proc. Natl. Acad. Sci. USA* **101**, 10398–10403 (2004).
28. Taylor, P.A. *et al.* B7 expression on T cells down-regulates immune responses through CTLA-4 ligation via T-T interactions. *J. Immunol.* **172**, 34–39 (2004).
29. Murphy, K.M., Heimberger, A.B. & Loh, D.Y. Induction by antigen of intrathymic apoptosis of $CD4^+CD8^+TCR^{lo}$ thymocytes *in vivo*. *Science* **250**, 1720–1723 (1990).
30. Scheu, S. *et al.* Targeted disruption of LIGHT causes defects in costimulatory T cell activation and reveals cooperation with lymphotoxin β in mesenteric lymph node genesis. *J. Exp. Med.* **195**, 1613–1624 (2002).
31. Arthos, J. *et al.* Biochemical and biological characterization of a dodecameric CD4-Ig fusion protein: implications for therapeutic and vaccine strategies. *J. Biol. Chem.* **277**, 11456–11464 (2002).
32. Arase, H. *et al.* Direct recognition of cytomegalovirus by activating and inhibitory NK cell receptors. *Science* **296**, 1323–1326 (2002).
33. Lybarger, L. *et al.* Enhanced immune presentation of a single-chain major histocompatibility complex class I molecule engineered to optimize linkage of a C-terminally extended peptide. *J. Biol. Chem.* **278**, 27105–27111 (2003).
34. Ouyang, W. *et al.* Stat6-independent GATA-3 autoactivation directs IL-4-independent Th2 development and commitment. *Immunity* **12**, 27–37 (2000).

nature immunology

BTLA is a lymphocyte inhibitory receptor with similarities to CTLA-4 and PD-1

Norihiko Watanabe[1,5], Maya Gavrieli[1], John R Sedy[1], Jianfei Yang[1,5], Francesca Fallarino[2], Susan K Loftin[1], Michelle A Hurchla[1], Natalie Zimmerman[3], Julia Sim[3], Xingxing Zang[4], Theresa L Murphy[1], John H Russell[3], James P Allison[4] & Kenneth M Murphy[1]

During activation, T cells express receptors for receiving positive and negative costimulatory signals. Here we identify the B and T lymphocyte attenuator (BTLA), an immunoglobulin domain–containing glycoprotein with two immunoreceptor tyrosine-based inhibitory motifs. BTLA is not expressed by naive T cells, but it is induced during activation and remains expressed on T helper type 1 (T_H1) but not T_H2 cells. Crosslinking BTLA with antigen receptors induces its tyrosine phosphorylation and association with the Src homology domain 2 (SH2)-containing protein tyrosine phosphatases SHP-1 and SHP-2, and attenuates production of interleukin 2 (IL-2). BTLA-deficient T cells show increased proliferation, and BTLA-deficient mice have increased specific antibody responses and enhanced sensitivity to experimental autoimmune encephalomyelitis. B7x, a peripheral homolog of B7, is a ligand of BTLA. Thus, BTLA is a third inhibitory receptor on T lymphocytes with similarities to cytotoxic T lymphocyte–associated antigen 4 (CTLA-4) and programmed death 1 (PD-1).

T cells receive costimulatory signals from antigen-presenting cells (APCs) that can be positive and negative. During the initiation of naive T cells, the primary positive costimulatory signal is mediated through the receptor CD28, whereas signaling through CTLA-4 has a negative effect on activation[1]. Both CD28 and CTLA-4 interact with the same set of ligands, B7-1 (also known as CD80) and B7-2 (CD86), expressed on APCs. Additional members of the CD28-B7 family have been identified. A second activating receptor on T cells is inducible costimulator (ICOS)[2], and its ligand B7h[3] (also known as B7RP-1 (ref. 4), GL50 (ref. 5), B7H2 (ref. 6) and LICOS[7]) is expressed on both lymphoid and nonlymphoid cells[8,9]. A second inhibitory receptor, PD-1 (refs. 10,11), binds to a pair of B7-related ligands PD-L1 (ref. 12), also known as B7-H1 (ref. 13), and PD-L2 (ref. 14), also known as B7-DC (ref. 15). B7-H3, another B7 homolog[16,17], binds an unidentified receptor on activated T cells.

Here we report the cloning and characterization of BTLA, an inhibitory receptor expressed by T lymphocytes. BTLA is induced on activation of naive T cells and is expressed by developing T_H1 and T_H2 cells. Expression of BTLA is subsequently lost on highly polarized T_H2 cells but remains on T_H1 cells. BTLA contains two cytoplasmic immunoreceptor tyrosine-based inhibitory motifs (ITIMs) and undergoes inducible tyrosine phosphorylation and association with SHP-1 and SHP-2. We show that coligation of BTLA partially inhibits CD3-induced secretion of IL-2 and that BTLA-deficient T cells have increased proliferation to antigen presented by dendritic cells (DCs), suggesting that BTLA exerts an inhibitory rather than activating influence on T cells. BTLA-deficient mice show a moderate increase in specific antibody response and an increased susceptibility to peptide antigen–induced experimental autoimmune encephalomyelitis (EAE), further suggesting an inhibitory role for BTLA. We also show that BTLA is recognized by an orphan B7 homolog, B7x. Thus, BTLA shares several structural and functional similarities with CTLA-4 and PD-1, the other two inhibitory receptors expressed on T lymphocytes.

RESULTS

Expression of BTLA mRNA

In a previous screen using Affymetrix arrays[18], we identified an anonymous T_H1-specific expressed sequence tag (EST). The full-length complementary DNA of this EST, cloned from a murine complementary DNA library (**Fig. 1** and **Supplementary Table 1** online), predicts a protein with a signal sequence, extracellular variable (V)-like immunoglobulin (Ig) domain, transmembrane region and intracellular domain of about 100 amino acids (**Fig. 1a**). By homology searching, we identified a single human gene homolog (**Fig. 1a,b**) with a similar domain structure. Notably, three tyrosine residues in the cytoplasmic domain are contained in sequence

[1]Department of Pathology & Immunology, Howard Hughes Medical Institute, Washington University School of Medicine, Box 8118, 660 South Euclid Avenue, St. Louis, Missouri 63110, USA. [2]Department of Experimental Medicine, University of Perugia, Via del Giochetto, 06122, Perugia, Italy. [3]Department of Molecular Biology & Pharmacology, Washington University School of Medicine, Box 8103, 660 South Euclid Avenue, St. Louis, Missouri, 63110, USA. [4]Howard Hughes Medical Institute, Department of Molecular and Cell Biology, Cancer Research Laboratory, University of California at Berkeley, Berkeley, California 94720, USA. [5]Present addresses: The Second Department of Internal Medicine, Chiba University School of Medicine, J1-8-1 Inohana, Chuo-ku, Chiba 260-8670, Japan (N.W.); Boehringer Ingelheim Pharmaceuticals, 900 Ridgebury Road, Ridgefield, Connecticut 06877, USA (J.Y.). Correspondence should be addressed to K.M.M. (murphy@immunology.wustl.edu).

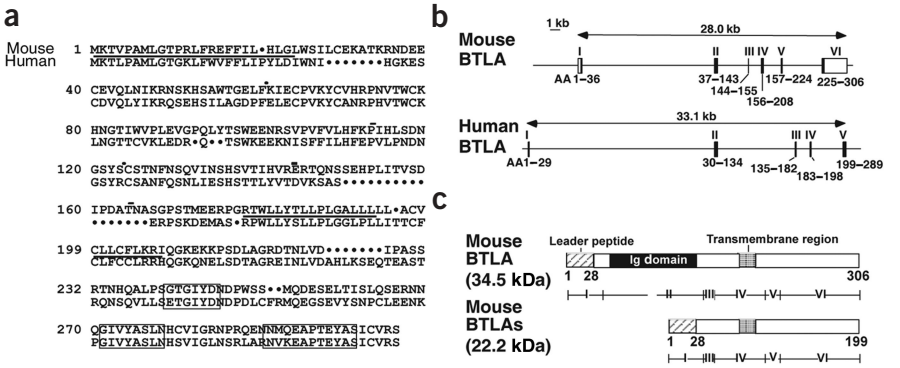

Figure 1 BTLA sequence and genomic structure. (**a**) Alignment of mouse and human BTLA. The signal peptide and the transmembrane region are underlined. Potential *N*-linked glycosylation sites (–) and cysteine residues (•) predicted to participate in disulfide bonds in the Ig domain are indicated. Spaces have been introduced for optimal comparison. Boxed sequences are tyrosine-based signaling motifs conserved between human and mouse BTLA, and are also conserved in the rat homolog (EST AI235902) expressed in normalized rat ovary. The mouse sequence is from the 129SvEv strain and the human sequence was cloned from the Ramos T cell line (Methods). (**b**) Exon and intron organization of mouse and human BTLA gene. Filled boxes indicate coding sequence in exons, and unfilled boxes indicate 3′ and 5′ untranslated regions. The amino acid number encoded by each exon is indicated below. (**c**) Predicted structural regions of mouse BTLA. Shown are full-length BTLA and a minor splice variant (BTLAs) that lacks exon 2 and thus the Ig domain. Roman numerals indicate the exon from which the predicted region is derived. The molecular weight of the predicted protein without posttranslational modifications is indicated in parentheses.

motifs that are conserved between mouse and human: the first is in a potential Grb2 interaction site[19] and the other two are in ITIM sequences[20]. In addition to BTLA, a minor alternatively spliced transcript, BTLAs, was detected by reverse transcription polymerase chain reaction (RT-PCR). BTLAs lacks exon 2 and thus the Ig domain (**Fig. 1c**).

BTLA mRNA is expressed strongly in spleen and lymph node tissues but very weakly or undetectably by several somatic tissues (**Fig. 2a**). It is expressed by both splenic B cell and T cells, with slightly higher levels in the former (**Fig. 2b**). By using an antigen-specific system to measure the expression of BTLA mRNA by northern analysis during T cell activation, we found low BTLA expression on day 2 after primary T cell activation, with no difference in expression between T_H1 and T_H2 conditions (**Fig. 2c**). On day 7 after primary T cell activation, expression of BTLA mRNA was increased, with slightly higher expression in T_H1 than in T_H2 cells (**Fig. 2c**). After a second week of *in vitro* culture under T_H1 or T_H2 polarization conditions, BTLA expression remained high in T_H1 cells, but by comparison was reduced in T_H2 cells (**Fig. 2d**).

Thus, expression of BTLA mRNA seems to be regulated during the activation and differentiation of T cells. BTLA expression is not strictly dependent on any single T_H1-inducing signal, because it remained expressed in T_H1 cells deficient for either signal transducer and activator of transcription 1 (STAT1) or STAT4. The A20 B cell line, but not macrophages or lymphokine activated killer (LAK) cells, also expressed BTLA mRNA (**Fig. 2b**).

BTLA surface expression and phosphorylation

To determine whether BTLA is a transmembrane protein, we expressed three forms of BTLA tagged with the Myc epitope in the Bjab cell line (**Fig. 3a**). Cell surface expression of wild-type BTLA was detected as predicted (**Fig. 3a**, top). Notably, deleting either the cytoplasmic or the Ig domain increased surface expression, suggesting that these domains have roles in controlling the amount of surface expression, similar to the regulation of surface CTLA-4 by its cytoplasmic domain[21,22].

Next, we confirmed that BTLA is a glycoprotein (**Fig. 3b**). Treatment with peptide *N*-glycosidase F (PNGase F) reduced the apparent molecular weight of both human and murine BTLA, consistent with the

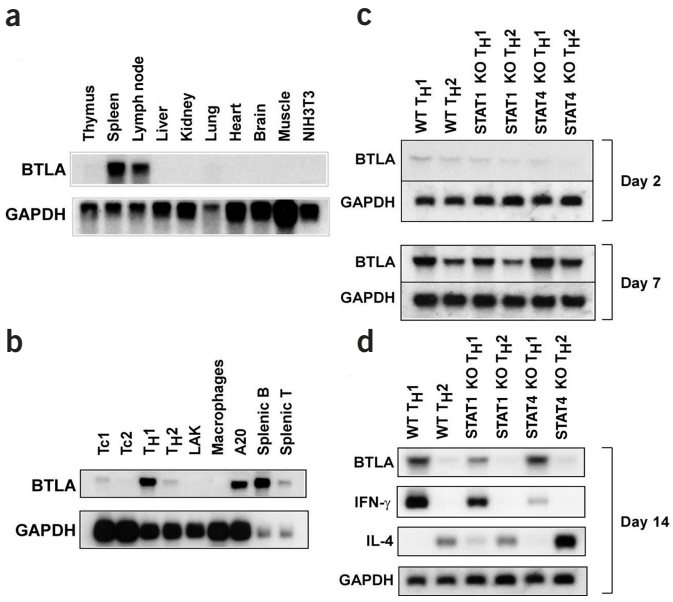

Figure 2 Expression of BTLA in lymphoid cells. (**a**) Tissue distribution of BTLA mRNA. Northern analysis of 10 μg of tissue or cellular RNA probed with full-length BTLA or GAPDH cDNA. (**b**) Northern analysis of total RNA from the indicated cells. Cytotoxic T cell type 1 (Tc1) and Tc2 cells were prepared from *in vitro*–polarized 2C[51] TCR transgenic T cells, LAK cells were prepared by culturing C57BL/6 splenocytes with 1,000 U/ml of IL-2 for 9 d, and macrophages were from BALB/c bone marrow derived with L-cell conditioned media and confirmed as >95% Mac-1$^+$. Splenic B and T cells were purified to >98% by cell sorting. (**c**) Total RNA was isolated from T cells on days 2 and 7 after 3 h of incubation with PMA plus ionomycin, and northern blots were probed for BTLA and GAPDH mRNA. Data for days 2 and 7 are from blots that were hybridized and exposed together. (**d**) Expression of BTLA in polarized T_H1 and T_H2 cells on day 14. Wild-type, STAT1-deficient and STAT4-deficient DO11.10 transgenic T cells[18] (3×10^6 per ml) were activated by 0.3 μM OVA peptide in T_H1 or T_H2 conditions and again after 7 d in the same conditions. Cells were collected on day 14 and stimulated with PMA plus ionomycin for 3 h, and total RNA was analyzed for BTLA, IFN-γ, IL-4 and GAPDH mRNA as described[18].

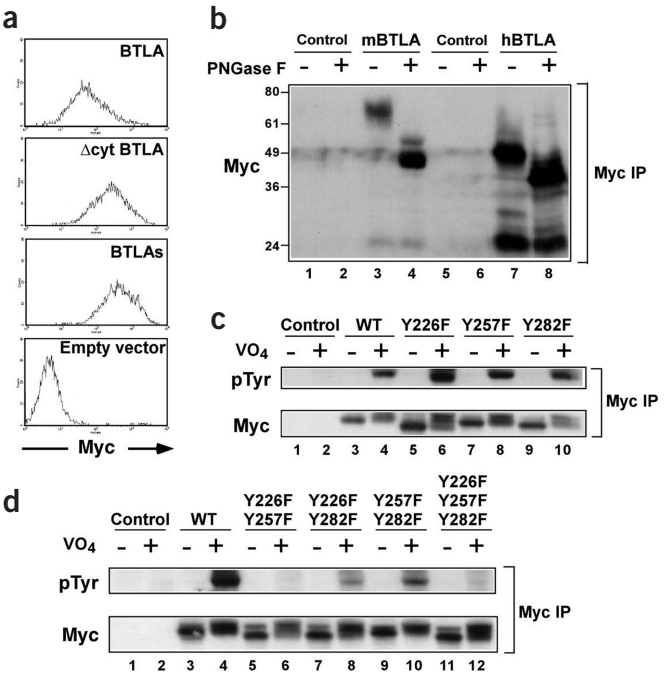

Figure 3 BTLA is transmembrane, glycoslyated, and tyrosine-phosphorylated on induction. (**a**) Transmembrane cell surface expression of BTLA. Bjab cells were infected with amphotrophic retrovirus containing empty vector, Myc_3-mBTLA-RV (BTLA), Δcyt-Myc_3-mBTLA-RV (Δcyt BTLA) and Myc_3-mBTLAs-RV (BTLAs). Expression of the Myc epitope was assayed on GFP-positive cells by FACS. (**b**) Murine and human BTLA contain *N*-linked oligosaccharides. A20 murine B lymphoma cells expressing control GFP-RV (lanes 1 and 2) or mBTLA-Myc_2-RV (lanes 3 and 4), and Bjab human B lymphoma cells expressing control GFP-RV (lanes 5 and 6) or hBTLA-Myc_3-RV (lanes 7 and 8) were prepared by infection with amphotrophic retrovirus, sorted for GFP expression and analyzed by immunoblotting (Methods). (**c**,**d**) Tyrosine phosphorylation of BTLA on stimulation with pervanadate. (**c**) Bjab cells infected with wild-type or single tyrosine mutants of hBTLA-Myc_3-RV were incubated in the absence (lanes 1, 3, 5, 7, 9) or presence (lanes 2, 4, 6, 8, 10) of pervanadate, and examined for tyrosine phosphorylation (Methods). (**d**) Bjab cells infected with double or triple tyrosine mutants of hBTLA-Myc_3-RV were analyzed for tyrosine phosphorylation (Methods).

N-linked glycosylation sites predicted in the extracellular region (**Fig. 1a**). The apparent molecular weight of human and murine BTLA treated with PNGase F was still higher than that predicted by its core amino acid sequence, suggesting that it has additional modifications such as *O*-linked glycosylation.

We also found that pervanadate treatment induced tyrosine phosphorylation of BTLA. Single mutation of tyrosines 226, 257 and 282 to phenylalanine had little effect on pervanadate-induced BTLA phosphorylation, but the triple tyrosine mutation blocked phosphorylation completely. The Y226F and Y257F double mutation severely reduced pervanadate-induced phosphorylation, suggesting that Y282 is either weakly phosphorylated or requires prior phosphorylation at Y226 or Y257 (**Fig. 3c**,**d**).

Thus, BTLA is an Ig domain-containing transmembrane glycoprotein that can be phosphorylated on tyrosines located in conserved cytoplasmic ITIM-like motifs.

Inducible SHP-1 and SHP-2 association

Sequences surrounding Y226 contain potential Grb2-binding motifs[23], Y257 seems to be an ITIM[20], and Y282 is similar to the immunoreceptor tyrosine-based switch motif (ITSM) in PD-1 (ref. 24) and SLAM (also called CD150 or IPO-3)[25]. To evaluate such potential interactions, we developed a system of inducible BTLA phosphorylation.

Extracellular Myc-tagged BTLAs was expressed stably in the DO11.10 hybridoma[26] (**Fig. 4a**). By a similar strategy to that used for crosslinking PD-1 with the B cell receptor complex[27], we crosslinked BTLA and the T cell antigen receptor (TCR) with antibodies to CD3 and the Myc epitope, and then carried out secondary crosslinking with goat anti–mouse IgG. Tyrosine phosphorylation of BTLA (**Fig. 4a**) was specific to BTLA-transduced cells, dependent on secondary crosslinking and not induced with anti-CD3 or anti-Myc alone (**Fig. 4a**,**b**). In addition, tyrosine phosphorylation of BTLA showed a time-dependent response: it appeared rapidly and peaked at 2–3 min, and was extinguished within 10 min of the secondary crosslinking (**Fig. 4a**).

We examined various signaling molecules for coimmunoprecipitation with Myc-BTLA. Notably, SHP-2 was strongly associated with BTLA. Association of SHP-2 correlated with phosphorylation of BTLA and was dependent on cocrosslinking (**Fig. 4a**, lanes 8–13). Pervanadate treatment also induced the association of SHP-2 with BTLA (**Fig. 4a**, lane 14), and this condition was used to examine further the association of BTLA with SHP-1 and SHP-2 (**Fig. 4c–e**). SHP-2 coprecipitated with pervanadate-treated BTLA (**Fig. 4c**,**d**, compare lanes 3 and 4). Coprecipitation of SHP-1 was also dependent on phosphorylation of BTLA (data not shown).

Inducible association of SHP-2 was also observed with human BTLA (**Fig. 4e**). Myc-tagged human BTLA was expressed in the human T cell line Jurkat. Myc-hBTLA coprecipitated with SHP-2 only in pervanadate-treated cells and was specific to expression of Myc-hBTLA (**Fig. 4e**). Likewise, only anti–SHP-2 immunoprecipitates from pervanadate-treated cells contained Myc-BTLA (**Fig. 4e**, lane 8). We also confirmed that SHP-1 associated with phosphorylated human BTLA (data not shown). The inducible association of BTLA with SHP-1 and SHP-2, a characteristic shared by CTLA-4 and PD-1, suggests that BTLA may have an inhibitory function in lymphocytes.

To explore the downstream effects of crosslinking BTLA with TCR, we examined the production of IL-2 in T cell hybridomas (**Fig. 4f**). Myc-tagged BTLA and BTLAs were stably expressed in DO11.10 hybridoma T cells[26]. Control DO11.10 hybridomas infected with the empty green fluorescent protein (GFP) retroviral vector, GFP-RV, showed anti-CD3–induced production of IL-2 that was unaffected by plate-bound anti-Myc (**Fig. 4f**). In contrast, production of IL-2 by DO11.10 cells expressing Myc-BTLA and Myc-BTLAs was dose-dependently inhibited by plate-bound anti-Myc (**Fig. 4f**). No differences in IL-2 production induced by phorbol 12-myristate 13-acetate (PMA) plus ionomycin were observed (**Fig. 4g**). Thus, it seems that BTLA can modestly inhibit antigen-induced, but not chemically induced, production of IL-2 by DO11.10 hybridoma cells.

Immune response in BTLA-deficient mice

To test whether BTLA has an inhibitory function *in vivo*, we targeted the *Btla* gene (**Fig. 5a**) to produce mice lacking BTLA (**Fig. 5b**). BTLA-deficient mice on a 129SvEv background lacked expression of BTLA

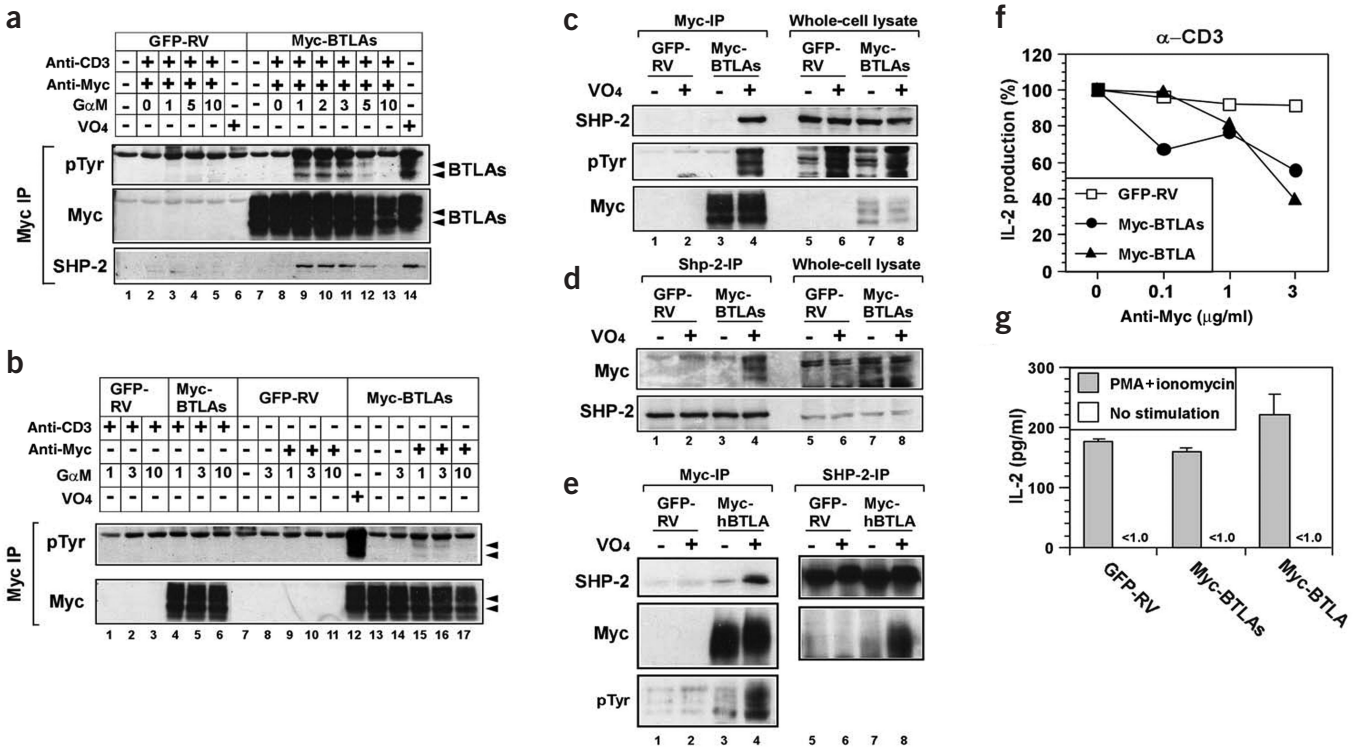

Figure 4 Inducible association of BTLA with SHP-2. (**a**) Tyrosine phosphorylation of BTLA on TCR crosslinking. DO11.10 hybridoma T cells were infected with empty vector (GFP-RV)[48] or Myc_3-mBTLAs-RV (Myc-BTLAs) and purified. After crosslinking (Methods), anti-Myc immunoprecipitates were analyzed with anti-pTyr (top), reprobed with polyclonal rabbit anti-Myc (middle), and then reprobed with rabbit anti–SHP-2 antibody (bottom). Arrowheads indicate the principal glycosylated forms of BTLAs. (**b**) BTLA tyrosine phosphorylation requires cocrosslinking. Cells in **a** were treated as indicated and analyzed for pTyr (top) or Myc (bottom). (**c**) Cells in **a** were incubated in the absence (–) or presence (+) of pervanadate for 2 min at 37 °C and lysed in 1% NP-40 lysis buffer. Anti-Myc immunoprecipitates and whole-cell lysates (25×10^6 cells) were analyzed sequentially for SHP-1 (data not shown), SHP-2, pTyr and Myc. (**d**) Cells were treated and lysed as in **c**. Anti–SHP-2 immunoprecipitates and whole-cell lysates were analyzed with anti-Myc (top), and reprobed with anti–SHP-2 (bottom). (**e**) Jurkat T cells were infected with GFP-RV or Myc_3-hBTLA-RV (hBTLA), sorted to >95% high surface expression of Myc-hBTLA, incubated in the absence (–) or presence (+) of pervanadate for 4 min at 37 °C, and lysed in 1% Triton X-100 lysis buffer. Anti-Myc (left) and anti–SHP-2 (right) immunoprecipitates were analyzed for Myc, SHP-2 and pTyr. (**f**,**g**) Crosslinking BTLA with TCR attenuates production of IL-2. DO11.10 cells expressing control vector (GFP-RV), Myc_3-mBTLAs-RV (Myc-BTLAs) or Myc_3-mBTLA-RV (Myc-BTLA) were stimulated with anti-CD3ε plus the indicated concentrations of anti-Myc (**f**) or with PMA plus ionomycin (**g**). The IL-2 concentration was determined by ELISA. In **f**, the IL-2 titer is normalized by the IL-2 concentration induced by stimulation with anti-CD3 alone.

mRNA in peripheral lymphocytes (**Fig. 5c**). No developmental defects in T or B cells in thymus or bone marrow were observed in these mice (**Supplementary Fig. 1** online). We produced BTLA-deficient DO11.10 TCR transgenic mice on a mixed 129SvEv and BALB/c background for the *in vitro* analysis of T cells (**Fig. 5d**). Fully polarized BTLA-deficient T_H1 cells showed a roughly twofold increase in proliferation in response to 0.3 μM OVA peptide presented by either $CD8^+$ or $CD8^-CD11c^+$ DCs (**Fig. 5d**).

We also examined T and B cells from wild-type and BTLA-deficient T cells for mitogen- and TCR-induced proliferation *in vitro* (**Fig. 6**). The proliferative response of wild-type and BTLA-deficient T cells to concanavalin A were comparable, but BTLA-deficient T cells showed a heightened response to stimulation with anti-CD3. Lipopolysaccharide (LPS)-induced proliferation was similar in wild-type and BTLA-deficient B cells, but BTLA-deficient B cells showed slightly greater responses to stimulation with anti-IgM. The increased *in vitro* responses, although not marked, were similar in magnitude to the increases in proliferation seen in PD-1-deficient T cells[11] and in CTLA-4-deficient $CD8^+$ T cells[28] *in vitro*. In fact, CTLA-4-deficient $CD4^+$ T cells show no enhancement of primary antigen-driven responses and only a twofold increase in secondary responses[29,30].

These results suggest that BTLA has an inhibitory, rather than activating, influence on T lymphocyte responses. Consistent with this, 4 weeks after immunization with nitrophenol-conjugated keyhole limpet hemocyanin (NP-KLH), BTLA-deficient mice showed a threefold increase in the amount of NP-KLH-specific IgG1, IgG2a and IgG2b isotypes as compared with control littermate 129/SvEv mice (**Table 1**).

EAE susceptibility in BTLA-deficient mice

As our data suggested that BTLA might be inhibitory, we used a model of EAE to detect potentially enhanced T cell responses in BTLA-deficient mice. Initially, we carried out an antigen dose titration of the myelin oligodendrocyte glycoprotein (MOG) peptide on the pure 129SvEv background to determine a dose that would generate a suboptimal disease capable of showing augmentation (**Fig. 7a**). We found that 10 μg and 50 μg of peptide induced severe disease in 129SvEv mice, whereas 2 μg induced milder disease with delayed onset (**Fig. 7a**). At this antigen dose, BTLA-deficient mice showed a higher incidence, increased clinical score, earlier onset and prolonged duration of disease as compared with wild-type littermate controls (**Fig. 7b**).

To ascertain any potential differences between the nature of MOG-induced EAE in BTLA-deficient mice and that in C57BL/6 control mice, we examined the lumbar spinal cords of affected mice (**Fig. 8**). There was an abundant cellular infiltrate in the lumbar spinal region of BTLA-deficient mice with a clinical score of 4, which was similar in severity to the infiltrate in C57BL/6 control mice induced with a high

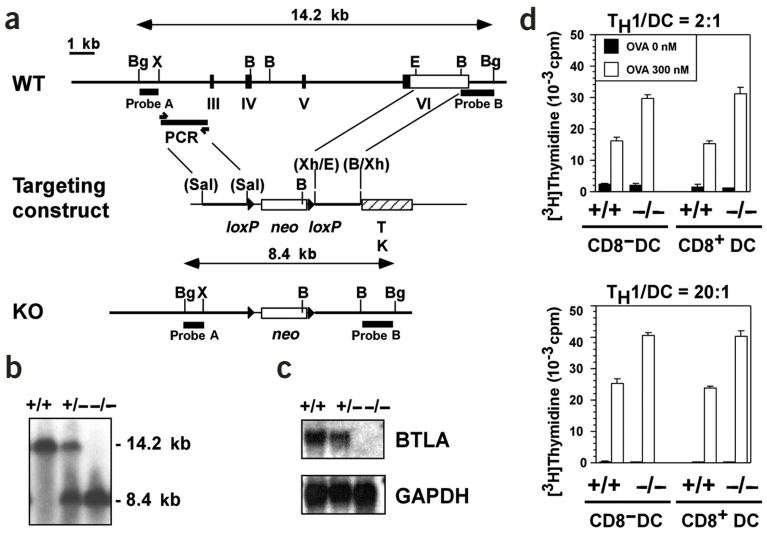

Figure 5 Generation and analysis of BTLA-deficient mice. (**a**) The *Btla* locus and targeting construct. Exons III–VI, encoding the extracellular, transmembrane and cytoplasmic regions, are indicated. *Bgl*II digestion of the germline locus generates a restriction fragment of 14.2 kb that hybridizes to probes A and B, and a fragment of 8.4 kb in correctly targeted clones. B, *Bam*HI; Bg, *Bgl*II; E, *Eco*RI; Sal, *Sal*I; X, *Xba*I; Xh, *Xho*I. TK, thymidine kinase gene; *neo*, neomycin resistance cassette. (**b**) Southern analysis. *Bgl*II-digested tail DNA hybridized with probe B. (**c**) Northern analysis. RNA was prepared directly from splenocytes of mice of the indicated genotype. Blots were hybridized to a full-length mouse BTLA cDNA probe, stripped and reprobed for GAPDH. (**d**) Proliferative responses of polarized T_H1 cells induced by incubation with antigen-pulsed DCs. Naive $CD4^+$ T cells from DO11.10 BTLA wild-type or BTLA-deficient mice were activated *in vitro* and passed biweekly in T_H1 conditions. Resting T_H1 cells (5×10^4) were incubated with BALB/c-derived $CD8^+$ or $CD8^-$ DCs (top, 2.5×10^4; bottom, 0.25×10^4), with or without 300 nM OVA peptide in a volume of 200 μl. Cell proliferation was measured by pulsing with [^{3}H]thymidine for 16 h.

dose of MOG peptide and also with a clinical score of 4 (compare **Fig. 8a** and **b**). Less abundant cellular infiltrates were observed in BTLA-deficient mice that were killed when the clinical score was 1.5 (**Fig. 8c**). Consistent with the MOG peptide–induced infiltrates observed in the C57BL/6 background[31], cellular infiltrates in BTLA-deficient mice consisted of both $CD4^+$ and $CD11b^+$ cells (**Fig. 8**), which were more frequent in mice with a clinical score of 4 than in those with a score of 1.5 (compare **Fig. 8f,g** and **d,e**).

Thus, loss of BTLA in 129SvEV mice increases the sensitivity to antigen-induced EAE, but the disease remains characterized by similar types of cellular infiltrate into the central nervous system (CNS).

BTLA interaction with a B7 homolog

The proposed similarity of BTLA to PD-1 and CTLA-4 is based primarily on the overall domain structure of the proteins, as each possesses a single extracellular Ig-like domain, a transmembrane region

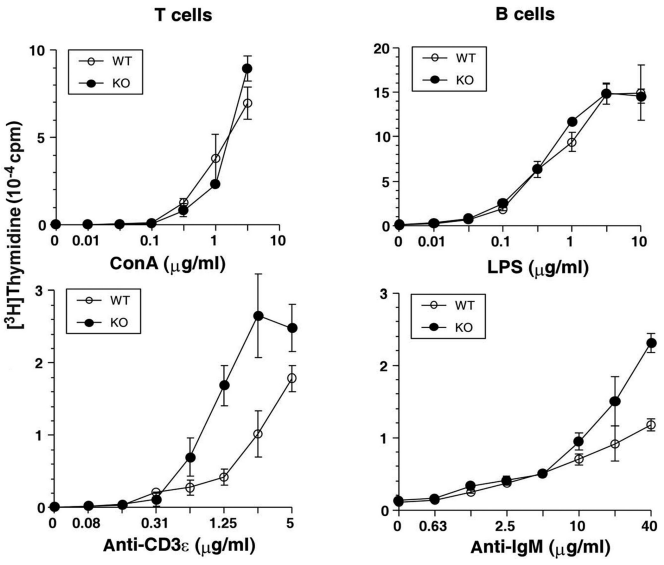

Figure 6 *In vitro* responses of BTLA-deficient lymphocytes. T and B cell from wild-type (WT) or BTLA-deficient (KO) mice were purified by cell sorting using anti-CD4–FITC, anti-CD8α–FITC or anti-B220–PE. Cells were stimulated with the indicated final concentrations of plate-bound anti-IgM, LPS, concanavalin A or plate-bound anti-CD3e. Cell proliferation was measured by pulsing with [^{3}H]thymidine for 16 h.

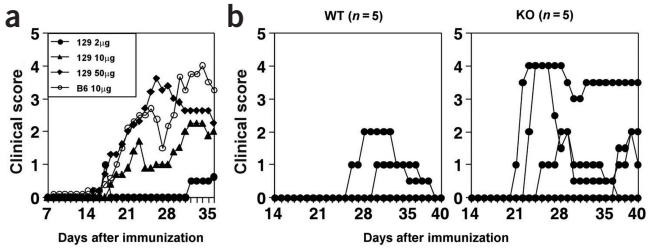

Figure 7 Increased EAE susceptibility in BTLA-deficient mice. (**a**) Titration of MOG peptide in 129SvEv mice. Mice were injected subcutaneously with MOG peptide at 2 μg, 10 μg and 50 μg ($n = 5$) in incomplete Freund's adjuvant and 500 μg of mycobacterium on day 0. Pertussis toxin (300 ng) of was injected intravenously on days 1 and 3. C57BL/6 (B6) mice injected with 10 μg of MOG were used as positive controls. Mice were monitored daily for symptoms. Clinical scores: 0, normal, no overt signs of disease; 1, limp tail or hindlimb weakness, but not both; 2, limp tail and hindlimb weakness; 3, partial hind limb paralysis; 4, complete hindlimb paralysis; 5, moribund state, death by EAE, killed for humane reasons. (**b**) Active induction of EAE by suboptimal dose of MOG peptide in BTLA-deficient mice. BTLA-deficient (KO) or wild-type (WT) littermate control 129SvEv mice aged 6–8 weeks ($n = 5$) were injected with 2 μg of MOG peptide as in **a**. Mean clinical scores: wild type, 0.6 ± 0.9; BTLA-deficient, 2.4 ± 1.7. Mean peak clinical score; wild type, 1.5 ± 0.7; BTLA-deficient 3.0 ± 1.2.

Table 1 Augmented IgG responses of BTLA-deficient mice to Td antigen

Anti-NP	*Btla*$^{+/+}$ (%)[a]	*Btla*$^{+/-}$ (%)	*Btla*$^{-/-}$ (%)
IgG1	157.9 ± 81.3	179.2 ± 160.6	272.1 ± 82.6[b]
IgG2a	110.0 ± 86.9	268.8 ± 203.9	306.7 ± 132.8[c]
IgG2b	92.51 ± 103.0	136.6 ± 38.8	249.8 ± 102.0[d]

[a]Data are presented as the percentage of mean isotype production as compared with wild-type BTLA serum, which was used as a uniform standard serum to determine relative titers of anti-NP. Data are the mean ± s.d. of measurements from five mice. [b]$P = 0.029$, [c]$P = 0.014$, [d]$P = 0.022$ versus wild-type BTLA.

and conserved intracellular ITIM motifs that interact with SHP-1 and SHP-2 phosphatases, and each has inhibitory rather than activating effects on lymphocytes. Both CTLA-4 and PD-1 interact with members of the B7 family[32], and we therefore tested whether BTLA also shares this feature. We identified a conserved B7 homolog, B7x, with high similarity between the mouse and human sequences. An alignment of human and murine B7x (**Supplementary Fig. 2** online) identified a predicted signal peptide and two Ig-like domains followed by a potential transmembrane region.

We generated a fusion protein of Ig and murine B7x and obtained additional Ig fusion proteins of B7h, PD-L1 and PD-L2. The B7h-Ig fusion protein showed no difference in binding between wild-type and BTLA-deficient T cells; this was expected, because B7h binds ICOS[3], which presumably should be expressed by both wild-type and BTLA-deficient T cells. In contrast, the B7x-Ig fusion protein bound to wild-type but not to BTLA-deficient T cells (**Fig. 9a**), suggesting that BTLA is responsible for most of the binding of B7x-Ig to T cells. PD-1 was expressed by both wild-type and BTLA-deficient T cells, but it was detected more strongly by anti–PD-1 than by the PD-L1 or PD-L2 Ig fusion proteins (**Fig. 9b**,**c**). In contrast, the B7-1 and B7-2 Ig fusion proteins generated stronger signals (**Fig. 9b**) on wild-type and BTLA-deficient T cells, consistent with the high affinity of CTLA-4 for B7-1 and B7-2.

Taken together, these results indirectly suggest that B7x is a ligand, although not necessarily the only ligand, for BTLA, thereby highlighting another similarity between BTLA and the other inhibitory receptors, CTLA-4 and PD-1, known to be expressed on T cells.

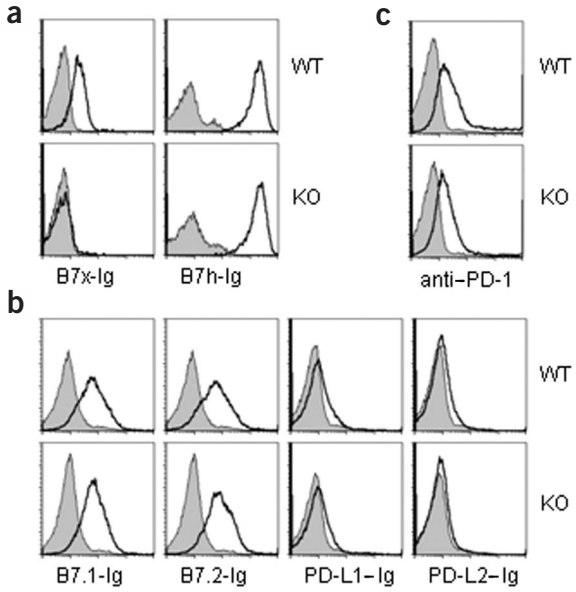

Figure 9 BTLA interacts with an orphan B7 B7x. (**a**) Spleen and lymph node cells from BTLA wild-type and BTLA-deficient DO11.10$^+$ TCR transgenic mice were collected and stimulated with 0.3 μM OVA peptide, 10 U/ml of IL-12 and neutralizing antibodies to IL-4, and assayed for Ig fusion binding after 4 d. Cells were stained with anti-CD4–FITC. Left, cells were stained with a human IgG1 antibody as a negative control (filled) or with a B7x-Ig fusion protein (open), followed by goat anti–human IgG–PE. Right, cells were unstained (filled) or stained with B7h-Ig (open), followed by biotinylated anti-Myc (murine IgG1 isotype) and streptavidin-PE. Anti-Myc was used as a negative control for the B7h-Ig fusion protein. (**b**,**c**) T_H1 cell lines derived from BTLA wild-type and BTLA-deficient DO11.10$^+$ mice were stimulated as above, collected on day 3, and assayed for binding to Ig fusion proteins. All cells were stained with anti-CD4–FITC. In **b**, Cells were stained with a human IgG1 antibody (filled) or with B7.1-Ig, B7.2-Ig, PD-L1–Ig and PD-L2–Ig fusion proteins (open), followed by goat anti–human Fcγ $F(ab')_2$–PE. In **c**, cells were stained with a hamster IgG2–PE as a negative control (filled) or with anti–PD-1–PE. Histograms are gated on CD4$^+$ cells.

DISCUSSION

BTLA seems to be a third inhibitory receptor expressed by T cells that, like PD-1, is induced on T cell activation but remains expressed more strongly on polarized T_H1 cells. Similar to PD-1 and CTLA-4 (ref. 27), BTLA can be induced to undergo phosphorylation and to associate with the SHP-1 and SHP-2 phosphatases by cocrosslinking with the TCR on T cells. The association with these phosphatases, the increased *in vivo* sensitivity to MOG peptide–induced EAE, and the increased rather than decreased *in vitro* proliferative responses suggest that

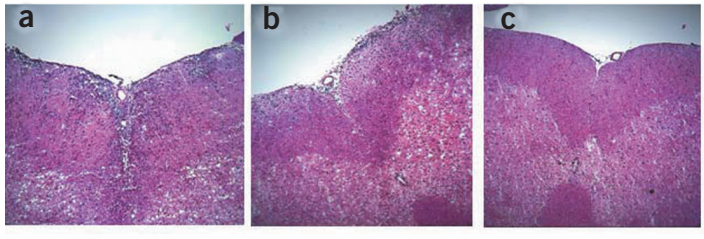

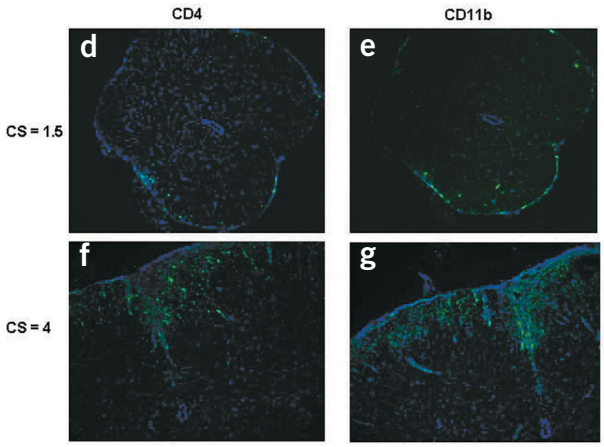

Figure 8 Infiltration of the CNS in MOG-induced EAE in BTLA-deficient mice. C57BL/6 control (**a**) or BTLA-deficient (**b**–**g**) mice immunized with MOG peptide were killed when showing the indicated clinical score (CS): (**a**) C57BL/6, CS 4; (**b**) BTLA-deficient, CS 4; (**c**-**e**) BTLA-deficient, CS 1.5; (**f**,**g**) BTLA-deficient, CS 4. Hematoxylin and eosin (**a**–**c**) or immunofluorescence staining for CD4 (left) and CD11b (right) (**d**–**g**) was done on frozen sections as described[31]. Immunofluorescent sections were counterstained with 4′,6-diamidino-2-phenylindole dihydrochloride (DAPI, blue).

BTLA may have an inhibitory function similar to that of PD-1 and CTLA-4, and may have a role in controlling late phases of immune responses and possibly autoimmunity.

The phenotypes generated by deficiencies in CTLA-4, PD-1 and BTLA suggest that PD-1 and BTLA may have partially redundant inhibitory signals. Of these three inhibitory receptors, deficiency in CTLA-4 produces by far the most marked *in vivo* phenotype[33]. In fact, the basis for spontaneous lymphoproliferative disease in CTLA-4-deficient mice is not fully understood, but it requires properties of the normal T cell repertoire *in vivo*, as it is abated or prevented when CTLA-4-deficient mice are crossed onto a TCR transgenic background[29] and delayed when crossed onto a FoxP3 transgenic background[34].

Antigen-specific proliferation or cytokine production in CTLA-4-deficient T cells is not enhanced during the primary response and shows modest, if any, increases during secondary responses[29,30]. This result indicates that the important inhibitory action of CTLA-4 is unlikely to be applied during the costimulation-dependent activation of T cells. Indeed, the greatest *in vitro* difference between wild-type and CTLA-4-deficient T cells occurs after the *in vivo* intravenous delivery of soluble antigen to induce anergy[30]. CTLA-4 may exert at least part of its regulatory activity by a non–cell-autonomous mechanism[35–37], contrary to the expected inhibitory action of SHP-1 or SHP-2 in cells expressing surface CTLA-4. A non–cell-autonomous inhibitory role for CTLA-4 might, for example, result from the engagement and crosslinking of B7 expressed by APCs[38], leading to an indirect regulatory action[39]. Thus, although CTLA-4 clearly has an important *in vivo* regulatory role, it is not yet totally clear how, when or where this action is exerted, or why no marked *in vitro* effect is seen.

In contrast to CTLA-4 deficiency, loss of PD-1 expression *in vivo* results in a phenotype that is variable and dependent on genetic background, being mild in 129SvEv mice[11] and more severe in BALB/c mice[40]. How the genetic background affects the requirement for PD-1 in regulating self-tolerance is not understood. *In vitro* analysis of PD-1-dependent T cell responses suggests that CD28-dependent, but not ICOS-dependent, costimulation overrides PD-1-dependent cellular inhibition[41]. In addition, inhibition by PD-1 of CD3-CD28–driven T cell activation is restricted to a very narrow range of activation; for example, it occurs at 1 μg/ml, but not at 2 μg/ml, of anti-CD3 *in vitro*[12] and is overcome by IL-2 (ref. 42). Thus, for both CTLA-4 and PD-1, the very modest effects seen in *in vitro* assays do not reflect the more marked and important actions of these inhibitory receptors observed *in vivo*.

In summary, whereas CTLA-4 deficiency produces a marked lymphoproliferative phenotype, PD-1 and BTLA deficiencies (on the 129SvEv background) individually produce a subtle phenotype characterized by enhanced propensity to autoimmunity. Although CTLA-4 can regulate both early events in T cell activation[43] and the later unfolding of autoimmunity[44,45], it seems that PD-1 and BTLA may function later in regulating effector responses, on the basis of their delayed expression in T cells. Conceivably, then, PD-1 and BTLA may have inhibitory actions that provide a redundant inhibitory system geared toward maintaining peripheral tolerance. An examination of mice deficient for both PD-1 and BTLA will be required to test this hypothesis.

CTLA-4 and PD-1 each interact with two known ligands, B7-1 and B7-2, and PD-L1 and PD-L2, respectively[32]. So far, we have identified only one candidate protein containing an Ig domain that may interact with BTLA. We may infer that an interaction occurs between BTLA and B7x from the loss of binding of the B7x-Ig fusion protein to BTLA-deficient T cells; however, it is conceivable that BTLA does not interact directly with the B7x-Ig fusion protein, but instead controls the expression of another, directly interacting, partner. On the basis of our interpretation that BTLA functions as an inhibitory receptor like PD-1 and CTLA-4, rather than as a regulator of protein transport, we favor the interpretation that there is a direct interaction between BTLA and B7x. Our analysis of potential BTLA-interacting candidates is in its early stages. So far, our search has been restricted to using Ig fusions of various B7 family members, which may limit the sensitivity of detecting interactions. For example, the limited sensitivity of Ig fusion proteins became evident in our control analysis of PD-1 expression. Anti–PD-1 detected a much higher signal that did the PD-L1 or PD-L2 Ig fusion proteins, probably a result of the lower affinities of the PD-L1 or PD-L2 Ig fusion proteins, as compared with the affinity of the PD-1 antibody, for PD-1. Thus, detecting additional BTLA-interacting proteins may require techniques with higher sensitivity.

The existence of a human homolog of BTLA that is very closely related to the mouse sequence, combined with the observation that murine and human BTLA cytoplasmic domains associate with the phosphatases SHP-1 and SHP-2, argue for a conserved inhibitory function. Polymorphisms in CTLA-4 may be linked to autoimmune disorders in humans[46,47]. Given the variable PD-1-deficient phenotype on different genetic backgrounds, and the quantitative nature of the BTLA-deficient phenotype, we propose that polymorphisms affecting the function of either of these inhibitory receptors could be a basis for variably penetrant susceptibility to autoimmunity in the human population. In this regard, we have noted variations among murine strains of the BTLA sequence (data not shown). Variations in receptor-ligand affinity, ligand expression or inherent receptor signaling could contribute to variable autoimmune susceptibility among individuals, particularly if these two inhibitory receptors provide a redundant shield for peripheral tolerance.

METHODS

Isolation of BTLA. We used an EST (aa839766) expressed by T_H1, but not T_H2, cells to screen a T_H1 cDNA phage library made in the Lambda ZAP vector (Stratagene) and isolated a partial clone, BTLAs, that lacked an Ig domain. Full-length BTLA cDNA, amplified from WEHI cell RNA by RT-PCR with primers J10-3K (5′-TTTGGCCTAAGATGCTGCTA-3′) and J10-7F (5′-CACAGATTGGGTACGACATG-3′), was inserted into the GEM-T Easy Vector (Promega) to produce mJ11W1. We obtained additional full-length BTLA cDNA isolates by screening a second mouse splenocyte cDNA library (Stratagene) using the 5′ region of mj11W1 as a probe. Coding sequence and intron-exon boundaries were further determined by sequencing 129SvEv strain bacterial artificial chromosome clones containing the BTLA region (Genome Systems). Some Ig domain sequence polymorphisms occur among mouse strains. Human BTLA cDNA, amplified from Ramos B lymphoma RNA by RT-PCR with primers hJ10 (5′-TTTTCCATCACTGATATGTGCAGG-3′) and hJ10 AS (5′-GGTCCCTGTTGGAGTCAGAAAC-3′) based on the Celera human genome assembly, was inserted into the GEM-T Easy Vector to produce hJ11#14u.

Plasmid constructions. Myc-tagged BTLA constructs were prepared as follows. The open reading frame of mBTLAs was amplified from a colony obtained from screening a DO11.10 T_H1 cDNA library with primers J10-RV1-Bgl2 (5′-AGCTCTGAAGATCTCTAGGGAGGAAG-3′) and J10-Xho1 (5′-CATGCTCGAGGAAGGTCCAGACAGAGGTATTG-3′). The product was digested with *Bgl*II and *Xho*I and cloned into the IRES-GFP-RV retrovirus[48] at the *Bgl*II and *Xho*I sites to produce mBTLAs-RV.

The N-terminal Myc-tagged version of mBTLAs (Myc_3-mBTLAs-RV) contains a triple Myc tag inserted downstream of the signal peptide. To produce this construct, a PCR product containing the mBTLA signal sequence and 3′ overhang homologous to the Myc tag was prepared with mBTLAs-RV as the template and primers J10-RV1-Bgl2 and J10-A2 (5′GTTCAGATCCAAGGATGCTCCAGAGGCCC-3′). This PCR product was annealed to a second PCR

product comprising three copies of the Myc epitope with 5′ and 3′ overhangs homologous to the N- and C-terminal portions of BTLA, respectively, which had been amplified from the triple Myc/Bluescript template with primers J10-A3 (5′-GAGCATCCTTGGATCTGAACAAAAGCTGATTA-3′) and J10-A4 (5′-CTTTCTCACAGAGCTCGTACAGGTCCTCT-3′). The triple Myc/Bluescript template contains 'anchor' sequences 5′ (GS) and 3′ (YEL) to the Myc_3 coding sequence, which are included in the final Myc-tagged mBTLA protein. We then amplified the two annealed pieces with primers J10-RV1-Bgl2 and J10-A4. This product was annealed to a third PCR product containing a 5′ Myc homologous tail and the C-terminal portion of BTLA amplified from the template mBTLAs-RV with primers J10-A5 (5′-GTACGAGCTCTGTGAGAAAGCTACTAA-GAGG-3′) and J10-Xho1, and the full-length chimeric cDNA was amplified with primers J10-RV1-Bgl2 and J10 Xho1. The resulting product was digested with *Bgl*II and *Xho*I and ligated into the *Bgl*II and *Xho*I sites of IRES-GFP-RV to yield Myc_3-mBTLAs-RV.

To produce the N-terminal Myc-tagged version of mBTLA (Myc_3-mBTLA-RV), primers J10-RV1-Bgl2 and J10-A4 were used to amplify the signal sequence linked to the triple Myc epitope from template Myc_3-mBTLAs-RV. A second PCR product was amplified with primers J10-A5 and J10 Xho1 and the template mJ11W1. The two PCR products were annealed and amplified with primers J10-RV1-Bgl2 and J10 Xho1, digested, and ligated into the retroviral vector to produce Myc_3-mBTLA-RV. A further modification was made by using the Quick Change mutagenesis kit (Stratagene) to convert a cysteine downstream of the Myc tag to alanine to mimic more accurately the predicted signal sequence processing in which this cysteine would be removed (SignalP V2.0).

Δcyt-Myc_3-mBTLA-RV was generated using Quick Change mutagenesis of Myc_3-mBTLA-RV with the primers mJ11 trunc top (5′-TGATATTCCATAAAC CTGCCACTGAGCCAG-3′) and mJ11 trunc bottom (5′-TGGCAGGTTTATG GAATATCAACCAGGTTAGTG-3′). mBTLA-Myc_2-RV, which expresses mBTLA with two C-terminal Myc epitopes, was generated by 'splicing by overlap extension' (SOEing) together two PCR products (generated from primers J10-RV1-Bgl2 and 3′ mj11 Myc tail (5′-GCTTTTGTTCACTTCTCACACAAATGGA TGC-3′) with template mJ11W1, and primers 5′ mjll Myc tail (5′-TGAGGAGTG AACAAAAGCTGATTAGCGAAG-3′) and new 3′ Xho Myc tail (5′-CCGCTCG AGCTCCTACAGGTCCTCTTC-3′) with template triple Myc/Bluescript) with primers J10-RV1-Bgl2 and new 3′ *Xho*I Myc tail and *Pfu* polymerase. After digestion with *Bgl*II and *Xho*I, the PCR product was ligated into the retroviral expression vector Tb-lym-GFP RV[49], which had been digested with *Bgl*II and *Xho*I, to generate mBTLA-Myc_2-RV.

The N-terminal Myc-tagged version of hBTLA containing a triple Myc tag inserted downstream of the signal peptide (Myc_3-hBTLA-RV) was prepared similarly. Three separate PCR products were generated using the following primers and templates: 5′ Bgl2 hj11 (5′-GAAGATCTGCAGGAAATGAAGACATTGCCT-3′) and 3′ Myc/hj11 bottom (5′-TCAGCTTTTGTTCCCCATGGATGTTCCA-GATGTCC-3′) with hj11#14u; 5′ hj11/Myc top (5′-CATCCATGGGGAACAAA AGCTGATTAGCGAAGAG-3′) and 3′ hj11/Myc bottom (5′-CACATGATTCTT TCAGGTCCTCTTCGCTAATCAGC-3′) with triple Myc/Bluescript; and 5′ Myc/hj11 top (5′-GAGGACCTGAAAGAATCATGTGATGTACAGCTTTA-3′) and 3′ Xho hj11 (5′-CCGCTCGAGTTGGAGTCAGAAACAGACTTAAC-3′) with hj11#14u. These PCR products were sequentially annealed and amplified, and cloned into tb-lym-GFP-RV, which had been digested with *Bgl*II and *Xho*I.

hBTLA containing three carboxy-terminal Myc epitopes (hBTLA-Myc_3-RV) was generated by SOEing together two PCR products (from primers 5′ Bgl2 hJ11 and 3′ hJ11 Myc tail (5′-TGAGGAGTGAACAAAAGCTGATTAGCGAAG-3′) with template hJ11#14u, and primers 5′ hj11 Myc tail (5′-TGAGGAGTGAA-CAAAAGCTGATTAGCGAAG-3′) and new 3′ Xho Myc tail with template triple Myc/Bluescript) with primers 5′ Bgl2 hJ11 and new 3′ Xho Myc tail and *Pfu* polymerase. After digestion with *Bgl*II and *Xho*I, the PCR product was ligated into retroviral expression vector Tb-lym-GFP-RV[49], which had been digested with *Bgl*II and *Xho*I, to generate hBTLA-Myc_3-RV. Embryonic stem cells (MC50) were a gift from R. Schreiber (Washington University School of Medicine, St. Louis, Missouri).

Tyrosine mutations. Single tyrosine-to-phenylalanine mutations of hBTLA-Myc_3-RV were produced using Quick Change mutagenesis and *Pfu* polymerase (Stratagene) with the following oligonucleotide pairs: Y226F top2 (5′-GA AACTGGAATTTATGATAATGACCCTGACCTTTG-3′) and Y226F bot (5′-GG GTCATTATCAAAAATTCCAGTTTCTGATAGCAG-3′); Y257F top2 (5′-ACCA GGCATTGTTTATGCTTCCCTGAACCATTCTG-3′) and Y257F bot (5′-AGG GAAGCAAAAACAATGCCTGGTTTGT-3′); Y282F top2 (5′-GCACCAACAG AATATGCATCCATATGTGTGAGG-3′) and Y282F bot (5′-ATATGGATGCAA ATTCTGTTGGTGCTTCTTTTA-3′).

We produced double and triple tyrosine-to-phenylalanine mutations of hBTLA-Myc_3-RV by using the oligonucleotide pair Y257F top2 and Y257F bot first with the Y226F-mutated hBTLA-Myc3-RV template to produce Y226F/Y257F and then with the Y282F-mutated template to produce Y257F/Y282F. The oligonucleotide pair Y282F top2 and Y282F bot was used with the Y226F-mutated template to produce Y226F/Y282F, and with the Y226F/Y257F-mutated template to produce Y226F/Y257F/Y282F.

Cell culture and expression analysis. Activation of DO11.10 TCR transgenic T cells[50] and retroviral infections, northern analysis and immunoblotting[49] were done as described. We prepared tissue and cellular RNA with the RNeasy Midi kit (Qiagen). A 20× stock of pervanadate was prepared 5 min before use by diluting 12.5 μl of 1 M $NaVO_4$ and 4 μl of 30% H_2O_2 to 600 μl in distilled water. The Opteia Mouse IL-2 set (PharMingen) was used to measure for IL-2 by enzyme-linked immunosorbent assay (ELISA).

Immunoblotting and analysis of *N*-linked glycosylation. To analyze the glycosylation status (**Fig. 3b**), cells (15×10^6 per ml) were lysed in Triton X-100 lysis buffer (25 mM HEPES (pH 7.5), 0.15 M NaCl, 1% Triton (v/v), 1 mM pervanadate, 1 μg/ml of leupeptin, 1 μg/ml of pepstatin, 1 μg/ml of aprotinin and 1 mM phenyl methylsulfonyl fluoride) for 30 min at 4 °C and centrifuged at 14,000*g* for 10 min. Extracts from 15×10^6 cells were immunoprecipitated with 1 μg of monoclonal antibodies to Myc (clone 9E10; Santa Cruz) and 20 μl of a 1:1 slurry of protein G–Sepharose (PGS) (Pharmacia). After being washed three times in Triton lysis buffer, the pellets were boiled for 10 min in 10 μl of PNGase denaturing buffer (NEB). After centrifugation to remove PGS, eluted proteins were transferred to PCR tubes containing 1 μl of 10% Nonidet P-40 (NP-40) and 1 μl of 10× G7 buffer (NEB), divided into two 6-μl aliquots, and treated without or with 1 μl of PNGase F (NEB) for 1 h at 37 °C. We boiled samples with 6 μl of 2× SDS-PAGE sample buffer and resolved them on 10% polyacrylamide gels. The proteins were transferred to nitrocellulose, blocked in 3% bovine serum albumin (BSA) in TBS-T buffer, blotted with rabbit anti-Myc (Santa Cruz) and horseradish peroxidase (HRP)-conjugated goat anti–rabbit IgG (Jackson), and analyzed by enhanced chemiluminescence (ECL).

To analyze the phosphorylation status (**Fig. 3c,d**), cells were treated with 1 mM pervanadate for 2 min at 37 °C, placed on ice for 1 min, lysed in an equal volume of 2× 1% Triton X-100 lysis buffer for 30 min and centrifuged for 10 min at 8,000*g*. Extracts from 15×10^6 cells were immunoprecipitated using 1 μg of anti-Myc (clone 9E10) and PGS. Blots were first analyzed for phosphotyrosine (pTyr) using HRP-conjugated (clone 4G10, Upstate Biotechnology), and then stripped and reanalyzed using rabbit anti-Myc and HRP-conjugated goat anti-rabbit IgG.

TCR crosslinking. To analyze the induction of tyrosine phosphorylation and association with SHP-1 and SHP-2 on TCR crosslinking, we infected DO11.10 hybridoma T cells with GFP-RV[48] or Myc_3-mBTLAs-RV and purified them by sorting. Cells were incubated with 4 μg/ml of hamster anti-CD3ε (clone 145-2C11, PharMingen) and 2 μg/ml of anti-Myc for 30 min at 4 °C, and crosslinked with 100 μg/ml of prewarmed goat anti–mouse IgG (GαM; Caltag) for various times, as indicated (**Fig. 4**). We used fluorescence-activated cell sorting (FACS) to confirm the cross-reactivity of goat anti–mouse IgG with hamster anti-CD3ε. As a positive control for phosphorylation, some cells were incubated with 1 mM pervanadate for 2 min at 37 °C. Cells were lysed in RIPA buffer, and 1 ml of lysates from 25×10^6 cells were immunoprecipitated with 2 μg of anti-Myc (9E10). We used the following antibodies to analyze the immunoprecipitates: anti-pTyr (RC20H, Transduction Laboratories), polyclonal rabbit anti-Myc (A-14, Santa Cruz), rabbit anti–SHP-2 (C-18, Santa Cruz), rabbit anti–SHP-1 antibody (C-19, Santa Cruz) and anti-Myc (9E10).

To measure the effect of crosslinking on IL-2 production, 3×10^4 DO11.10 cells expressing GFP-RV, Myc_3-mBTLAs-RV or Myc_3-mBTLA-RV were stimulated with 1 μg/ml of immobilized anti-CD3ε in combination with various concentrations of immobilized polyclonal rabbit anti-Myc or 50 ng/ml of PMA

plus 1 μM ionomycin. Culture supernatants of triplicate cultures were collected after 24 h, and the IL-2 concentration was determined by ELISA.

Antibody responses. Eight-week-old littermate wild-type, *Btla*$^{+/-}$ and *Btla*$^{-/-}$ mice on a pure 129SvEv background ($n = 5$) were injected intraperitoneally with 100 μg of NP^{17}-KLH (Biosearch Technologies) in alum (Pierce) on days 0 and 14. Sera was collected on day 28, and the titers of anti-NP were determined by ELISA using NP^{25}-BSA (Biosearch Technologies) for antibody capture and the SBA Clonotyping system/HRP kit for IgG subclass-specific ELISA (Southern Biotech).

***In vitro* responses of BTLA-deficient lymphocytes.** T and B cells from wild-type or BTLA-deficient mice were purified by cell sorting using fluorescein isothiocyanate (FITC)-conjugated anti-CD4 (Caltag), FITC-conjugated anti-CD8α (PharMingen) or phycoerythrin (PE)-conjugated anti-B220 (PharMingen). Cells (5×10^5 per ml) were stimulated with various concentrations of plate-bound anti-IgM (Affinipure F(ab′)$_2$ fragment goat anti–mouse IgM 115-006-075, Jackson ImmunoResearch), LPS (serotype 055:B5, Sigma), concanavalin A or plate-bound anti-CD3e (PharMingen, 145-2C11). Cell proliferation was measured after 48 h by pulsing with [^{3}H]thymidine for 16 h.

Production and interaction of B7x-Ig. In the public databases we identified a B7 homolog, B7x, that was conserved in mouse (accession code XP_143450.2 and AAH32925.1), rat (accession code XP_227553.1) and human (accession code NP_078902.1) and was highly conserved in sequence. B7x-Ig was prepared by fusing the coding region of the extracellular domain of B7x to the CH2-CH3 domain of mouse IgG1 and a Myc-His tag in pcDNA4 (a gift of W. Sha, Univ. California Berkeley, Berkeley, California, USA). The construct was linearized with *Bgl*II and transfected into 293T cells with FuGENE 6 (Roche). Stable transfectants were selected in 1 mg/ml of Zeocin (Invitrogen). To obtain fusion protein, we cultured stable transfectants in serum-free Dulbecco's modified Eagle's medium for 72 h, collected the supernatant and purified B7x-Ig by affinity column chromatography over His-Bind resin (Novagen). The purity of the fusion protein was confirmed by SDS-PAGE and by immunoblotting with antibodies against Myc and mouse IgG.

The following reagents were used to measure receptor and B7 ligand interactions (**Fig. 9**): anti-CD4–FITC (Caltag); human IgG1 antibody (Sigma); biotinylated anti-Myc (Santa Cruz); streptavidin-PE (PharMingen); B7.1-Ig, B7.2-Ig, PD-L1-Ig and PD-L2-Ig fusion proteins (Fc portion; human IgG1 isotype; R&D Systems); goat anti–human Fcγ F(ab′)$_2$–PE (Jackson ImmunoResearch); and anti–PD-1–PE (PharMingen).

FACS analysis. Human IgG1 and goat anti–human PE were gifts of M. Cella (Washington Univ., St. Louis, Missouri, USA). The construct for the B7h-Ig fusion protein[3], a gift of W. Sha (Univ. California Berkeley), and the cDNA encoding the fusion protein were inserted into the GFP-RV retroviral vector[48], and the retrovirus was used to infect J558 cells. We purified fusion protein from infected J558 supernatant with His-Bind resin (Novagen). B7.1-Ig, B7.2-Ig, PD-L1-Ig and PD-L2-Ig fusion proteins (Fc portion; human IgG1 isotype) were obtained from R&D Systems. All analyses were done on a FACSCalibur.

To measure the surface expression of BTLA, Bjab cells were infected with amphotrophic retrovirus prepared in Phoenix A packaging cells to express empty vector, Myc$_3$-mBTLA-RV, Δcyt-Myc$_3$-mBTLA-RV and Myc$_3$-mBTLAs-RV. Expression of the Myc epitope on GFP-positive cells was assayed on a FACScalibur with rabbit anti-Myc polyclonal serum (Santa Cruz) and PE-conjugated goat F(ab′)$_2$ anti–rabbit IgG (Jackson Research Laboratories).

Histological analysis. CNS tissues were removed from mice and frozen and 10-μm sections were prepared. Sections shown are from lumbar spinal cord. We prepared sections stained with hematoxylin and eosin, and measured the expression of CD4 and CD11b by immunofluorescence microscopy as described[31].

Accession codes. Murine BTLA, AY293285; human BTLA, AY293286; murine B7x, XP_14350.2 and AAH32925.1; rat B7x, XP_227553.1; human B7x, NP_078902.1 (http://www.ncbi.nlm.nih.gov/entrez/query.fcgi?db=protein). From the NCBI Protein database.

Note: Supplementary information is available on the Nature Immunology website.

ACKNOWLEDGMENTS

We thank B. Sleckman for help with gene targeting; M. White for generating chimeric mice; M. Gimenez for help with immunohistochemistry; and W. Sha for discussions. This work was supported in part by grants from the National Institutes of Health. J.P.A. and K.M.M. are Investigators of the Howard Hughes Medical Institute.

COMPETING INTERESTS STATEMENT

The authors declare that they have no competing financial interests.

Received 13 January; accepted 13 May 2003
Published online 8 June 2003; doi:10.1038/ni944

1. Coyle, A.J. & Gutierrez-Ramos, J.C. The expanding B7 superfamily: increasing complexity in costimulatory signals regulating T cell function. *Nat. Immunol.* **2**, 203–209 (2001).
2. Hutloff, A. *et al.* ICOS is an inducible T-cell co-stimulator structurally and functionally related to CD28. *Nature* **397**, 263–266 (1999).
3. Swallow, M.M., Wallin, J.J. & Sha, W.C. B7h, a novel costimulatory homolog of B7.1 and B7.2, is induced by TNFα. *Immunity* **11**, 423–432 (1999).
4. Yoshinaga, S.K. *et al.* T-cell co-stimulation through B7RP-1 and ICOS. *Nature* **402**, 827–832 (1999).
5. Ling, V. *et al.* Cutting edge: identification of GL50, a novel B7-like protein that functionally binds to ICOS receptor. *J. Immunol.* **164**, 1653–1657 (2000).
6. Wang, S. *et al.* Costimulation of T cells by B7-H2, a B7-like molecule that binds ICOS. *Blood* **96**, 2808–2813 (2000).
7. Brodie, D. *et al.* LICOS, a primordial costimulatory ligand? *Curr. Biol.* **10**, 333–336 (2000).
8. Liang, L. & Sha, W.C. The right place at the right time: novel B7 family members regulate effector T cell responses. *Curr. Opin. Immunol.* **14**, 384–390 (2002).
9. Liang, L., Porter, E.M. & Sha, W.C. Constitutive expression of the B7h ligand for inducible costimulator on naive B cells is extinguished after activation by distinct B cell receptor and interleukin 4 receptor–mediated pathways and can be rescued by CD40 signaling. *J. Exp. Med.* **196**, 97–108 (2002).
10. Ishida, Y. *et al.* Induced expression of PD-1, a novel member of the immunoglobulin gene superfamily, upon programmed cell death. *EMBO J.* **11**, 3887–3895 (1992).
11. Nishimura, H. *et al.* Immunological studies on PD-1 deficient mice: implication of PD-1 as a negative regulator for B cell responses. *Int. Immunol.* **10**, 1563–1572 (1998).
12. Freeman, G.J. *et al.* Engagement of the PD-1 immunoinhibitory receptor by a novel B7 family member leads to negative regulation of lymphocyte activation. *J. Exp. Med.* **192**, 1027–1034 (2000).
13. Dong, H. *et al.* B7-H1, a third member of the B7 family, co-stimulates T-cell proliferation and interleukin-10 secretion. *Nat. Med.* **5**, 1365–1369 (1999).
14. Latchman, Y. *et al.* PD-L2 is a second ligand for PD-l and inhibits T cell activation. *Nat. Immunol.* **2**, 261–268 (2001).
15. Tseng, S.Y. *et al.* B7-DC, a new dendritic cell molecule with potent costimulatory properties for T cells. *J. Exp. Med.* **193**, 839–846 (2001).
16. Chapoval, A.I. *et al.* B7-H3: a costimulatory molecule for T cell activation and IFN-γ production. *Nat. Immunol.* **2**, 269–274 (2001).
17. Sun, M. *et al.* Characterization of mouse and human B7-H3 genes. *J. Immunol.* **168**, 6294–6297 (2002).
18. Yang, J. *et al.* IL-18-stimulated GADD45β required in cytokine-induced, but not TCR-induced, IFN-γ production. *Nat. Immunol.* **2**, 157–164 (2001).
19. Tomasello, E. *et al.* Signaling pathways engaged by NK cell receptors: double concerto for activating receptors, inhibitory receptors and NK cells. *Semin. Immunol.* **12**, 139–147 (2000).
20. Bolland, S. & Ravetch, J.V. Inhibitory pathways triggered by ITIM-containing receptors. *Adv. Immunol.* **72**, 149–177 (1999).
21. Shiratori, T. *et al.* Tyrosine phosphorylation controls internalization of CTLA-4 by regulating its interaction with clathrin-associated adaptor complex AP-2. *Immunity* **6**, 583–589 (1997).
22. Zhang, Y. & Allison, J.P. Interaction of CTLA-4 with AP50, a clathrin-coated pit adaptor protein. *Proc. Natl. Acad. Sci. USA* **94**, 9273–9278 (1997).
23. Songyang, Z. *et al.* Specific motifs recognized by the SH2 domains of Csk, 3BP2, fps/fes, GRB-2, HCP, SHC, Syk, and Vav. *Mol. Cell. Biol.* **14**, 2777–2785 (1994).
24. Nishimura, H. *et al.* Development of lupus-like autoimmune diseases by disruption of the PD-1 gene encoding an ITIM motif-carrying immunoreceptor. *Immunity* **11**, 141–151 (1999).
25. Shlapatska, L.M. *et al.* CD150 association with either the SH2-containing inositol phosphatase or the SH2-containing protein tyrosine phosphatase is regulated by the adaptor protein SH2D1A. *J. Immunol.* **166**, 5480–5487 (2001).
26. Haskins, K. *et al.* The major histocompatibility complex–restricted antigen receptor on T cells. I. Isolation with a monoclonal antibody. *J. Exp. Med.* **157**, 1149–1169 (1983).
27. Okazaki, T. *et al.* PD-1 immunoreceptor inhibits B cell receptor–mediated signaling by recruiting Src homology 2-domain-containing tyrosine phosphatase 2 to phosphotyrosine. *Proc. Natl. Acad. Sci. USA* **98**, 13866–13871 (2001).
28. Chambers, C.A. *et al.* Secondary but not primary T cell responses are enhanced in CTLA-4-deficient CD8$^+$ T cells. *Eur. J. Immunol.* **28**, 3137–3143 (1998).

29. Oosterwegel, M.A. *et al.* The role of CTLA-4 in regulating Th2 differentiation. *J. Immunol.* **163**, 2634–2639 (1999).
30. Greenwald, R.J. *et al.* CTLA-4 regulates induction of anergy *in vivo*. *Immunity* **14**, 145–155 (2001).
31. Sabelko-Downes, K.A., Cross, A.H. & Russell, J.H. Dual role for Fas ligand in the initiation of and recovery from experimental allergic encephalomyelitis. *J. Exp. Med.* **189**, 1195–1205 (1999).
32. Sharpe, A.H. & Freeman, G.J. The B7-CD28 superfamily. *Nat. Rev. Immunol.* **2**, 116–126 (2002).
33. Tivol, E.A. *et al.* Loss of CTLA-4 leads to massive lymphoproliferation and fatal multiorgan tissue destruction, revealing a critical negative regulatory role of CTLA-4. *Immunity.* **3**, 541–547 (1995).
34. Khattri, R. *et al.* An essential role for Scurfin in $CD4^+CD25^+$ T regulatory cells. *Nat. Immunl.* **4**, 337–342 (2003).
35. Bachmann, M.F. *et al.* Cutting edge: lymphoproliferative disease in the absence of CTLA-4 is not T cell autonomous. *J. Immunol.* **163**, 1128–1131 (1999).
36. Bachmann, M.F. *et al.* Normal pathogen-specific immune responses mounted by CTLA-4-deficient T cells: a paradigm reconsidered. *Eur. J. Immunol.* **31**, 450–458 (2001).
37. Tivol, E.A. & Gorski, J. Re-establishing peripheral tolerance in the absence of CTLA-4: complementation by wild-type T cells points to an indirect role for CTLA-4. *J. Immunol.* **169**, 1852–1858 (2002).
38. Grohmann, U. *et al.* CTLA-4-Ig regulates tryptophan catabolism *in vivo*. *Nat. Immunol.* **3**, 1097–1101 (2002).
39. Finger, E.B. & Bluestone, J.A. When ligand becomes receptor—tolerance via B7 signaling on DCs. *Nat. Immunol.* **3**, 1056–1057 (2002).
40. Nishimura, H. *et al.* Autoimmune dilated cardiomyopathy in PD-1 receptor–deficient mice. *Science* **291**, 319–322 (2001).
41. Bennett, F. *et al.* Program death-1 engagement upon TCR activation has distinct effects on costimulation and cytokine-driven proliferation: attenuation of ICOS, IL-4, and IL-21, but not CD28, IL-7, and IL-15 responses. *J. Immunol.* **170**, 711–718 (2003).
42. Carter, L. *et al.* PD-1:PD-L inhibitory pathway affects both $CD4^+$ and $CD8^+$ T cells and is overcome by IL-2. *Eur. J. Immunol.* **32**, 634–643 (2002).
43. Brunner, M.C. *et al.* CTLA-4-mediated inhibition of early events of T cell proliferation. *J. Immunol.* **162**, 5813–5820 (1999).
44. Luhder, F. *et al.* Cytotoxic T lymphocyte-associated antigen 4 (CTLA-4) regulates the unfolding of autoimmune diabetes. *J. Exp. Med.* **187**, 427–432 (1998).
45. Luhder, F. *et al.* Pinpointing when T cell costimulatory receptor CTLA-4 must be engaged to dampen diabetogenic T cells. *Proc. Natl. Acad. Sci. USA* **97**, 12204–12209 (2000).
46. Abiru, N., Kawasaki, E. & Eguch, K. Current knowledge of Japanese type 1 diabetic syndrome. *Diabetes Metab. Res. Rev.* **18**, 357–366 (2002).
47. Ueda, H. *et al.* Association of the T-cell regulatory gene CTLA4 with susceptibility to autoimmune disease. *Nature*; advance online publication 30 April 2003/ doi 10.1038/nature01621.
48. Ranganath, S. *et al.* GATA-3-dependent enhancer activity in IL-4 gene regulation. *J. Immunol.* **161**, 3822–3826 (1998).
49. Afkarian, M. *et al.* T-bet is a STAT1-induced regulator of IL-12R expression in naive $CD4^+$ T cells. *Nat. Immunol.* **3**, 549–557 (2002).
50. Hsieh, C.S. *et al.* Development of TH1 $CD4^+$ T cells through IL-12 produced by Listeria-induced macrophages. *Science* **260**, 547–549 (1993).
51. Sha, W.C. *et al.* Selective expression of an antigen receptor on CD8-bearing T lymphocytes in transgenic mice. *Nature* **335**, 271–274 (1988).